STUDY ON POTENTIAL OF CHRYSIN AND ITS NANOFORMULATIONS IN AMELIORATING PULMONARY INFLAMMATORY DISORDERS

THESIS SUBMITTED TO JADAVPUR UNIVERSITY
FOR THE DEGREE OF
DOCTOR OF PHILOSOPHY (PHARMACY)

By

SAHELI ROY, M.S (Pharm)

DEPARTMENT OF PHARMACEUTICAL TECHNOLOGY
FACULTY COUNCIL OF ENGINEERING AND TECHNOLOGY
JADAVPUR UNIVERSITY
KOLKATA- 700032, INDIA

2022

JADAVPUR UNIVERSITY

KOLKATA-700032, INDIA

INDEX NO: 258/17/Ph

1. **Title of the thesis**: Study on potential of chrysin and its nano formulations in ameliorating pulmonary inflammatory disorders

2. **Name, Designation & Institution of the Supervisor/ s:**

Prof. Tarun Jha

Professor

Department of Pharmaceutical Technology

Jadavpur University, Kolkata-32, India

Dr. Krishna Das Saha

Principal Technical Officer

Cancer Biology & Inflammatory Disorder Division

CSIR-Indian Institute of Chemical Biology

Kolkata-32, India

3. **List of publications:**

Publication related to thesis

1. **Roy S**, Manna K, Jha T, Saha KD. Chrysin-loaded PLGA attenuates OVA-induced allergic asthma by modulating TLR/NF-κB/NLRP3 axis. Nanomedicine. 2020 Nov;30: 102292. doi: 10.1016/j.nano.2020.102292. Epub 2020 Aug 25. PMID: 32853785.
2. Synergistic effect of Chrysin functionalized gold nanoparticles and paclitaxel on lung cancer cell line by modulating the AKT/PPAR-ϒ/β-Catenin pathway. **Saheli Roy**, Tarun Jha, Krishna Das Saha (under communication)

Other Publications

1. Chakraborty S, Ehsan I, Mukherjee B, Mondal L, **Roy S**, Saha KD, Paul B, Debnath MC, Bera T. Therapeutic potential of andrographolide-loaded nanoparticles on a murine asthma model. Nanomedicine. 2019 Aug;20: 102006. doi: 10.1016/j.nano.2019.04.009. Epub 2019 May 3. PMID: 31059793.
2. Banerji B, Chandrasekhar K, Sreenath K, **Roy S**, Nag S, Saha KD. Synthesis of Triazole-Substituted Quinazoline Hybrids for Anticancer Activity and a Lead Compound as the EGFR Blocker and ROS Inducer Agent. ACS Omega. 2018 Nov 30;3(11):16134-16142. doi: 10.1021/acsomega.8b01960. Epub 2018 Nov 28. PMID: 30556027; PMCID: PMC6288807.

3. Role effectuated by immunomicroenvironment on prognosis of COVID-19 infected asthmatic patients and the potentialities of repurposing immunomodulatory drugs. **Saheli Roy**, Krishna Das Saha (under communication)

4. **List of Patents**: Nil

5. **List of Presentation in National / International conference/ workshop :**

1) Bioterm 2019, IIT-Kanpur. Poster presented on "Chrysin loaded PLGA ameliorates OVA-induced allergic asthma by modulation of NF-κB/NLRP3 axis."

2) ISNSCON 2018.Poster presentation on "Chrysin loaded PLGA ameliorates ova-induced allergic asthma by modulation of NF-κB pathway."

3) XI global health care summit 2017: Health care, Commerce &Career: American Association of Physicians of Indian Origin. Poster presented on topic "PLGA encapsulated nano andrographolide ameliorates OVA-induced allergic asthma in mice by upregulating Th2 type cytokines and targeting 5-LOX pathway."

"Statement of Originality"

I, *SAHELI ROY* registered on 24th April 2017, do hereby declare that this thesis entitled "*STUDY ON POTENTIAL OF CHRYSIN AND ITS NANOFORMULATIONS IN AMELIORATING PULMONARY INFLAMMATORY DISORDERS.*" contains literature survey and original research work done by the undersigned candidate as part of Doctoral studies. All information in this thesis have been obtained and presented in accordance with existing academic rules and ethical conduct. I declare that, as required by these rules and conduct, I have fully cited and referred all materials and results that are not original to this work. I also declare that I have checked this thesis as per the "Policy on Anti Plagiarism, Jadavpur University, 2019", and the level of similarity as checked by iThenticate software is 8 %

Saheli Roy

Signature of Candidate

Date: 20/07/2022

Certified by Supervisor(s):

Tarun Jha
20.7.2022

Prof. Tarun Jha

Professor

Department of Pharmaceutical Technology

Jadavpur University, Kolkata-32, India

TARUN JHA, Ph.D
Professor
Dept. of Pharm. Tech.
Jadavpur University
Kolkata-700 032

Krishna Das Saha 20/07/22

Dr. Krishna Das Saha

Principal Technical Officer

Cancer Biology & Inflammatory Disorder Division

CSIR-Indian Institute of Chemical Biology

Kolkata-32, India

Dr. (Mrs.) Krishna Das Saha
Principal Technical Officer
Cancer Biology & Inflammatory Disorder Division
CSIR - Indian Institute of Chemical Biology
4, Raja S. C. Mullick Road, Kolkata - 700 032

CERTIFICATE FROM THE SUPERVISOR/S

This is to certify that the thesis entitled ***"Study on potential of Chrysin and its nano formulations in ameliorating pulmonary inflammatory disorders"*** submitted by Saheli Roy, who got his/her name registered on 24th April 2017 for the award of Ph.D. (~~Engg~~ / Pharmacy) degree of Jadavpur University is absolutely based upon his/her own work under the supervision of **Prof. Tarun Jha**, Pharmaceutical Technology, Jadavpur University, Kolkata, India & **Dr. Krishna Das Saha**, Cancer Biology and Inflammatory Disorder Division, CSIR-Indian Institute of Chemical Biology, Kolkata, India and that neither ~~his~~/her thesis nor any part of the thesis has been submitted for any degree/diploma or any other academic award anywhere before.

Tarun Jha 20.7.2022

Prof. Tarun Jha

Professor

Department of Pharmaceutical Technology

Jadavpur University, Kolkata

TARUN JHA, Ph.D
Professor
Dept. of Pharm. Tech.
Jadavpur University
Kolkata-700 032

Krishna Das Saha 20/07/22

Dr . Krishna Das Saha

Principal Technical Officer

Cancer Biology & Inflammatory Disorder Division

CSIR-Indian Institute of Chemical Biology ,Kolkata

Dr. (Mrs.) Krishna Das Saha
Principal Technical Officer
Cancer Biology & Inflammatory Disorder Division
CSIR - Indian Institute of Chemical Biology
4, Raja S. C. Mullick Road, Kolkata - 700 032

DEDICATED TO

MY BELOVED

PARENTS

Acknowledgement

I want to thank almighty for bestowing his blessings in completing this rigorous journey of Ph.D. I want to commence by expressing my sincere gratitude and respect to my Ph.D supervisors Prof. Tarun Jha, Department of Pharmaceutical Technology, Jadavpur university, and Dr. Krishna Das Saha, Cancer Biology and Inflammatory Disorder Division, CSIR-Indian Institute of Chemical Biology, Kolkata for their continuous inspiration, priceless guidance, insightful criticism, and scientific advice over the course of my research. I am grateful to Dr. Arun Bandopadhyay, Director, and Prof Samit Chattopadhyay, Ex Director of CSIR- I.I.C.B Kolkata, for providing me all the necessary facilities to carry out this work. Special thanks to my lab colleagues cum friends Moumita Saha, Sanchaita Mondal, Saswati Banerjee, Sayoni Nag, Snehasis Mishra, Tanushree Das, Sanjib Das and seniors Krishnendu Da, Dipayan da, Somenath Da, Sujata Di for the memorable good times spent during this period.

I want to thank my friends in CSIR-IICB Tresha, Nilanjana Di, Sreyashi, Kamran, Sumangal for continuous help and support at all times during my work.

I express my sincerest gratitude and due respects to my beloved parents and my little sister Manali whose constant inspiration and encouragement helped me a lot to complete this Ph.D work.

I want to thank my husband Shashi Kant for his unwavering support and extending help in my research work without which it would have been difficult to complete my thesis successfully. Last but not least my little son-shine Shaurya for being in my life and for being my constant source of motivation.

***Indian Council of Medical Research(ICMR)** offered financial assistance during my whole research as JRF and SRF fellowship, which I gratefully acknowledge.*

Finally, I'd want to thank everyone who helped me benevolently either directly or indirectly.

Saheli Roy

List of Abbreviations

g gram

mg milligram

µg microgram

Au Gold

AEC Animal ethics committee

AFM Atomic force microscopy

AHR Airway hyper-responsiveness

AKT Protein Kinase B

ANOVA one-way analysis of variance

BSA Bovine serum albumin

B-NP Blank nanoparticle

CD4 Cluster of differentiation 4

CHR-Chrysin

CHR-NP Chrysin loaded PLGA nanoparticle

CHR-AuNP Chrysin functionalized gold nanoparticle

DCM Dichloromethane

DEX Dexamethasone

DMEM Dulbecco's modified eagles medium

DSC Differential scanning calorimetry

DL Drug loading

DMSO Dimethyl sulfoxide

DNA Deoxyribonucleic acid

EE Entrapment efficiency

ELISA Enzyme linked immunosorbent assays

FBS Fetal bovine serum

FDA Food and drug administration

FESEM Field emission scanning electron microscopy

FITC Fluorescein isothiocyanate

FTIR Fourier-transform infrared spectroscopy

HEPES (4-(2-hydroxyethyl)-1-piperazineethanesulfonic acid)

HRP Horseradish peroxidase

IC 50 Inhibitory concentration 50%

IFN- γ Interferon γ

IgE Immunoglobulin E

IL Interleukin

i.p Intraperitoneal

NF- κB Nuclear factor κ B

NP-nano particle

NLRP3 NLR family pyrin domain containing 3

OVA Ovalbumin

PI3K Phosphoinositide 3-kinase

PBS Phosphate buffered saline

PDI Polydispersity index

PLGA Poly(D,L-lactic-coglycolic acid)

PS Phospatidyl serine

PVA Polyvinyl alcohol

ROS Reactive oxygen species SD Standard deviation

SDS-PAGE Sodium dodecyl sulphate-polyacrylamide gel electrophoresis

TEM Transmission electron microscope

Th2 Type 2 T helper cell

TLR-Toll like receptor

TNF α Tumor necrosis factor α

WHO World Health organization

WNT Wingless Integrated

XRD X ray diffraction

ZP Zeta potential

CONTENT

CHAPTER 1

INTRODUCTION

INTRODUCTION

Asthma

Asthma is a chronic ailment typified by airway inflammation, restricted airflow, hyper-reactivity, and remodelling. The introduction of inhaled corticosteroids and beta-adrenergic agonists has shifted the treatment paradigm for asthma, and a better knowledge of the pathological mechanism of asthma is likely to foster the growth of new medicines.

Currently, asthma pharmacological therapy is mostly centred on the prescription of anti-inflammatory drugs to avoid symptoms and pain relievers during exacerbations. Among people who have access to specialised asthma medication, there is a notably high prevalence of usage of herbal plants (Newman & Cragg, 2012; Park et al., 2010). Flavonoids which is found abundantly in plants have been found to have therapeutic benefits in asthmatic models in several investigations, however data from epidemiological research and human clinical trials is still sparse.

Epidemiology Around the World

Asthma incidence varies greatly around the globe due to diverse genetic, environmental, and occupational risk factors. However, this discrepancy appears to be diminishing as the frequency in high-income nations reaches a plateau while it rises in low and middle-income countries (Loftus & Wise, 2015). Asthma is estimated to affect roughly 334 million people worldwide, with the condition accounting for 250,000 fatalities per year. The disease's prevalence is increasing, and the global prevalence is expected to rise by 100 million by 2025 (Enilari & Sinha, 2019).

The present state of asthma treatment

The pathophysiology of asthma is unknown and has been related to a number of genetic, environmental, viral, and dietary variables. As a result, asthma is challenging to treat. A combination of β -adrenoceptor agonists and steroids has been found to be effective.

In recent years, corticosteroids have become the first-line treatment for allergic diseases and immunological disorders. Inhaled corticosteroids are the most often used asthma medication. Oral corticosteroids are used to treat severe asthma episodes. Bronchodilators can also be used to enhance other therapies. However, they just alleviate bronchospasm and have little or no effect on the inflammatory phase, providing patients only symptomatic relief. Mast cell stabilisers, such as sodium cromoglycate, are commonly used in the treatment of asthma. In addition to these drugs, leukotriene inhibitors are used for maintenance therapy. Omalizumab, an anti-IgE immunotherapy, has been demonstrated to be extremely successful. It is a monoclonal antibody that binds to serum IgE and reduces IgE levels.

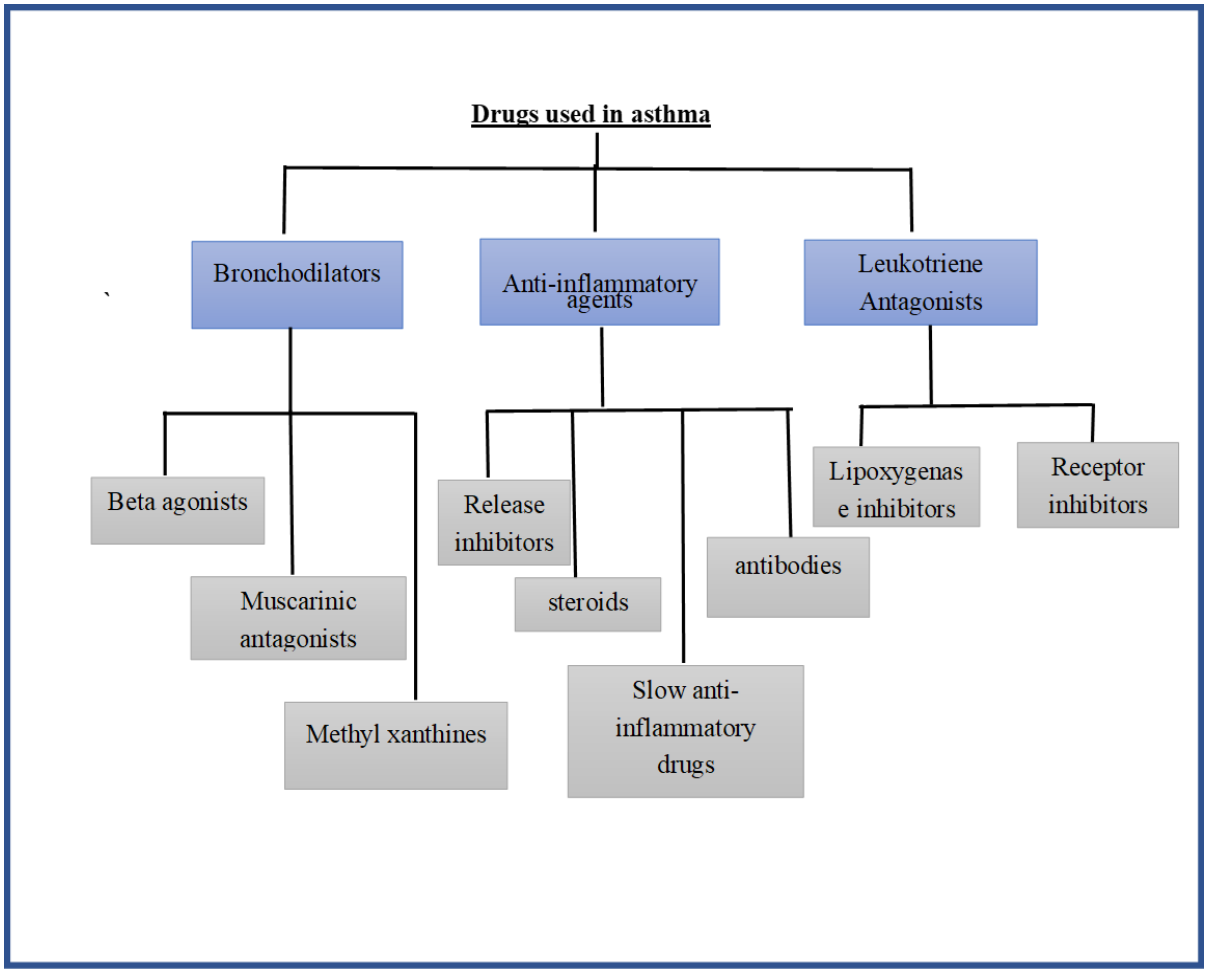

Classification of antiasthmatic drugs Trevor AJ, K. B. K.-H. M. (n.d.). *Katzung and Trevor' s Pharmacology: Examination and board review, 11. Ed, Chapter 5, 2015; 169.*

Corticosteroids' Limitations

Although corticosteroids are currently the best available remedy, they have a number of adverse effects when used long term. Oral corticosteroids cause long-term adverse effects such as fluid retention, weight gain, loss of appetite, osteoporosis. All inhaled corticosteroids (ICS) are absorbed directly through the lungs and can cause systemic and local side effects (Marandi et al., 2013). Additionally, ICS are disseminated throughout the body and eliminated quickly. A significant amount of medication with repeated dosage is required to obtain the effective therapeutic concentration.

Natural products in treatment of asthma

Notwithstanding significant breakthroughs in chemical and pharmaceutical technologies for synthesising novel molecules, natural-source pharmaceuticals are continually being discovered and developed for novel treatments. These investigations are based on the traditional usage of natural materials, which attracts pharmaceutical firms' interest due to their ease of use and low cost. Presently, a few natural-based active substances such as ipratropium bromide, theophylline, epinephrine, and sodium cromoglycate are available on the market for asthma treatment (Amaral-Machado et al., 2020).

Lung Cancer

Lung cancer is among the biggest killers globally. It originates in lung tissues due to uncontrolled cellular proliferation and when unaddressed, it has the potential to invade beyond the lung.

According to the most recent GLOBOCAN figures, 2,094,000 new cases of lung cancer were discerned worldwide in 2018, making lung cancer the top driver of cancer death. Lung cancer

is predicted to affect 1,369,000 people and is the second most prevalent cancer in males, behind prostate cancer, and the most frequent cancer in women. With 725,000 cases, it is the second most frequent malignancy in women after breast cancer cases (Thandra et al., 2021).

The huge majority of lung cancers, referred to as primary lung cancers, are epithelial-derived carcinomas and classified into two types.

a) Small-cell lung carcinoma (SCLC)

b) Non-small-cell lung carcinoma (NSCLC)

Treatment for NSCLC.

NSCLC may be treated in five different ways:

Surgery, Radiation therapy, Chemotherapy, Adjuvant therapy and therapy that is specific to the patient ie , Immunotherapy. The kind and stage of cancer, as well as other characteristics, influence therapeutic strategies (Indini et al., 2020).

Surgery

Surgery is often performed if the tumor is reselectable.(Thai et al., 2021) Stage I, II and IIIA NSCLC patient often undergo surgery (Howington et al., 2013).

Adjuvant

Adjuvant therapy may help certain individuals who have had lung cancer resection surgery minimize their chance of recurrence.(Pennell et al., 2019) Radiation, chemotherapy, and targeted therapy are examples of adjuvant therapy (Zhong et al., 2018).

Chemotherapy

Approximately 40% of lung cancer patients who are newly diagnosed are in stage IV. The purpose of treatment for these individuals is to increase survival while reducing disease-related complications. The first-line treatment for stage IV NSCLC is cytotoxic combination chemotherapy with a platinum compound (cisplatin or carboplatin) along with paclitaxel, gemcitabine, docetaxel, vinorelbine, irinotecan (Felip et al., 2010).

Radiotherapy

In radiotherapy, high-energy photons are used to disrupt the DNA of cancer cells, causing them to perish. Those patients whose cancer has metastasised are ideal candidate for radiotherapy (Vinod & Hau, 2020).

Immunotherapy

The FDA authorised the first immunotherapy to treat a subgroup of lung cancer patients in 2015. Immunotherapy is a type of treatment that uses a person's own immune system to assist the body eradicate or control cancer. Recent clinical trials using immunotherapy, either alone or in combination with other treatments, have shown significant patient progress, prompting the FDA to approve several other immunotherapy options for more lung cancer patients, including approvals to use immunotherapy as a first-line therapy instead of conventional treatment (Thai et al., 2021).

Early-stage lung cancer treatment (stage I and Stage II)

Stage I NSCLC patients have a 60%–80% five-year survival rate following surgical resection, while stage II NSCLC patients have a 30%–50% five-year survival rate. Primary

radiation, can be utilised for patients who refuse surgical resection or who have unresectable tumours. For stage I and II patients, regrettably, post-surgery radiation is not advised. Adjuvant platinum-based chemotherapy is said to be successful in patients with stage II NSCLC, and it is the recommended therapeutic option for those who have had their tumor completely excised (Howington et al., 2013).

Stage III Lung Cancer Treatment

In individuals with resectable stage IIIA NSCLC, conventional treatment involves surgery followed by chemotherapy. Adjuvant chemotherapy has been demonstrated to enhance control of resected stage IIIA-N2 illness in clinical studies. Adjuvant radiation treatment has also been proven to improve control of resected stage IIIA-N2 disease in clinical studies. Neoadjuvant chemotherapy improves five-year survival by 5% to 6%, according to meta-analyses of several clinical studies (Yang et al., 2020).

Phytochemicals in cancer treatment

Over many years, natural products have been employed extensively as lead molecules for anticancer treatments. Since 1940 till date over fifty % of the anticancer drug belong to the plant origin. Alkaloids, terpenoids, organosulfur compounds, polyphenols are plentiful in many plant-based foods which are taken in regular diet. These plant-derived compounds have been linked to a variety of anticancer effects, including antioxidant, antiproliferative, proapoptotic, antiangiogenic, antimetastatic, and anti-inflammatory properties. Furthermore, the safety profile of these substances has been established as a result of their long-term dietary intake (Li et al., 2022). Vinca, taxane , camptothecin , and epipodophyllotoxin are examples of plant-derived anticancer agents. Other examples are combretastatins,

homoharringtonine (omacetaxine mepesuccinate, cephalotaxine alkaloid), and ingenol mebutates,

Co-Therapy of Drugs

Integrating the benefits of traditional and contemporary medicine has previously been proposed as a viable way to discovering and bringing novel plant-based drugs. The synergistic or additive effects of chemotherapeutic drug and phytochemical molecule combinations in cancer cells has tolerable side effects (Chen et al., 2020). Thus, due to their low toxicity in normal cells but dramatic effects in malignant cells, phytochemicals' anticancer and chemopreventive qualities have piqued the interest of oncology researchers in recent years (Yu et al., 2012).

When cancer drugs are taken concurrently, they are most efficacious. The goal of combination therapy is to combine medications that function through diverse pathways, reducing the chances of cancer cells developing resistance. When several drugs with varying impacts are combined, each drug can be taken at its optimal dose without generating overly severe adverse effects. Patients with advanced tumours who are not candidates for radiation therapy or surgery for example, people with non–small cell lung cancer, esophageal cancer, or bladder cancer that cannot be entirely removed by surgery may benefit from combination medication therapy.

Nano formulation of natural product

Nanotherapeutics have shown potential in circumventing the constraints of traditional drug delivery systems. It has been observed that natural product based nanoformulations have greater accessibility and reduced toxicity (Li et al., 2022). Nanoparticles can selectively target tumour cells, increasing the specificity and efficacy of cancer therapy modalities and,

as a result, improving patient response and survival. The combination of ethnomedicine with nanotechnology in the therapeutic context may improve patients' pharmaceutical responses and clinical outcomes.

Nano formulations based on polymers

Plant-derived natural compounds can be delivered using polymer-based nanomaterials .

When made from biocompatible and biodegradable polymers, can be utilised to regulate the release and delivery of bioactive substances. Natural polymers (alginate and chitosan) and synthetic polymers (for example, polyvinyl alcohol, poly [L-lactic acid], polyethylene glycol [PEG], and poly [lactic-co-glycolic acid]) are commonly utilised in the fabrication of polymer-based nanoparticles (Kamaly et al., 2016).

Nano formulations using inorganic materials

Plant-based natural compounds can be administered utilising very stable, hydrophilic, and biocompatible inorganic nanoparticles. They provide regulated medication delivery while simultaneously preventing stomach acid and enzyme breakdown. Aqueous colloid solutions containing inorganic nanoparticles such as gold, silver, and zinc oxide are employed for delivering bioactive molecules (Kim & Hyeon, 2014).

Chrysin

Chrysin (5,7 dihydroxyflavone) found abundantly in propolis, passion flower,honey has demonstrated anticancer (Phan et al., 2011), (Anari et al., 2016) anti-asthmatic and plethora of other disease alleviating properties. However, due to its low oral bioavailability, its medicinal uses have been limited. Its severe first-pass metabolism is the primary cause of its low bioavailability. Plenty of research have been undertaken to improve its pharmacokinetics and investigate the potential targets for its mechanism of action.

REFERENCES

Amaral-Machado, L., Oliveira, W. N., Moreira-Oliveira, S. S., Pereira, D. T., Alencar, É. N., Tsapis, N., & Egito, E. S. T. (2020). Use of Natural Products in Asthma Treatment. *Evidence-Based Complementary and Alternative Medicine*, *2020*, 1–35. https://doi.org/10.1155/2020/1021258

Anari, E., Akbarzadeh, A., & Zarghami, N. (2016). Chrysin-loaded PLGA-PEG nanoparticles designed for enhanced effect on the breast cancer cell line. *Artificial Cells, Nanomedicine and Biotechnology*, *44*(6), 1410–1416. https://doi.org/10.3109/21691401.2015.1029633

Chen, Y. J., Wang, Z. W., Lu, T. L., Gomez, C. B., Fang, H. W., Wei, Y., & Tseng, C. L. (2020). The Synergistic Anticancer Effect of Dual Drug- (Cisplatin/Epigallocatechin Gallate) Loaded Gelatin Nanoparticles for Lung Cancer Treatment. *Journal of Nanomaterials*, *2020*. https://doi.org/10.1155/2020/9181549

Enilari, O., & Sinha, S. (2019). The global impact of asthma in adult populatio. In *Annals of Global Health* (Vol. 85, Issue 1, pp. 1–7). Ubiquity Press. https://doi.org/10.5334/aogh.2412

Felip, E., Rosell, R., Maestre, J. A., Rodríguez-Paniagua, J. M., Morán, T., Astudillo, J., Alonso, G., Borro, J. M., González-Larriba, J. L., Torres, A., Camps, C., Guijarro, R., Isla, D., Aguiló, R., Alberola, V., Padilla, J., Sánchez-Palencia, A., Sánchez, J. J., Hermosilla, E., & Massuti, B. (2010). Preoperative Chemotherapy Plus Surgery Versus Surgery Plus Adjuvant Chemotherapy Versus Surgery Alone in Early-Stage Non–Small-Cell Lung Cancer. *Journal of Clinical Oncology*, *28*(19), 3138–3145. https://doi.org/10.1200/JCO.2009.27.6204

Howington, J. A., Blum, M. G., Chang, A. C., Balekian, A. A., & Murthy, S. C. (2013). Treatment of Stage I and II Non-small Cell Lung Cancer. *Chest*, *143*(5), e278S-e313S. https://doi.org/10.1378/chest.12-2359

Indini, A., Rijavec, E., Bareggi, C., & Grossi, F. (2020). Novel treatment strategies for early-stage lung cancer: the oncologist's perspective. *Journal of Thoracic Disease*, *12*(6), 3390–3398. https://doi.org/10.21037/jtd.2020.02.46

Kamaly, N., Yameen, B., Wu, J., & Farokhzad, O. C. (2016). Degradable controlled-release polymers and polymeric nanoparticles: Mechanisms of controlling drug release. In *Chemical Reviews* (Vol. 116, Issue 4, pp. 2602–2663). American Chemical Society. https://doi.org/10.1021/acs.chemrev.5b00346

Kim, T., & Hyeon, T. (2014). Applications of inorganic nanoparticles as therapeutic agents. *Nanotechnology*, *25*(1), 012001. https://doi.org/10.1088/0957-4484/25/1/012001

Li, Z., Zhao, T., Li, J., Yu, Q., Feng, Y., Xie, Y., & Sun, P. (2022). Nanomedicine Based on Natural Products: Improving Clinical Application Potential. In *Journal of Nanomaterials* (Vol. 2022). Hindawi Limited. https://doi.org/10.1155/2022/3066613

Loftus, P. A., & Wise, S. K. (2015). Epidemiology and economic burden of asthma. In *International Forum of Allergy and Rhinology* (Vol. 5, pp. S7–S10). John Wiley and Sons Inc. https://doi.org/10.1002/alr.21547

Marandi, Y., Farahi, N., & Hashjin, G. S. (2013). Asthma: Beyond corticosteroid treatment. *Archives of Medical Science*, *9*(3), 521–526. https://doi.org/10.5114/aoms.2013.33179

Newman, D. J., & Cragg, G. M. (2012). Natural products as sources of new drugs over the 30 years from 1981 to 2010. In *Journal of Natural Products* (Vol. 75, Issue 3, pp. 311–335). https://doi.org/10.1021/np200906s

Park, H. S., Kim, S. R., Kim, J. O., & Lee, Y. C. (2010). The roles of phytochemicals in bronchial asthma. *Molecules*, *15*(10), 6810–6834. https://doi.org/10.3390/molecules15106810

Pennell, N. A., Neal, J. W., Chaft, J. E., Azzoli, C. G., Jänne, P. A., Govindan, R., Evans, T. L., Costa, D. B., Wakelee, H. A., Heist, R. S., Shapiro, M. A., Muzikansky, A., Murthy, S., Lanuti, M., Rusch, V. W., Kris, M. G., & Sequist, L. v. (2019). SELECT: A Phase II Trial of Adjuvant Erlotinib in Patients With Resected Epidermal Growth Factor Receptor–Mutant Non–Small-Cell Lung Cancer. *Journal of Clinical Oncology*, *37*(2), 97–104. https://doi.org/10.1200/JCO.18.00131

Phan, T. A., Yu, X. M., Kunnimalaiyaan, M., & Chen, H. (2011). Antiproliferative effect of chrysin on anaplastic thyroid cancer. *Journal of Surgical Research*, *170*(1), 84–88. https://doi.org/10.1016/j.jss.2011.03.064

Reddel, H. K., FitzGerald, J. M., Bateman, E. D., Bacharier, L. B., Becker, A., Brusselle, G., Buhl, R., Cruz, A. A., Fleming, L., Inoue, H., Ko, F. W. S., Krishnan, J. A., Levy, M. L., Lin, J., Pedersen, S. E., Sheikh, A., Yorgancioglu, A., & Boulet, L. P. (2019). GINA 2019: a fundamental change in asthma management: Treatment of asthma with short-acting bronchodilators alone is no longer recommended for adults and adolescents. In *The European respiratory journal* (Vol. 53, Issue 6). NLM (Medline). https://doi.org/10.1183/13993003.01046-2019

Thai, A. A., Solomon, B. J., Sequist, L. v, Gainor, J. F., & Heist, R. S. (2021). Lung cancer. *The Lancet*, *398*(10299), 535–554. https://doi.org/10.1016/S0140-6736(21)00312-3

Thandra, K. C., Barsouk, A., Saginala, K., Aluru, J. S., & Barsouk, A. (2021). Epidemiology of lung cancer. In *Wspolczesna Onkologia* (Vol. 25, Issue 1, pp. 45–52). Termedia Publishing House Ltd. https://doi.org/10.5114/wo.2021.103829

Vinod, S. K., & Hau, E. (2020). Radiotherapy treatment for lung cancer: Current status and future directions. *Respirology*, *25*(S2), 61–71. https://doi.org/10.1111/resp.13870

Yang, Z.-R., Liu, M.-N., Yu, J.-H., Yang, Y.-H., Chen, T.-X., Han, Y.-C., Zhu, L., Zhao, J.-K., Fu, X.-L., & Cai, X.-W. (2020). Treatment of stage III non-small cell lung cancer in the era of immunotherapy: pathological complete response to neoadjuvant pembrolizumab and chemotherapy. *Translational Lung Cancer Research*, *9*(5), 2059–2073. https://doi.org/10.21037/tlcr-20-896

Yu, Y. L., Su, K. J., Chen, C. J., Wei, C. W., Lin, C. J., Yiang, G. T., Lin, S. Z., Harn, H. J., & Chen, Y. L. S. (2012). Synergistic anti-tumor activity of isochaihulactone and paclitaxel on human lung cancer cells. *Journal of Cellular Physiology*, *227*(1), 213–222. https://doi.org/10.1002/jcp.22719

Zhong, W.-Z., Wang, Q., Mao, W.-M., Xu, S.-T., Wu, L., Shen, Y., Liu, Y.-Y., Chen, C., Cheng, Y., Xu, L., Wang, J., Fei, K., Li, X.-F., Li, J., Huang, C., Liu, Z.-D., Xu, S., Chen, K.-N., Xu, S.-D., … Shi, J.-H. (2018). Gefitinib versus vinorelbine plus cisplatin as adjuvant treatment for stage II–IIIA (N1–N2) EGFR-mutant NSCLC (ADJUVANT/CTONG1104): a randomised, open-label, phase 3 study. *The Lancet Oncology*, *19*(1), 139–148. https://doi.org/10.1016/S1470-2045(17)30729

CHAPTER 2

LITERATURE REVIEW

LITERATURE REVIEW

Nature has always functioned as a shining example of the remarkable dynamics of synergy. Nature's biotic and abiotic elements are all inextricably linked. Plants are extremely vital for mankind to maintain their basic lifestyle providing all fundamental necessities of life (Petrovska et al., 2012). Minus the plants, the fate of human civilisation on this planet would be questionable. Medicinal herbs are becoming more and more popular each day. Roughly 80% of individuals in developing nations continue to rely on traditional methods for their primary healthcare (Karunamoorthi et al., 2013). Traditional health care is greatly strived after due to the exorbitant cost of Western drugs and health care.

The widespread usage of synthetic medications is linked to a gradual deterioration of the body's resistance mechanisms, whilst plants have an edge in terms of protracted human use. Bioactive component derived from plants that are non-hazardous are safe for prolonged use. The application of natural products may be traced all the way back to ancient Mesopotamia. India is haven to a multitude of medicinal plants that are employed in traditional medicine. Approximately 20,000 medicinal plants were recently been recognized in India, however well over 500 traditional populations mostly use roughly 800 medicinal plants to treat various maladies (Pandey et al., 2013). Presently, natural products account for more than half of all pharmaceuticals sold in the globe.

Inflammation has been associated to the onset or progression of a number of non-infectious disorders. As a result of tissue injury and genetic changes generated by continual low-grade inflammation in and around the affected tissue or organ, a variety of chronic ailments such as cancer, diabetes, asthma, cardiovascular problems, autoimmune diseases, and neurodegenerative disorders occur (Hunter, 2012). Conventional medicines for those kinds of chronic disorders can have more detrimental side effects than the disease itself, necessitating

the development of safer, lesser hazardous, and far more cost-effective medical interventions for patients. Flavonoids and their formulations have been implemented to cure myriad of disorders for centuries, and their use has perpetuated through the years (Cazarolli et al., 2008) (Tungmunnithum et al., 2018).

Chrysin

Chrysin (CHR) is a therapeutically active flavonoid found in a variety of plants, honey, and propolis. It, like all the other flavonoids, has a wide range of pharmacological actions, including anti-asthmatic, anti-diabetic, anti-inflammatory, antioxidant, antihypertensive, and anticancer properties. The IUPAC designations for CHR is 5,7-dihydroxyflavone (Mehdi et al., 2018).

Sources

In 1949, Gösta Linstedt of the KTH Royal Institute of Technology extracted Chrysin from the bark of pine trees (*Pinus spp.)* (Stockholm).CHR is a flavone found naturally in honey, propolis. It is also available from medicinal bitter melon, wild Himalayan pear but more abundantly from passion fruit (*Passiflora sp*.), honey, and propolis. *Radix scutellariae*, a well-known medicinal plant, is mostly made up of chrysin and its derivatives. The presence of chrysin has also been confirmed in walnut pellicles and flowers, and the foliage and fruits of doum palms (*Hyphaene thebaica*), *Chaetomium globosum*, which is an endophytic fungus (Mani & Natesan, 2018).

Chemical structure of Chrysin

CHR is a dihydroxyflavone with the hydroxyl groups (5-OH and 7-OH positions) attached to the aromatic ring. The chemical formula is C15H10O4, and a molar mass of 254.241 gmol1. Based on its structural categorization, CHR is classed as a flavone. CHR's structure includes two benzene rings. It also has one oxygen-containing heterocyclic ring. It has 2–3 carbon

double bond and a carbonyl group is attached to the fourth carbon. The fifth and seventh carbon atoms likewise have –OH groups. In one of the benzene rings CHR has no oxygenation, unlike other flavonoids (Siddiqui et al., 2018).

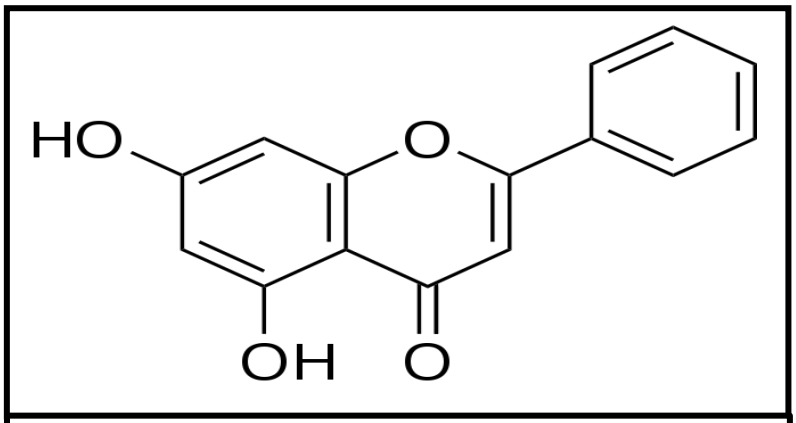

Chemical structure of Chrysin

Biological activity of chrysin

Between all of CHR's therapeutic properties, anticancer quality is universally acknowledged. It functions by inducing apoptosis and inhibiting cancer cell migration. Its anticancer activities have been demonstrated for a variety of tumours. Reports of activity on lung cancer (Samarghandian et al., 2014), thyroid cancer (Phan et al., 2011), breast cancer (Anari et al., 2016a), melanoma (Tavakoli et al., 2018) are numerous.

CHR exerts antiviral effects against different viruses like influenza virus, human rhino virus etc (Liu et al., 2022). CHR also possesses antiallergic property by impacting airway inflammation in vivo studies. It also reduced overall IgE levels in blood as well as the total number of inflammatory cells and eosinophils in BAL fluid in several reports (Du et al., 2012). CHR has also been reported to have effect on bleomycin induced lung fibrosis (Kseibati et al., 2020).

CHR benefits the liver by shielding the cells from hazardous chemicals (Hermenean et al., 2017). It also protects against hepatic necrosis. CHR reduced the levels of liver enzyme that had previously been elevated by d-galactosamine administration in research reported by (Pushpavalli et al., 2010).

CHR controls neurogenesis in memory loss that happens in aged person. CHR also showed neuroprotective impact on neuronal cells that have been treated with diclofenac. CHR may be used to treat neuronal disorders such as Parkinson's disease in near future (Nabavi et al., 2015).

Nanotechnology

Nanotechnology is harnessing of materials unique features at nanoscale. Nanotechnology refers to materials and technologies with structure and function suitable for tiny scales ranging from nanometers (10^{-9} m) to micrometres (10^{-6}m). Object attributes are defined at about this level, just above the size of a single atom. As a result, both artificial and biological systems are related to nanoscale events. The significant portion of fundamental biological macromolecules and cells are the same size as nanomaterials. A standard carbon-carbon bond, for example, is between 0.12 and 0.15 nanometers long; the diameter of a DNA double-helix is roughly 2 nanometers; and the tiniest cellular life form, Mycoplasma bacterium, is around 200 nanometers long (Kargozar & Mozafari, 2018).

Nanomedicine is the implementation of nanotechnology in medicine and healthcare, and it has been utilised to address some of the most prevalent ailments, such as cardiovascular disease and cancer. The implementation of nanotechnologies in medicine and healthcare is referred to as nanomedicine (Gökçay & Arda, n.d.). Nanomedicine is the use of nanotechnology in medicine, defined as the use of nanoparticles for medical diagnosis, monitoring, control, prevention, and therapy (Tinkle et al., 2014). Conversely, numerous scientific and international regulatory organisations have questioned the idea of nanomaterial. Nanomaterials have distinct

physicochemical traits that differ from their bulk chemical counterparts due to their microscopic scale, and various attempts have been made to develop a consensual definition. These qualities significantly broaden the spectrum of possibilities in pharmaceutical research, yet, specific safety concerns have arisen. Nanotechnology has noteworthy prospects in medicine and have integrated treatment of a wide range of diseases such as cardiovascular disease, cancer, diabetes, infectious disease etc.

Nanoparticles and Bioavailability

As previously stated, bioavailability refers to the percentage of a bioactive substance that enters systemic circulation and performs functions in the body. Blood plasma levels must be measured in order to evaluate bioavailability. There are endless studies linked with phytochemicals demonstrating their efficacy and safety but the bioavailability is unknown. Many factors such as hydrophobicity, poor stability influence the bioavailability of various nutraceuticals, including dosage, possible interactions with the food matrix, such as protein and fibres, the hydrophobicity of the compound, low chemical stability, intestinal first-pass metabolism. The physicochemical characteristics of nanoparticles can have a major impact on therapeutic bioavailability.

Chrysin nanoparticles

Drug delivery systems for CHR employing liposomes, micelles, and nanoparticles as carriers have been reported. To the best of our knowledge, the greatest strategy to overwhelm the poor bioavailability of CHR was regarding the attempts to encapsulate chrysin in nanoparticles. Some of the reports are mentioned herewith. CHR-loaded nanostructured lipid carriers (NLCs) could affect apoptosis in MCF-7 cancer cells by inhibiting the Nrf2 pathway. Loading with PLGA-PEG nanoparticles elevated the solubility and cytotoxicity of CHR, and reduced its toxic effects in the breast cancer cell line (T47D) (Anari et al., 2016b). CHR chitosan

nanoparticles was also predicted to useful in cancer by inhibiting mitochondrial complex II (Ragab et al., 2022).

Nanotechnology in drug - delivery systems for respiratory disorders

The incidence of respiratory disorders is escalating attributed to increasing levels of air pollution, frequent episodes of microbial infections, notably in vulnerable populations with weakened immune systems. Respiratory diseases claim the lives of almost 4,000,000 individuals every year all throughout world. Lung cancer and allergic asthma are the most common respiratory illnesses. Despite advances in diagnostic and therapeutic tools, effective treatment of severe and chronic illness remains a challenge. Furthermore, most medications have difficulty reaching the lower respiratory tract with a sufficient dosage and minimal adverse effects. As a result, there is an urgent need to improve treatment quality in an efficient and cost-effective manner.

Cancer therapy and nanotechnology

Conventional cancer medicines have the propensity to impair healthy tissue while seeking to undermine malignant cells. Scientists are now developing nanotechnology-based treatments to circumvent this constraint and improve the chances of survival in a variety of cancer types.

How Nanotechnology Aids Cancer Treatment

By directing medications to selectively target cancer cells, nanotechnology improves chemotherapy and decreases its side effects. It also improves the precision of surgical tumour excision and increases the efficacy of radiotherapies and other existing therapeutic options. As a result, the patient is at lower danger and has a better chance of surviving.

Scientists are creating innovative treatments using recently formulated nanoparticles with novel features that can be used in medical research. Nanoparticles, despite their microscopic

size can contain minuscule medicinal molecules. Nanoparticles' relatively enormous surface area allows them to be ornamented with ligands, DNA and RNA strands, peptides, or antibodies. These 'add-ons' provide the nanoparticle with extra functionality that boosts the therapeutic impact or aids in the targeting of a nanoparticle (Zhang et al., 2019).

Nanoparticles with sizes ranging from 10 to 100 nm are often utilised in cancer treatment since they may transport drugs efficiently while also improving permeability and retention (EPR). Smaller particles (less than 1–2 nm) can readily leak through normal vasculature and be filtered by kidneys (less than 10 nm in diameter) whereas particles larger than 100 nm are more likely to be removed from circulation by phagocytes (Decuzzi et al., 2009). Additionally, the bioavailability and half-life of NPs may be influenced by their surface characteristics.

When compared to standard therapeutics, NPs of different sorts, including organic and inorganic NPs are vastly used in the treatment of many cancer types. NP-based drug delivery systems outperform traditional therapies in terms of pharmacokinetics, biocompatibility, tumour targeting, and stability, while also reducing systemic toxicity and overcoming drug resistance. NP-based drugs can be widely employed in chemotherapy, targeted treatment, radiation, hyperthermia, and gene therapy because of these advantages. Nanocarrier delivery technologies also provide improved platforms for combination treatment. By addressing several aspects with dual-drug loading, enhancing specificity with triggered release, and eliminating malignant cells with physical modalities, nano formulations can overcome resistance mechanisms.

Nanoscale carriers can traverse tumour endothelium and passively collect in tumours. Furthermore, nanomaterials have distinct physicochemical features that are used in very sensitive diagnostic procedures, enabling for early cancer identification and improved patient prognosis. Cancer diagnostics are gradually shifting away from invasive, complex procedures

and toward very sensitive point-of-care liquid biopsies, where nanomaterials have proven to be extremely useful for biomarker identification. Certain features also allow for significant advancements in imaging techniques used for surgical guiding and tumour monitoring, allowing for very targeted surgical procedures.

Tumour intricacy, diversity, and heterogeneity severely constrain treatment's therapeutic potential. As a result, the current clinical research trend has steadily evolved from a focus on monotherapy to a focus on combination therapy for improved therapeutic efficacy. More crucially, coordinated enhanced interactions amongst forms of monotherapy lead to the emergence of multimodal synergistic treatment, resulting in exceptional super additive (i.e., "1 + 1 > 2") benefits that outperform any single therapy or their putative combination (Parashar et al., 2019).

Asthma therapy and nanotechnology

Nanoparticles (NPs) are regarded to have several advantages over standard treatments for the respiratory system, including homogeneous drug distribution, enhanced solubility or dissolution rate, longer release, macromolecule delivery, and appropriate cell internalisation.

Therapeutic agents such as nano-modified anti-asthma drugs, can be delivered through nanomedicine. The precise delivery of drugs to the lungs looks to be a potential treatment strategy. To put it differently, the lungs' distinctive architectural form, which includes characteristics such as a thin epithelial barrier with a large alveolar-region surface area, as well as a high degree of vascularization and low proteolytic activity, contributes to this.

Many researchers are now developing innovative drug delivery systems for asthma in order to minimise dose frequency and drug-related toxicity (L. Wang et al., 2019).

(Patil-Gadhe et al., 2014) demonstrated that a nanostructured lipid carrier containing montelukast circumvented hepatic metabolism, lowering hepatobiliary toxicity and thereby increasing the drug's therapeutic value.

(Oyarzun-Ampuero et al., 2011) synthesized chitosan–hyaluronic acid nanoparticles coated with heparin for asthma therapy.

(Dhayanandamoorthy et al., 2020) produced an aerosolized, ferulic acid-loaded chitosan nanoparticle using a vibrating mesh nebulizer as a strategic combination of drug, nanocarrier, and delivery mechanism for effective asthma therapy.

PEG-PLGA nanoparticles encapsulating bavachinin were tested in a mouse model of asthma treatment caused by OVA sensitization. These NPs demonstrated extremely strong anti-asthmatic therapeutic benefits in a mouse allergic asthma model when administered orally (K. Wang et al., 2018).

(Casula et al., 2021) developed a multicomponent formulation for water-based nanosuspension administration of curcumin (CUR) and beclomethasone dipropionate (BDP) into the lungs.

Polymeric nanoparticles

Polymeric nanoparticles emerge out as an imperative tool for improving drug bioavailability or site-specific delivery. Polymers biocompatibility and biodegradability makes them potentially suitable as carrier. Various polymers are used to construct various types of carriers for drug delivery (Bennet & Kim, 2014).

Poly (D, L-lactic-co-glycolic acid) and polymeric nanoparticles (PLGA)

PLGA is one of the favoured materials for producing nanoparticles. This biodegradable polymer hydrolyses into metabolite monomers, lactic acid and glycolic acid, in the body after systemic absorption (Acharya & Sahoo, 2011). PLGA is a biocompatible polymer that has been approved for use in injectable formulations by the US Food and Drug Administration (USFDA) and the European Medicines Agency (EMA). This polymer offers a diverse variety of produced nanoparticle, including drug molecules or biological molecules that are entrapped or conjugated with the nanoparticles.

Chemistry of PLGA

PLGA is a linear copolymer that may be comprised of two monomers: Lactic acid with glycolic acid.

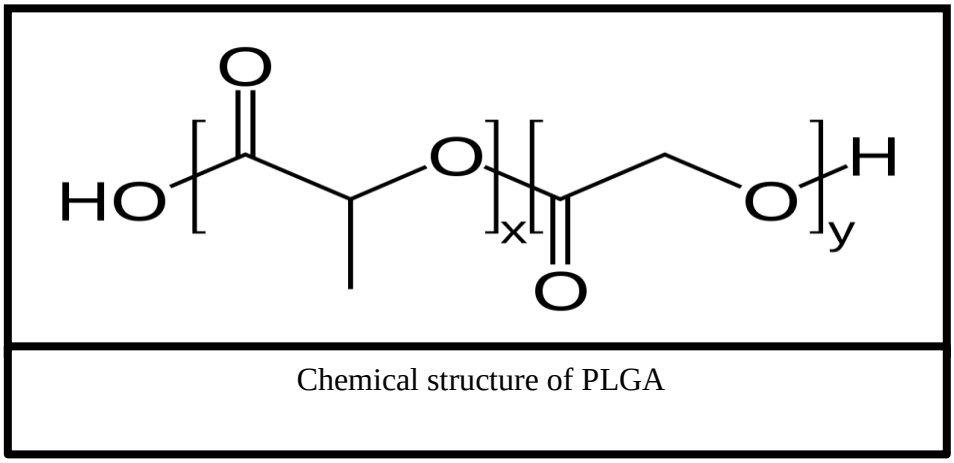

Chemical structure of PLGA

Varieties of PLGA

Different kinds of PLGA can be manufactured by varying the ratio of lactide and glycolide monomers. Some instances are PLGA 50:50 , PLGA 65:35, PLGA 75:25, and PLGA 85:15.

Gold nanoparticles

Noble metal nanoparticles are becoming incredibly popular. Gold nanoparticles (AuNPs) have piqued the interest of scientists, who are investigating their various properties and possible applications, bioimaging, cancer therapy etc (Madkour, 2018).

Gold (Au) was unearthed as one of the first metals thousands of years ago. Au and its complexes have been used in medicine for a long time. Colloidal gold nanoparticles suspended in a liquid was first referenced in ancient Chinese, Arabian, and Indian records from the V–IV centuries BC, where it was advised for the treatment of a variety of ailments despite the fact that the mechanism of action was unknown. Throughout the Middle Ages, alchemists investigated colloidal gold extensively, and it was used to cure mental illnesses, syphilis, diarrhoea, and was even promoted as a lifespan elixir.

Gold nanoparticles(AuNP) are of tremendous interest for therapeutic applications, particularly anticancer treatment, due to their unique features. Depending on the intended use, a variety of synthetic processes can be used to create nanogold particles with appropriate architecture and properties. At the moment, nanoparticle functionalization is a major focus of study, with great progress being made toward the development of biocompatible, multifunctional particles for use in cancer detection and therapy. AuNPs are being researched as potential drug delivery agents for medicine administration into tumour cells in the field of oncology therapy (Sardar et al., 2009).

REFERENCES

Acharya, S., & Sahoo, S. K. (2011). PLGA nanoparticles containing various anticancer agents and tumour delivery by EPR effect. *Advanced Drug Delivery Reviews*, *63*(3), 170–183. https://doi.org/10.1016/j.addr.2010.10.008

Anari, E., Akbarzadeh, A., & Zarghami, N. (2016a). Chrysin-loaded PLGA-PEG nanoparticles designed for enhanced effect on the breast cancer cell line. *Artificial Cells, Nanomedicine and Biotechnology*, *44*(6), 1410–1416. https://doi.org/10.3109/21691401.2015.1029633

Anari, E., Akbarzadeh, A., & Zarghami, N. (2016b). Chrysin-loaded PLGA-PEG nanoparticles designed for enhanced effect on the breast cancer cell line. *Artificial Cells, Nanomedicine and Biotechnology*, *44*(6), 1410–1416. https://doi.org/10.3109/21691401.2015.1029633

Bennet, D., & Kim, S. (2014). Polymer Nanoparticles for Smart Drug Delivery. In *Application of Nanotechnology in Drug Delivery*. InTech. https://doi.org/10.5772/58422

Casula, L., Lai, F., Pini, E., Valenti, D., Sinico, C., Cardia, M. C., Marceddu, S., Ailuno, G., & Fadda, A. M. (2021). Pulmonary Delivery of Curcumin and Beclomethasone Dipropionate in a Multicomponent Nanosuspension for the Treatment of Bronchial Asthma. *Pharmaceutics*, *13*(8), 1300. https://doi.org/10.3390/pharmaceutics13081300

Cazarolli, L., Zanatta, L., Alberton, E., Bonorino Figueiredo, M. S., Folador, P., Damazio, R., Pizzolatti, M., & Barreto Silva, F. R. (2008). Flavonoids: Prospective Drug Candidates. *Mini-Reviews in Medicinal Chemistry*, *8*(13), 1429–1440. https://doi.org/10.2174/138955708786369564

Decuzzi, P., Pasqualini, R., Arap, W., & Ferrari, M. (2009). Intravascular Delivery of Particulate Systems: Does Geometry Really Matter? *Pharmaceutical Research*, *26*(1), 235. https://doi.org/10.1007/s11095-008-9697-x

Dhayanandamoorthy, Y., Antoniraj, M. G., Kandregula, C. A. B., & Kandasamy, R. (2020). Aerosolized hyaluronic acid decorated, ferulic acid loaded chitosan nanoparticle: A promising asthma control strategy. *International Journal of Pharmaceutics*, *591*, 119958. https://doi.org/10.1016/j.ijpharm.2020.119958

Du, Q., Gu, X., Cai, J., Huang, M., & Su, M. (2012). Chrysin attenuates allergic airway inflammation by modulating the transcription factors T-bet and GATA-3 in mice. *Molecular Medicine Reports*, *6*(1), 100–104. https://doi.org/10.3892/mmr.2012.893

Gökçay, B., & Arda, B. (n.d.). *NANOTECHNOLOGY, NANOMEDICINE; ETHICAL ASPECTS WHAT IS NANOTECHNOLOGY AND NANOMEDICINE?*

Hermenean, A., Mariasiu, T., Navarro-González, I., Vegara-Meseguer, J., Miuțescu, E., Chakraborty, S., & Pérez-Sánchez, H. (2017). Hepatoprotective activity of chrysin is mediated through TNF-α in chemically-induced acute liver damage: An in vivo study and molecular modeling. *Experimental and Therapeutic Medicine*, *13*(5), 1671–1680. https://doi.org/10.3892/etm.2017.4181

Hunter, P. (2012). The inflammation theory of disease. *EMBO Reports*, *13*(11), 968–970. https://doi.org/10.1038/embor.2012.142

Kargozar, S., & Mozafari, M. (2018). Nanotechnology and Nanomedicine: Start small, think big. *Materials Today: Proceedings*, *5*(7), 15492–15500. https://doi.org/10.1016/j.matpr.2018.04.155

Karunamoorthi, K., Jegajeevanram, K., Vijayalakshmi, J., & Mengistie, E. (2013). Traditional Medicinal Plants. *Journal of Evidence-Based Complementary & Alternative Medicine*, *18*(1), 67–74. https://doi.org/10.1177/2156587212460241

Kseibati, M. O., Sharawy, M. H., & Salem, H. A. (2020). Chrysin mitigates bleomycin-induced pulmonary fibrosis in rats through regulating inflammation, oxidative stress, and hypoxia. *International Immunopharmacology*, *89*, 107011. https://doi.org/10.1016/j.intimp.2020.107011

Liu, Y., Song, X., Li, C., Hu, H., Li, W., Wang, L., Hu, J., Liao, C., Liang, H., He, Z., & Ye, L. (2022). Chrysin Ameliorates Influenza Virus Infection in the Upper Airways by Repressing Virus-Induced Cell Cycle Arrest and Mitochondria-Dependent Apoptosis. *Frontiers in Immunology*, *13*. https://doi.org/10.3389/fimmu.2022.872958

Madkour, L. H. (2018). Applications of gold nanoparticles in medicine and therapy. *Pharmacy & Pharmacology International Journal*, *6*(3). https://doi.org/10.15406/ppij.2018.06.00172

Mani, R., & Natesan, V. (2018). Chrysin: Sources, beneficial pharmacological activities, and molecular mechanism of action. *Phytochemistry*, *145*, 187–196. https://doi.org/10.1016/j.phytochem.2017.09.016

Mehdi, S. H., Nafees, S., Zafaryab, M., Khan, M. A., & Alam Rizvi, Md. M. (2018). Chrysin: A Promising Anticancer Agent its Current Trends and Future Perspectives. *European Journal of Experimental Biology*, *08*(03). https://doi.org/10.21767/2248-9215.100057

Nabavi, S. F., Braidy, N., Habtemariam, S., Orhan, I. E., Daglia, M., Manayi, A., Gortzi, O., & Nabavi, S. M. (2015). Neuroprotective effects of chrysin: From chemistry to medicine. *Neurochemistry International*, *90*, 224–231. https://doi.org/10.1016/j.neuint.2015.09.006

Oyarzun-Ampuero, F. A., Goycoolea, F. M., Torres, D., & Alonso, M. J. (2011). A new drug nanocarrier consisting of polyarginine and hyaluronic acid. *European Journal of Pharmaceutics and Biopharmaceutics*, *79*(1), 54–57. https://doi.org/10.1016/j.ejpb.2011.04.008

Pandey, M. M., Rastogi, S., & Rawat, A. K. S. (2013). Indian Traditional Ayurvedic System of Medicine and Nutritional Supplementation. *Evidence-Based Complementary and Alternative Medicine*, *2013*, 1–12. https://doi.org/10.1155/2013/376327

Parashar, P., Tripathi, C. B., Arya, M., Kanoujia, J., Singh, M., Yadav, A., Kaithwas, G., & Saraf, S. A. (2019). A synergistic approach for management of lung carcinoma through folic acid functionalized co-therapy of capsaicin and gefitinib nanoparticles: Enhanced apoptosis and metalloproteinase-9 down-regulation. *Phytomedicine*, *53*, 107–123. https://doi.org/10.1016/j.phymed.2018.09.013

Patil-Gadhe, A., Kyadarkunte, A., Patole, M., & Pokharkar, V. (2014). Montelukast-loaded nanostructured lipid carriers: Part II Pulmonary drug delivery and in vitro–in vivo aerosol performance. *European Journal of Pharmaceutics and Biopharmaceutics*, *88*(1), 169–177. https://doi.org/10.1016/j.ejpb.2014.07.007

Petrovska, B. (2012). Historical review of medicinal plants′ usage. *Pharmacognosy Reviews*, *6*(11), 1. https://doi.org/10.4103/0973-7847.95849

Phan, T. A., Yu, X. M., Kunnimalaiyaan, M., & Chen, H. (2011). Antiproliferative effect of chrysin on anaplastic thyroid cancer. *Journal of Surgical Research*, *170*(1), 84–88. https://doi.org/10.1016/j.jss.2011.03.064

Pushpavalli, G., Kalaiarasi, P., Veeramani, C., & Pugalendi, K. V. (2010). Effect of chrysin on hepatoprotective and antioxidant status in d-galactosamine-induced hepatitis in rats. *European Journal of Pharmacology*, *631*(1–3), 36–41. https://doi.org/10.1016/j.ejphar.2009.12.031

Ragab, E. M., el Gamal, D. M., Mohamed, T. M., & Khamis, A. A. (2022). Study of the inhibitory effects of chrysin and its nanoparticles on mitochondrial complex II subunit activities in normal mouse liver and human fibroblasts. *Journal of Genetic Engineering and Biotechnology*, *20*(1), 15. https://doi.org/10.1186/s43141-021-00286-0

Samarghandian, S., Nezhad, M., & Mohammadi, G. (2014). Role of Caspases, Bax and Bcl-2 in Chrysin-Induced Apoptosis in the A549 Human Lung Adenocarcinoma Epithelial Cells. *Anti-Cancer Agents in Medicinal Chemistry*, *14*(6), 901–909. https://doi.org/10.2174/1871520614666140209144042

Sardar, R., Funston, A. M., Mulvaney, P., & Murray, R. W. (2009). Gold Nanoparticles: Past, Present, and Future. *Langmuir*, *25*(24), 13840–13851. https://doi.org/10.1021/la9019475

Siddiqui, A., Akhtar, J., Uddin M.S., S., Khan, M. I., Khalid, M., & Ahmad, M. (2018). A Naturally Occurring Flavone (Chrysin): Chemistry, Occurrence, Pharmacokinetic, Toxicity, Molecular Targets and Medicinal Properties. *Journal of Biologically Active Products from Nature*, *8*(4), 208–227. https://doi.org/10.1080/22311866.2018.1498750

Tavakoli, F., Jahanban-Esfahlan, R., Seidi, K., Jabbari, M., Behzadi, R., Pilehvar-Soltanahmadi, Y., & Zarghami, N. (2018). Effects of nano-encapsulated curcumin-chrysin on telomerase, MMPs and TIMPs gene expression in mouse B16F10 melanoma tumour model. *Artificial Cells, Nanomedicine and Biotechnology*, *46*(sup2), 75–86. https://doi.org/10.1080/21691401.2018.1452021

Tinkle, S., McNeil, S. E., Mühlebach, S., Bawa, R., Borchard, G., Barenholz, Y. C., Tamarkin, L., & Desai, N. (2014). Nanomedicines: addressing the scientific and regulatory gap. *Annals of the New York Academy of Sciences*, *1313*(1), 35–56. https://doi.org/10.1111/nyas.12403

Tungmunnithum, D., Thongboonyou, A., Pholboon, A., & Yangsabai, A. (2018). Flavonoids and Other Phenolic Compounds from Medicinal Plants for Pharmaceutical and Medical Aspects: An Overview. *Medicines*, *5*(3), 93. https://doi.org/10.3390/medicines5030093

Wang, K., Feng, Y., Li, S., Li, W., Chen, X., Yi, R., Zhang, H., & Hong, Z. (2018). Oral delivery of bavachinin-loaded PEG-PLGA nanoparticles for asthma treatment in a murine

model. *Journal of Biomedical Nanotechnology*, *14*(10), 1806–1815. https://doi.org/10.1166/jbn.2018.2618

Wang, L., Feng, M., Li, Q., Qiu, C., & Chen, R. (2019). Advances in nanotechnology and asthma. *Annals of Translational Medicine*, *7*(8), 180–180. https://doi.org/10.21037/atm.2019.04.62

Zhang, Y., Li, M., Gao, X., Chen, Y., & Liu, T. (2019). Nanotechnology in cancer diagnosis: progress, challenges and opportunities. *Journal of Hematology & Oncology*, *12*(1), 137. https://doi.org/10.1186/s13045-019-0833-3;

CHAPTER 3

AIMS AND OBJECTIVE

Broad Objectives

- ❖ Synthesis and characterization of chrysin (CHR) nanoparticles to enhance its bioactivity.
- ❖ Evaluation of the therapeutic efficacy of the nano formulations in vitro and in vivo in different pulmonary inflammatory disease models.

Sub Objectives

- ➢ Synthesis of CHR loaded PLGA nanoparticle (CHR-NP) and its characterization.
- ➢ Evaluation of protective role of CHR-NP in OVA-induced murine allergic asthma model.
- ➢ Synthesis and characterization of CHR functionalized gold nanoparticle (CHR-AuNP).
- ➢ Exploration of cytotoxic activity of CHR-AuNP in combination with Paclitaxel (PTX) in A549 cell line in vitro.

Plan of study for CHR-NP

- Synthesis of CHR loaded PLGA (poly lactide glycolic acid) nanoparticle (CHR-NP) by solvent displacement technique.
- Assessment of possible interactions between the drug and any excipients used in the study by Fourier transform infrared spectroscopy (FTIR).
- Physio-chemical characterization as well as microscopic characterization of CHR-NP done by DLS, ZP, DSC, XRD, AFM, SEM, TEM.
- Determination of drug loading(DL) and entrapment efficiency(EE).
- In vitro release study in PBS (pH 7.4)
- In vitro cellular uptake study in A549 cells.

In vivo studies

- Establishment of a murine model of allergic asthma
- Determination of non-toxic dose of CHR-NP.
- Treatment of the different experimental group with the experimental drugs and standard drug Dexamethasone (DEX).
- Quantifying the inflammatory cells present in the different experimental group mice by Giemsa staining.
- Assesement of IgE in serum and Th2 cytokines in the BAL fluid.
- Lung histopathological studies by staining with HE, PAS and MT stain.
- Expression level of NF-κB, TLR2/4, NLRP3 pathway molecules via western blot and immunofluorescence.
- Statistical Analysis.

Plan of study for CHR-AuNP

- Synthesis of CHR functionalised gold nanoparticle (CHR-AuNP)
- Physico-chemical characterization of CHR-AuNP by FTIR, DLS, ZP, UV spectroscopy and microscopic characterization by AFM microscopy.
- Exploration of cytotoxic activity of CHR-AuNP in combination with PTX in A549 cell line in vitro by MTT assay.
- Combination effect determined by Compusyn software.
- Apoptotic studies performed by AO/EtBr dual staining of A549 cells and Annexin V assay.
- Reactive oxygen species (ROS) generation determination by flow cytometry and spectroflourimetry.

- Mitochondrial Membrane potential (MMP) determination by JC-1 assay and Rhodamine 123 by flow cytometry and spectroflourimetrically respectively.
- Cytochrome C level alteration determination via spectroflourimetry.
- Levels of activated Caspase-3 and Caspase-9 determination colorimetrically by ELISA kits.
- Changes in the level of pro- and anti-apoptotic proteins detection in A549 cells by western blot and immunofluorescence.
- Western Blot and immunofluorescence assay to detect the changes in the protein level of PPAR-Ɣ and molecules of PI3K-AKT pathway.
- Western Blot and immunofluorescence assay to detect the changes in the protein expression level of molecules involved in the Wnt / β catenin pathway.
- Statistical analysis.

CHAPTER 4

EXPLORATION OF ANTIASTHMATIC POTENTIAL OF CHRYSIN LOADED PLGA NANOPARTICLES

Background

Asthma is a multifaceted illness characterised by chronic inflammation of the airways, wheezing, shortness of breath, chest tightness, and dyspnoea caused by airway obstruction. (Bousquet et al., 2010)

In the early days of asthma treatment, the focus was on easing bronchoconstriction using a bronchodilator. However, the identification of airway inflammation as a critical pathophysiological factor was a game-changer and eventually led to the adoption of inhaled corticosteroids as the primary treatment option (Bousquet et al., 2000; Marandi et al., 2013).

In asthma, T helper-2 (Th2)-related responses are frequently linked to airway inflammation (Bousquet et al., 2000). Along with that eosinophil overproduction is seen, as is an increase in Th2 cytokine levels, particularly Interleukins (IL)-4 and IL-5, and IL-13 and IgE overproduction. Both IL-4 and IL-13 promote acute inflammatory responses(Nakajima & Takatsu, 2007).

The Global Asthma Initiative (GINA) (*Global Asthma Network The Global Asthma Report*, 2018)released updated asthma treatment guidelines, mandating the use of inhaled corticosteroids, as well as bronchodilators and leukotriene receptor antagonists. Existing medications must be improved in terms of side effect profiles or oral formulations, as well as the prevention of recurrence following treatment termination, which is common with corticosteroids. The use of phytochemicals particularly flavonoids which have inherent anti-inflammatory antioxidant properties have emerged out as alternate therapy (Park et al., 2010).

CHR (5,7 dihydroxflavone) is one such phytochemicals which has been discovered to have antiasthmatic qualities (Stompor-gorący et al., 2021).(Du et al., 2012) (Naz et al., 2019)However, its poor pharmacokinetics constrain its prospect. For the administration of hydrophobic pharmaceuticals such as CHR, a biodegradable carrier such as PLGA was used,

and its anti-asthmatic potential was investigated in a murine asthmatic model. The involvement of TLR receptors in detecting allergens (Kawai & Akira, 2011) (Salazar & Ghaemmaghami, 2013)and thereby activating NF-kB (Schuliga, 2015a) that is present downstream has been documented in the literature (Mogensen, 2009). It was also recently reported that the NLRP3 inflammasome is involved in the inflammation associated with allergic asthma (Peng et al., 2016), (Tran et al., 2012). Hence , in our work, we not only assessed CHR- NP's anti-asthmatic capability, but also its effect on the TLR/NF-κB /NLRP3 pathway.

Materials and Methods:

Chemical ingredients used in this study

S. No	Name	Source
1.	Acetone	Merck Life Science Pvt. Ltd, Bengaluru, India
2.	Alum	Sigma-Aldrich Co, St Louis, MO, USA
3.	Chrysin (CHR) (purity ≥ 97.0%),	Sigma-Aldrich Co, St Louis, MO, USA
4.	Dexamethasone (Dex)	Sigma-Aldrich Co, St Louis, MO, USA
5.	PLGA (85:15)	Sigma-Aldrich Co, St Louis, MO, USA
6.	Fluorescein isothiocyanate (FITC)	Sigma-Aldrich Co, St Louis, MO, USA
7.	Ovalbumin	Sigma-Aldrich Co, St Louis, MO, USA
8.	4,6 -diamidino-2-phenylindole (DAPI	Sigma-Aldrich Co, St Louis, MO, USA
9.	Fetal bovine serum (FBS	Sigma-Aldrich Co, St Louis, MO, USA
10.	Penicillin-Streptomycin	Hi Media Laboratories, Mumbai, India

11.	PVA	Merck Life Science Pvt. Ltd, Bengaluru, India
12.	Primary antibodies	Santa Cruz Biotechnology (Santa Cruz, CA)
8.	Secondary antibodies	Santa Cruz Biotechnology (Santa Cruz, CA)
9.	Serum alanine aminotransferase (ALT)	BioVision, Milpitas, CA, USA.
10.	Serum aspartate aminotransferase (AST)	BioVision, Milpitas, CA, USA.
11.	(ELISA) kits	R&D system (MN, USA).
12	OVA-specific Ig E ELISA kit	Cayman Chemical, Ann Arbor, MI, United States
13	A549 cell line	National Centre for Cell Science (Pune, India).

Animals

Male inbred BALB/C mice which were of age (6-8 weeks) were used for the in vivo experiments. The CSIR-IICB's Animal Ethics Committee (AEC) approved all testing protocols, which were carried out in accord with AEC standards. All animals were provided a regular meal and had access to plenty of water.

Methods

CHR-NP synthesis

The nanoprecipitation technique also known as the solvent displacement method was employed in our study to synthesize CHR-NP (Fessi et al., 1989a). The detailed process of the nanoparticle synthesis is discussed hereunder. Firstly, PLGA and CHR were commixed in

acetone (20ml) in a ratio (5:1) and probe sonicated to form a homogenous organic phase solution. The aqueous phase was established with PVA (1% W/V) dissolved in double distilled water. The PVA solution was kept under constant magnetic stirring in order to generate a clear transparent solution as the aqueous phase. The organic phase solution was then dropped into PVA solution while magnetic stirring was maintained consistently. The organic phase was thereafter dropwise added into 50 ml of PVA solution with unceased magnetic stirring. Following the addition of the organic phase into the aqueous phase, the solution was kept overnight to allow the evaporation of the acetone. The nanoparticles were then ultracentrifuged at 20,000 rpm for 30 minutes and washed twice to eliminate CHR from the surface of the nanoparticles. Thereafter, the nanoparticles were lyophilized, and the freeze-dried nanoparticles were kept at 4°C for future use.

CHR-NP physico-chemical characterization

FTIR studies, particle size analysis, surface charge analysis (ZP), surface morphology by TEM and AFM microscopy, drug encapsulation efficiency, drug release study, percentage drug loading, DSC, XRD , and cellular uptake effectiveness study were the varied methods manoeuvred to study and establish the proper formation of CHR-NP based on a physicochemical parameter.

Particle size measurement

The average diameter of the synthesized CHR-NP was enumerated using Dynamic light scattering (DLS) technique to determine the size of the nanoparticles. Malvern Zetasizer Nano ZS were used to determine particle size (Malvern Instruments, UK).

At a temperature of 25°C, the mean diameter value of the nanoparticles was obtained in 10 mm diameter cells at a 90° angle. To achieve an appropriate scattering intensity, all samples were

diluted with twofold distilled water before being assessed. The measurements were repeated thrice for an individual sample.

Surface Charge analysis:

Aggregation is regulated by the charge on the nanoparticles. The presence of a higher relative number of positive or negative charges repels each other, deterring aggregation.

Malvern Zetasizer 3000 was the instrument employed to measure the zeta potential (ZP). The ZP of freeze-dried materials was evaluated by dissolving them in distilled water.

Polydispersity index

The polydispersity index (PDI) was determined using Malvern Zetasizer 3000. Particles with a polydispersity index of less than 0.2 were deemed acceptable. It was computed using the formula PDI= D (0.9)-D (0.1)/ D (0.5).

D (0.9) represents the particle size that is more than 90% of the test sample. Similarly, D (0.5) and D (0.1) represents the particle size that is more than 50% and 10% of the test sample respectively,

Fourier transform infra-red spectroscopy (FTIR)

A FTIR study was carried out to investigate any potential interactions between the chosen excipients and the crude drug. The powdered freeze-dried samples were blended with KBr to produce pellets. CHR, PLGA, and CHR-NP IR spectra were recorded. The FT-IR spectrometer (Bruker). was used to record FT-IR spectra in the absorbance mode The existence of distinct groups was surmised from various peaks in the IR spectra.

Differential Scanning Calorimetry(DSC)

DSC scrutinise the physicochemical compatibility of drug and polymer. DSC was conducted with lyophilised test specimens CHR, PLGA, and CHR loaded PLGA (CHR-NP). The thermograms were acquired on a differential scanning calorimeter (Q2000 model, TA equipment). The heating rate was kept at 5^{o}C/min and temperature range was kept in between 0 to 290 during performing this experiment.

X-Ray Diffraction (XRD)

The crystalline or amorphous state of CHR in CHR-NP was determined using X-ray diffraction (XRD). XRD analysis was conducted on crude CHR, freeze-dried CHR-NPs, and PLGA. In a X-ray diffractometer (Bruker D8 ADVANCE SWAX Diffractometer) calibrated with 40kV voltage and 40mA current and standardised by nickel filter Cu K α(=0.15406nm) radiation the diffraction angle 2θ of all the samples was recorded.

Transmission Electron Microscopy with High Resolution (HR-TEM)

The size and structure of the manufactured CHR-NP were determined using transmission electron microscopic examination (TEM). A drop of CHR-NP solution was deposited on the carbon-coated copper grids and the sample was dried. After drying, the copper grid was put into the specimen holder. TEM images were acquired by evaluating the prepared grids using (HR-TEM) (Jeol, JEM 2100, Tokyo, Japan).

Drug loading and entrapment efficiency

CHR-NP was ultracentrifuged and the supernatant containing free CHR was collected. The free CHR in the supernatant was required to deduce the percentage drug loading and entrapment efficiency of CHR in CHR-NP. UV-visible spectrophotometer was used to determine drug loading and entrapment efficiency of CHR-NP (JASCO V-730, Spectrophotometer, Tokyo,

Japan) at 348 nm. Prior to measuring the amount of chrysin in CHR-NP, a standard calibration curve of CHR (10–100 g/ml) was plotted. The solvent used for plotting the standard curve was acetone. The following equations were used to calculate the actual amount of CHR in CHR-NP.

$$\% \text{ EE } = \frac{\text{Amount of drug in entrapment } - \text{ Amount of drug in supernatant}}{\text{Total amount of CHR in the formulation}} \times 100$$

Drug release study

The drug release study was performed for a period of 120 hours. Phosphate buffer saline (PBS) of pH 7.4 was used in the study. In a dialysis bag having a cutoff size of 5 k Da, CHR-NP was disseminated in 1 mL of PBS. Thereafter, in 100 mL of PBS under constant magnetic stirring the dialysis bag was suspended. The quantity of CHR released from CHR-NP was determined by calculating the absorbance at 348 nm at intermittent interval.

Cellular uptake study of CHR-NP in vitro

Cellular uptake study was performed in A549 cells seeding them in tissue culture plates incubating overnight at 37 °C, 5% CO_2. The cells were subsequently treated for 1 hr ,2 hr and 6 hr with FITC tagged CHR-NP. The free FITC tagged CHR-NP were removed after treatment by washing thrice. The A549 cells were then fixed for observation under microscope. 4% paraformaldehyde was used to fix the cells. Confocal microscopy (Olympus Fluo View FV10i) was employed to observe CHR-NP internalisation.

Establishment of in vivo asthma model

An experimental in vivo mice asthma model was established to examine anti-asthmatic efficacy of CHR-NP. The protocol that was adapted for the model development is described here.

The Development of a Murine Asthma Model was in accord with standard protocol with minor modification. On the 1st, 7th, and 14th days, all mice were intraperitoneally sensitised with 100 µ g of OVA dissolved in 200 µL phosphate-buffered saline (PBS). 2 mg aluminium hydroxide was also added in PBS. Schematic Diagram (scheme1) represents the asthma model development. From day 21, mice were sedated and administered an intranasal challenge thrice a week for four weeks. For intranasal challenge 50 µg of OVA dissolved in PBS was used. All the control mice were sensitised and given PBS as a challenge. Finally, all the mice were euthanized 48 hours after completing the last challenge.

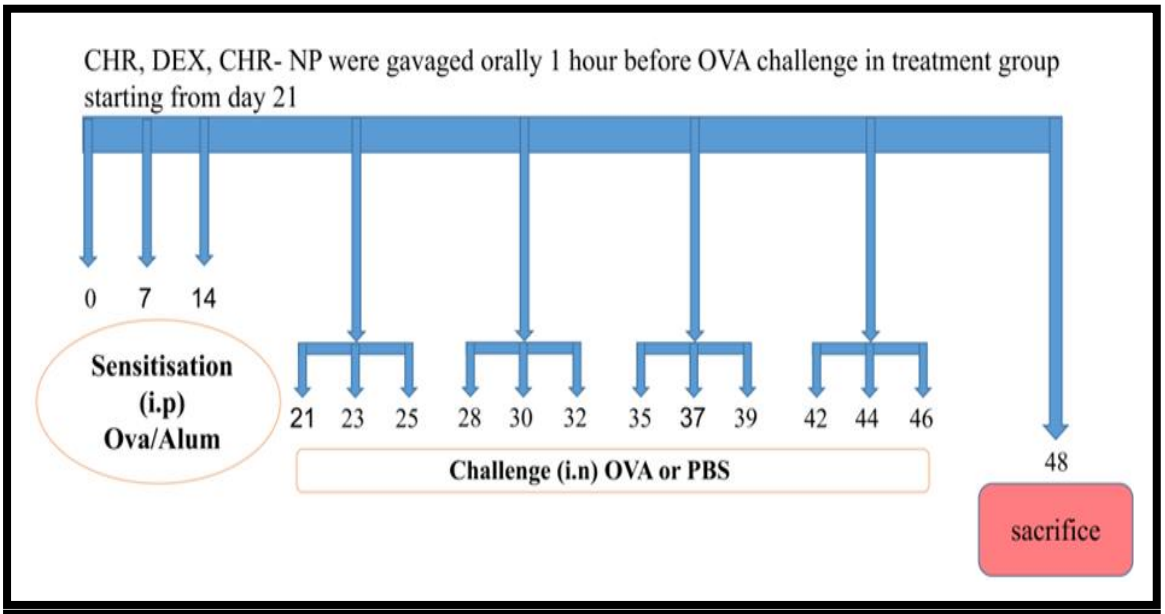

Schematic diagram of in vivo asthma model developement

Treatment groups

Five groups with five animals in each group were formed , out of which three groups received treatment. In one group, CHR-NP was dissolved in PBS and given orally to asthmatic mice once a day, three times a week for four weeks, commencing one hour before the ova challenge on day 21. The quantity of CHR-NP used was equivalent to 50mg/Kg body weight of CHR. In the other treatment groups, free chrysin (CHR) (50 mg/kg body weight) dissolved in PBS and dexamethasone (DEX) (1 mg/kg body weight) were given. The OVA-only group received no intervention, whereas the control group received just PBS. The mice were killed two days after the final OVA exposure, and their tissues and blood were collected for histological and cytokine analysis.

ALT and AST activity assay in serum

During the preliminary dosage selection of CHR-NP, blood was drawn from the tail vein of mice at weekly intervals post CHR-NP administration. The collected blood was centrifuged for 5 minutes at 3000 g and the serum was extracted. Serum (ALT) and serum (AST) activities were measured following the guidelines on the commercial test kit.

Ig E level measurement in serum

IgE level detection is of prime importance in allergic asthma disease. Following OVA exposure, the mice were extravasated (from the tail vein). This extravasation process was carried out on the 14th, 28th, or 35th day. The enzyme-linked immunosorbent assay (ELISA) kit was used to assess the amount of OVA-specific Ig E in the serum.

Cytokines analysis from BALF and serum

24 hours after the final OVA exposure, mice from all experimental group were sedated and serum is extracted from blood collected by retro orbital bleeding by centrifuging at 3000 g for

5 minutes. The serum thus collected was kept at a temperature of -80 °C until it was being used. The levels of different inflammatory cytokines in the serum were determined using commercially available ELISA kits according to the manufacturer's procedure. The lung lobes were cleansed 2 times with 0.5 ml of ice-cold PBS by intratracheal instillation preceding BALF collection and centrifugation (10 min, 4 °C, 1000 rpm). The supernatants were stashed at -80°C before differential cell counting, and the cell pellets were reconstituted in 30µl ice-cold PBS. A hemocytometer was used to quantify the total number of different inflammatory cells in BALF, and commercial ELISA kits were utilised to determine the levels of IL-(4,5,13).

Histological analyses

After sacrificing the mice, small amount of lung tissues from all animals were fixed using 10% formalin (neutral-buffered). After fixing the tissues were cut into sections. The lung sections were stained with hematoxylin and eosin (H&E), Masson Trichome (MT), and Periodic acid–Schiff (PAS) stains and investigated using an Olympus IX70 microscope at 20X magnification.

Analysis of protein expression by Western Blot

Each group of experimental mice's lung tissue was fractionated into cytosolic and nuclear fractions. After that protein estimation was done from the fractions according to the documented procedure with minor modifications. After combining protein samples with loading dye (4:1), they were segregated on a 10–15 percent SDS-polyacrylamide gel and transferred to PVDF membranes. The membranes were then blocked, washed, and incubated overnight with specific primary antibodies before being conjugated with horseradish peroxidase for two hours the next day. Finally, a chemidoc method was employed to evaluate protein expression using the horseradish peroxidase substrate (peroxidase/luminol).

Immunofluorescence-based estimation of protein expression

Indirect immunofluorescence was utilized to assess for protein expression in the unstained lung sections of all test groups, and images were acquired using a ZEISS LSM 980 Confocal Microscope. To summarise, the unstained lung sections were deparaffinized and thereafter hydrated in graded ethanol. In the next step the sections were blocked with (0.3 percent hydrogen peroxide) for 20 minutes to suppress endogenous peroxidase activity. The antigen was retrieved in a microwave oven using citrate buffer (10 mM, pH 6.0) at temperatures ranging from 95°C to 98°C for 15 minutes, and the sections were then further blocked with BSA (5%) for 30 minutes at 37°C. Following blocking, in the next step the lung sections were incubated overnight at 4°C with the primary antibody (dilution: 1:250). After rinsing the samples in PBS, the sections were incubated for 1 hour at 37°C with anti-rabbit/ mice-FITC/ phycoerythrin (PE)/allophycocyanin (APC) secondary antibodies, followed by nuclear staining with DAPI for 10 minutes and finally the images were acquired in confocal microscopy.

The sections were then blocked utilizing (0.3 % hydrogen peroxide) lasting 20 minutes to inhibit endogenous peroxidase activity. The antigen was retrieved by heating in a microwave oven for 15 minutes at temperatures ranging from 95°C to 98°C. Citrate buffer of pH 6.0 was used for antigen retrieval. Post retrieval the lung sections were blocked with BSA (5%) at 37°C for a time period of 30 mins. Following blocking, the lung sections were incubated with the primary antibody for overnight at 4°C. Following a PBS rinse, the sections were incubated for 1hour at 37°C with anti-rabbit/mice-FITC/phycoerythrin(PE)/allophycocyanin (APC) secondary antibodies. Finally nuclear staining with DAPI was done for 10 minutes before image acquiring.

Results

DLS, Zeta potential, drug loading study, and encapsulation efficiency

The size, encapsulation efficiency, drug loading, zeta potential, and PDI of CHR-NP are displayed in Table 1. The formulation's mean particle sizes were 99.034±9.494 and had a high encapsulation efficacy of 91.4%, with a drug loading of 8.37±0.12%. The PDI score was 0.084, suggesting that the formulation was narrowly scattered. At pH 7.4, the potential value was -13.1 mV, while at pH 6.8 and pH 2, it was -9.33±0.5 mV and -6.10±0.7 mV, respectively.

Generally, PLGA NPs have a negative zeta-potential (ZP) due to the carboxylic group, which is also evident in the formulation.

Mean size	**Polydispersity index (PDI)**	**Encapsulation efficiency (EE)%**	**Drug loading (DL)%**	**Zeta potential (ζ-potential) mV**		
				pH2	**pH6.8**	**pH7.4**
99.034±9.494	**0.084**	**91.45 ±1.4**	**8.37±0.12**	**-6.10±0.7**	**-9.33±0.5**	**-13.1±2.9**

Table 1: Particle mean size, polydispersity index, encapsulation efficiency, drug loading percentage and zeta potential

Morphological analysis of CHR-NPs

AFM study

The CHR-NPs AFM picture affirmed the structure of the CHR-NP at the nanoscale (Fig 1).2D and 3D images of CHR-NP were acquired from AFM microscope. The images obtained showed spherical shaped nanoparticles with size ~77nm.The surface of the synthesized nanoparticles were observed to be smooth in surface morphology.

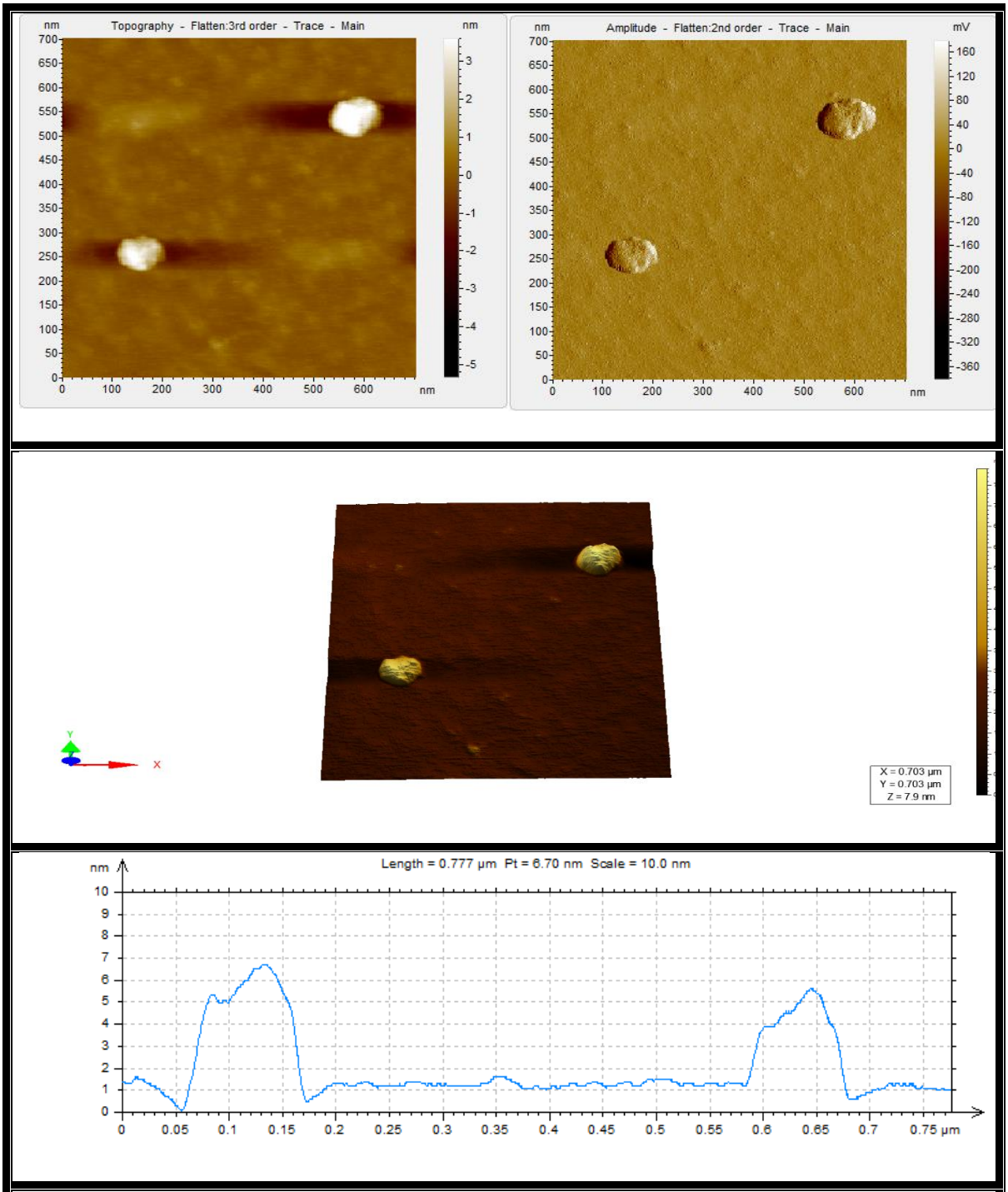

Fig1: Microscopic assessment of CHR-NP by Atomic force microscopy

Two-dimensional and three-dimensional AFM images with topography and distance measurement for CHR-NP are shown. Note: The topography shows the height of each nanoparticle from the mica sheet's substratum.

TEM analysis

Transmission electron microscopy also revealed the structure of CHR-NP along with the size which ranged from 55-80 nm. (Fig.2) TEM images showed homogenous particle size distributions that were in line with the data obtained from DLS study.

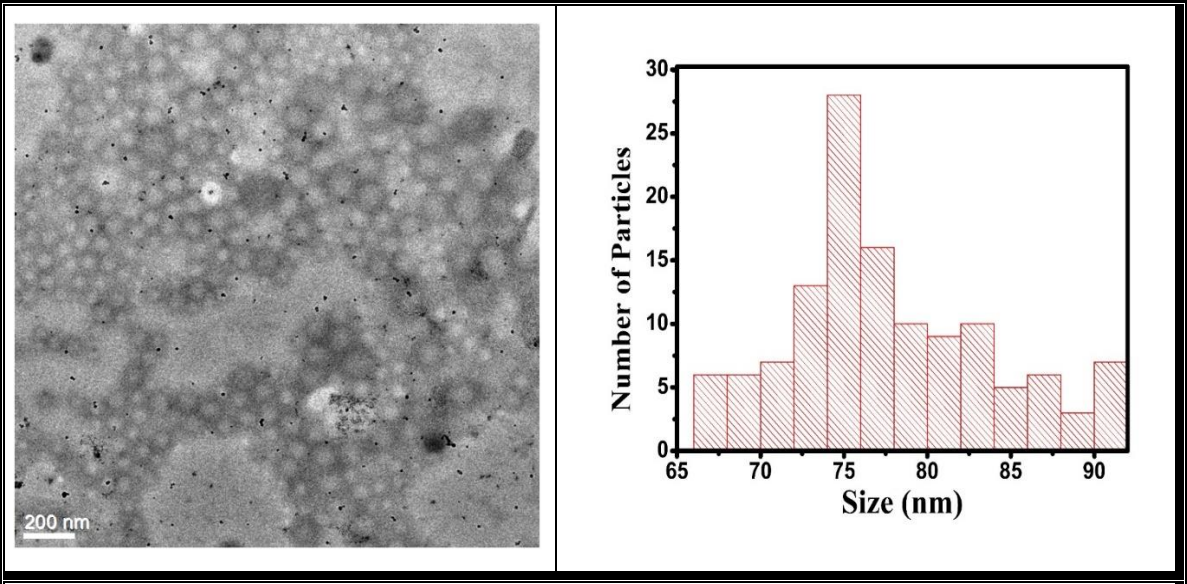

Fig 2: Microscopic assessment of CHR-NP by Transmission electron microscopy (TEM). Size distribution of the particles obtained in TEM

DSC studies

By examining the temperature of items, DSC provides information on the crystalline or amorphous characteristics of the samples. For assessing the status of CHR in CHR-NP, the samples were run through a differential scanning calorimeter.

The physical state of both the drug (CHR) and the polymer (PLGA) were also examined since it would affect the drug's release kinetics.

DSC investigation disclosed that crude CHR has a strong endothermic peak at 293.5°C, whereas that of B-NP has a glass transition temperature (Tg) of 51°C. The thermogram of CHR-NP revealed a PLGA peak at 51°C. However, the sharp peak of the CHR at 293.5°C was missing (Fig 3), suggesting that the drug had relinquished its crystalline form and had been incorporated into the polymer matrix.

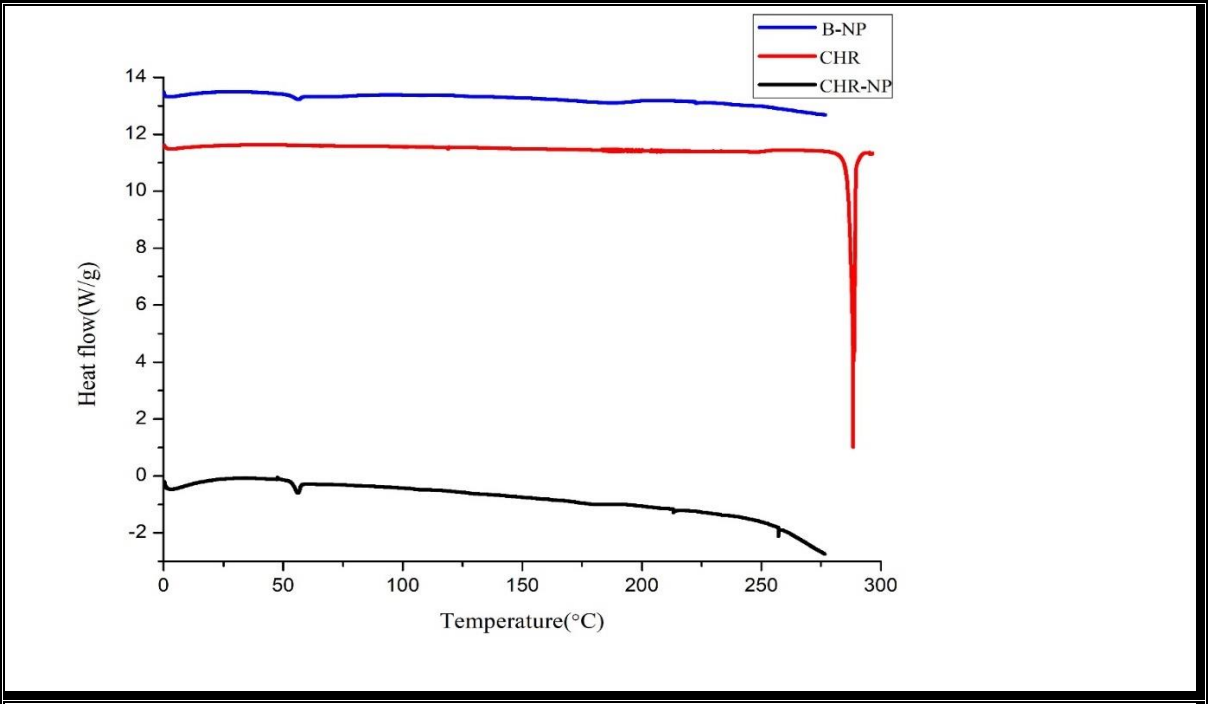

Fig 3 : DSC analysis of pure Chrysin (CHR), Blank nanoparticle (B-NP), and Chrysin loaded poly (lactic-co-glycolic acid)(CHR-NP)

FTIR analysis

FTIR was used to investigate the functional groups found in CHR, CHR-NP, and B-NP (Blank nanoparticle). The following figure depicts the FTIR spectra of pure CHR, CHR-NP, and B-NP (Fig4). The copolymer's terminal hydroxyl groups are allocated to the absorption band at

3387.5 cm-1. C-H stretching generates the absorption bands at 2944.6cm-1 and 2997 cm-1, whereas C=O stretching yields the band at 1759 cm -1. C-O stretching generates the bands at (1190.2 – 1093.4) cm -1. The C–H stretching and C=H are accountable for the bands at 2931 cm- 1, 2710 cm- 1, and 2632 cm- 1 in CHR. The bands at 1653.3 cm- 1 are carbonyl group vibration coupled with a double bond at the gamma benzopyrone ring, while the absorption bands at 1612 cm- 1, 1576 cm- 1, and 1449.7 cm- 1 are owing to carbon vibration in benzene and pyrone ring .

The disappearance of CHR's distinctive peak in CHR-NP, as well as the similarities between CHR-NP and B-NP, imply that free drug didn't exist on the surface of CHR-NP. (Fig 4)

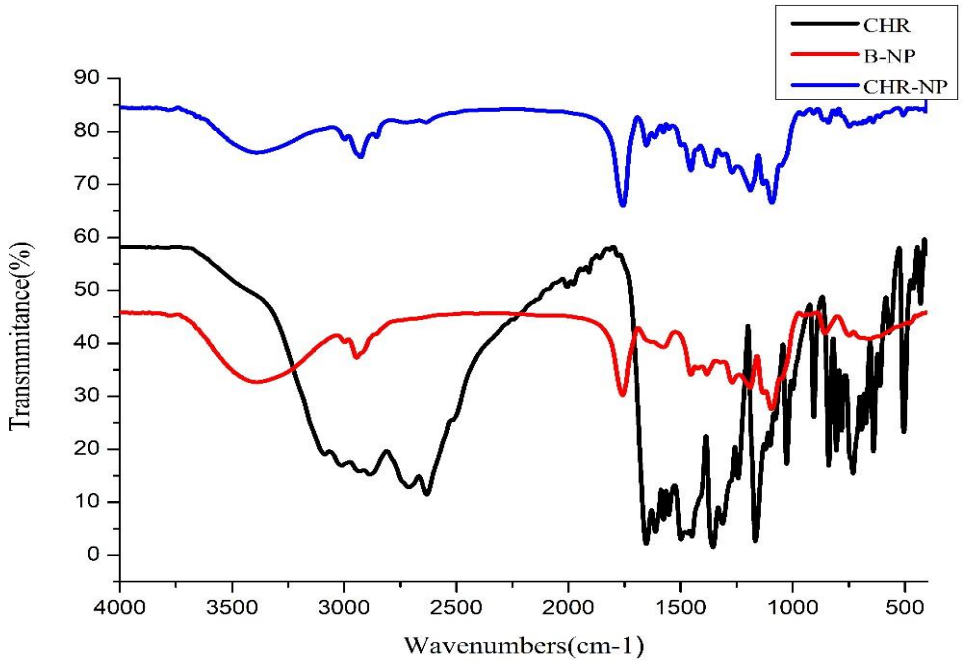

Fig 4: FTIR analysis of pure Chrysin (CHR), Blank nanoparticle(B-NP), and Chrysin loaded poly (lactic-co-glycolic acid) (CHR-NP)

Results

XRD analysis

XRD spectra of CHR, B-NP, and CHR-NP were acquired. The XRD spectrum of CHR demonstrated multiple different sharp peaks at 2θ depicting its crystallinity.

The XRD Spectra of CHR-NP had dramatically reduced peak intensity as compared to CHR (Fig 5). CHR's crystallinity changed once it was mixed with PLGA, according to the findings. As a consequence, XRD data confirmed the total loss of CHR crystallinity following inclusion in PLGA and were congruent with DSC findings.

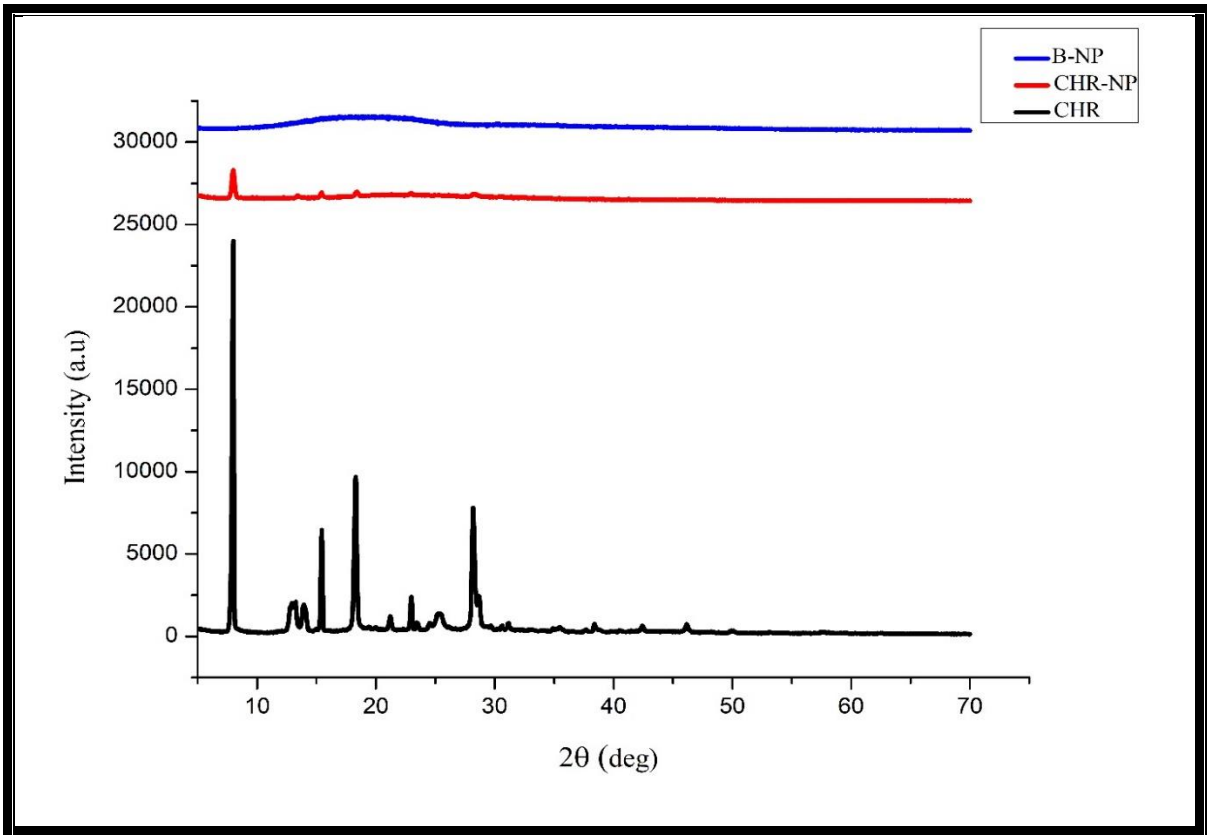

Fig 5: XRD analysis of pure Chrysin (CHR), Blank nanoparticle(B-NP), and Chrysin loaded poly (lactic-co-glycolic acid)

Study of drug release

CHR release from CHR-NPs was investigated in vitro using the dialysis technique at pH 7.4. At pH 7.4, the drug release pattern demonstrated a burst release in the first eight hours followed by a controlled drug release for the next 120 hours, with about 63.5 % of CHR released from the CHR-NPs during this time. (Fig 6)

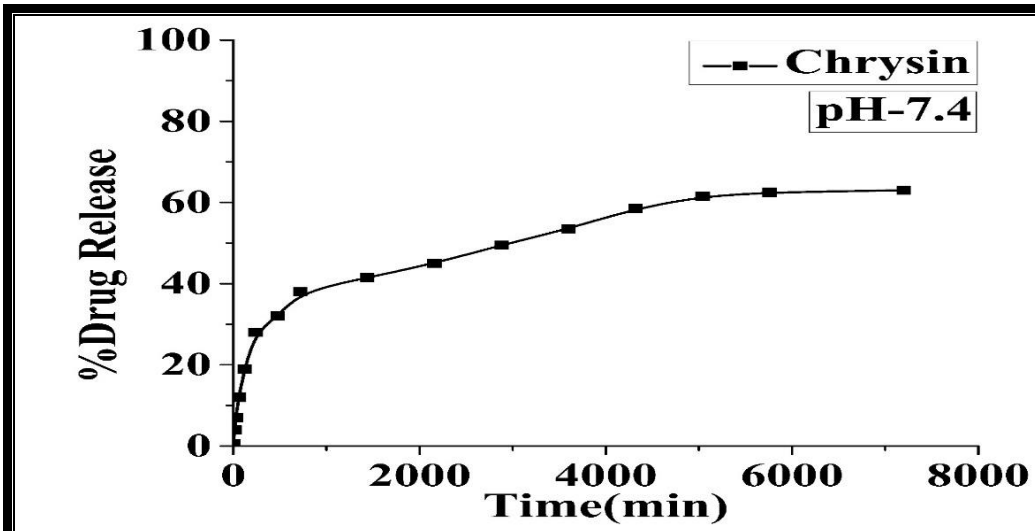

Fig 6: Release profile of CHR from CHR-NP in PBS buffer (pH 7.4) over a period of 120 hours

Cellular uptake in vitro

In a cellular uptake study, A549 cells treated with FITC-CHR-NP displayed green fluorescence in the cytoplasm, indicating that FITC-CHR-NP accumulates in the cells over time. (Fig 7)

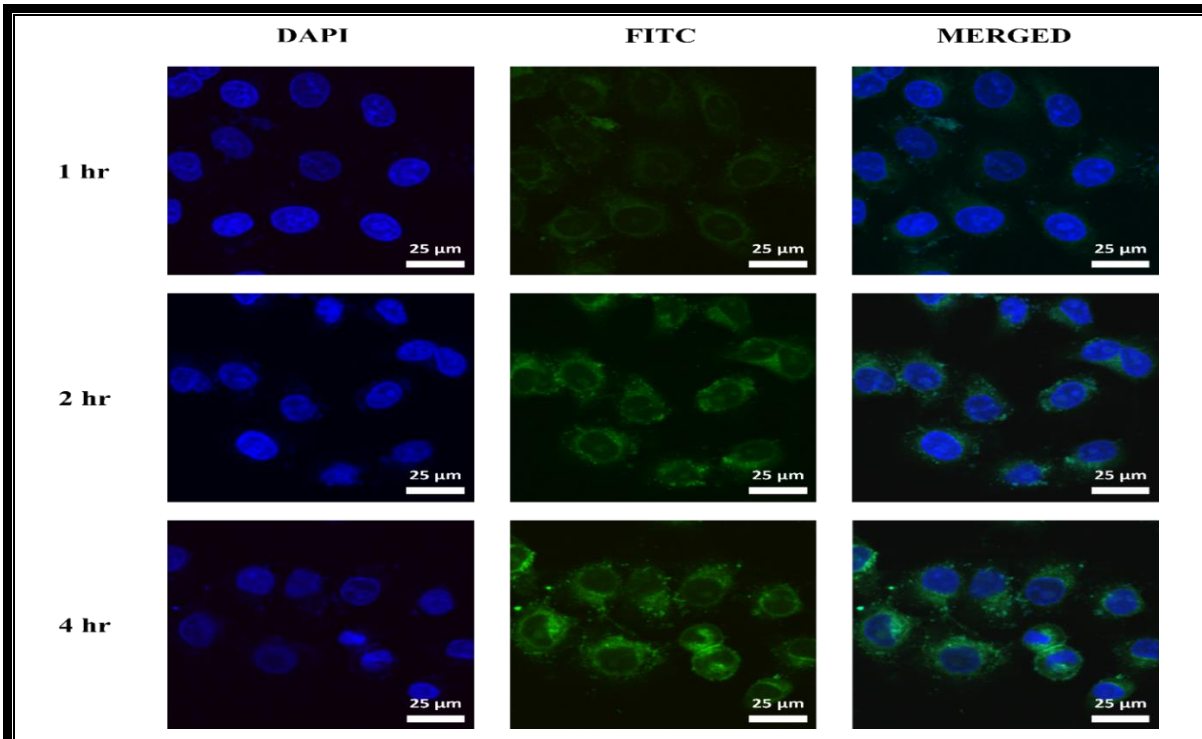

Fig 7: Cellular uptake study of FITC tagged CHR-NP on A549 cell line for 4 hours

CHR-NP Dose Selection

Multiple dosages of CHR-NP (proportional to 10 mg, 50 mg, 250 mg, or 500 mg /kg CHR) were orally administered to mice on alternate days for 30 days. To assess the toxicity of the dosages, liver function parameters (AST, ALT) were measured on a weekly basis. For 30 days, mice were given different doses of CHR-NP (corresponding to 10mg, 50mg, 250mg, or 500mg of CHR) orally on alternating days. On the 7th, 14th, 21st, and 30th days, liver function markers (AST, ALT) were evaluated in the serum of these mice. In our study, the liver function markers were not elevated with (10mg and 50mg)/ kg doses till the 30th day, but they were elevated with (250mg and 500mg)/ kg doses on the 21st day (Fig 8). As a result, CHR-NP (dosage equivalent to 50mg/kg CHR) and free CHR (dose equivalent to 50mg/kg CHR) were utilised. CHRNP (dosage corresponding to 50mg/kg of CHR) was chosen for our investigation based on blood levels of liver function parameters.

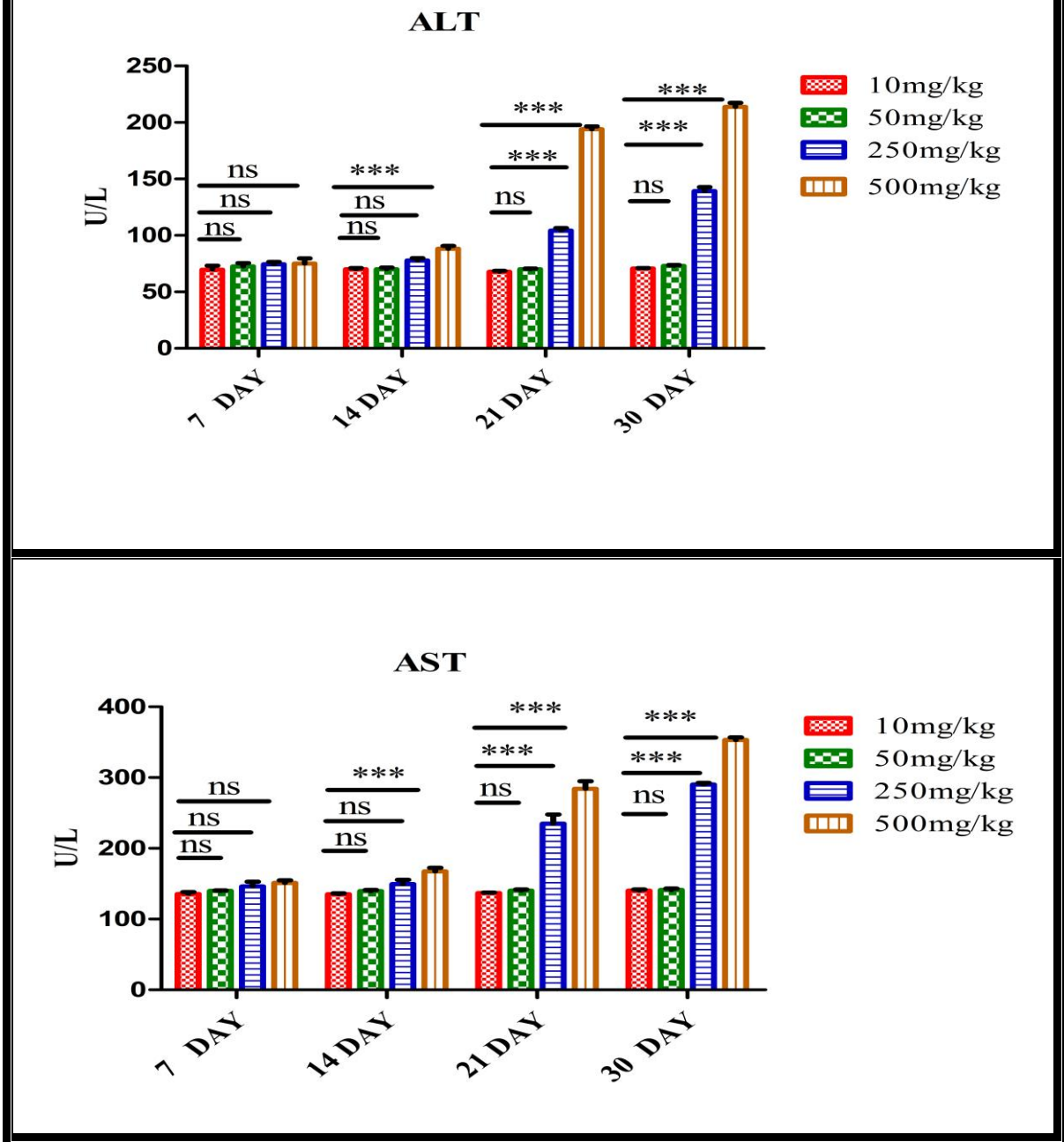

Fig 8: Serum ALT (on the top) and AST levels (on the bottom) of mice treated with various concentrations of CHR-NP (corresponding to 10mg, 50mg, 250mg, and 500mg) /kg CHR

CHR-NP affects serum Ig E levels

We initially determined the innoxious dosages of CHR-NP for this study and CHR-NP equivalent to 50 mg/kg CHR was selected to be administered.

On the 21st, 28th, 35th, and 42nd days of the experimental allergic asthma model development, serum IgE levels were monitored in all experimental groups. IgE levels, which had continually increased over time, were curbed after treatment with CHR-NP and the conventional drug dexamethasone (DEX) (Fig 8). Free CHR had no effect on ovalbumin (OVA)-induced IgE levels in OVA-sensitized mice, but CHR-NP had a nearly equivalent effect on IgE levels in OVA-sensitized mice treated with DEX (Fig 9).

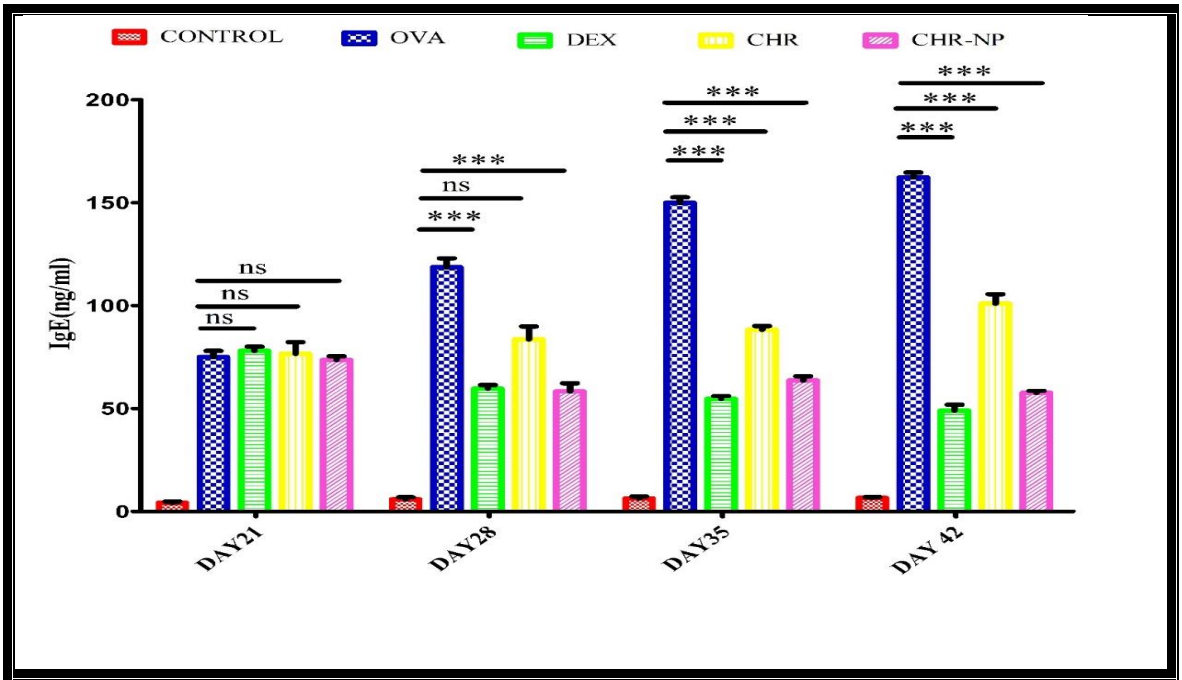

Fig 9: Ig E level detection in all the experimental groups (treated and non-treated)

Lung histopathology in OVA-treated mice

The mice were sacrificed on the 48th day of the experiment, at which point lung tissue histology was performed. According to the PAS staining results, the OVA group had excessive production of mucus in the bronchial airways due to goblet cell hyperplasia and mucus hyperproduction. Both groups of CHR-NP and DEX significantly lowered it, while CHR did not (upper panel, Fig 10). Increased collagen deposition is one of the hallmarks of pulmonary remodelling. In the OVA group, Masson's trichrome (MT) staining indicated thick collagen deposition in the peribronchial area, denoting enhanced fibroblast proliferation and collagen secretion. CHR-NPs and DEX effectively diminished collagen deposition, but the free CHR group had no affect (middle panel, Fig 10). The peribronchial infiltrates appeared to be enlarged histologically.

CHR-NPs and DEX significantly reduced collagen deposition, but the free CHR group had no impact (middle panel, Fig 10). In the OVA group, histological staining indicated increased peribronchial infiltrates with many inflammatory cells. The administration of CHR-NPs to OVA-challenged mice resulted in a significant reduction in inflammatory cell recruitment in peribronchial areas, compared to a modest reduction in inflammatory cells in the free CHR group (lower panel, Fig 10). The histological characteristics of the DEX-treated group and the control group were nearly identical.

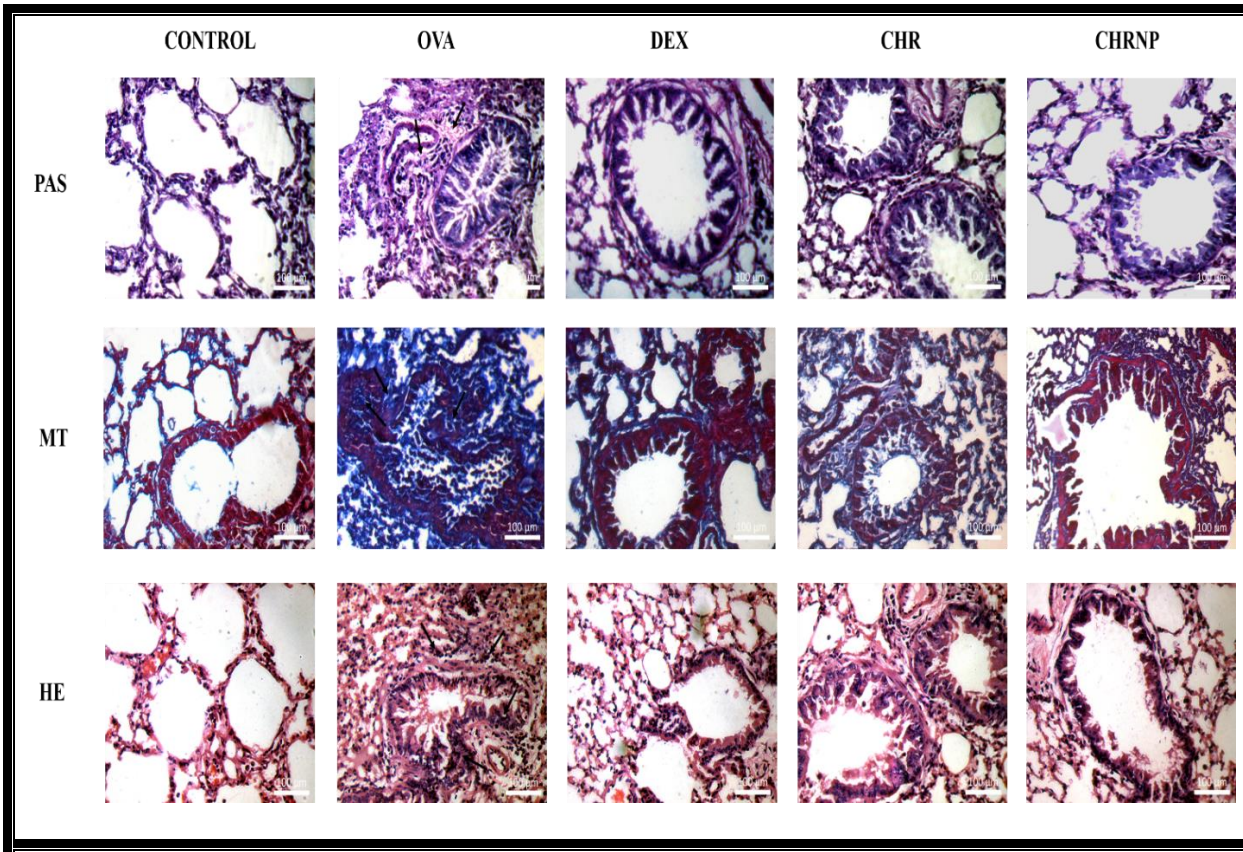

Fig 10: Lung Histological analysis of all the experimental groups (treated and non-treated)

OVA-induced airway inflammatory cell infiltration and Th2 cytokine levels in BALF were reduced by CHR-NP.

The number of inflammatory cells, such as macrophages, neutrophils, lymphocytes, and eosinophils, were reported to be significantly escalated in OVA-sensitized / challenged mice BALF compared to control mice after the animals were sacrificed on the 48th day. When compared to the OVA-sensitized / challenged animals, the CHR-NP treated mice had significantly lower numbers of eosinophils and macrophages. (Fig 11 A) The amount of Th2 cytokines (IL-4, IL-5, and IL-13) was likewise raised by OVA, which was reduced by CHR-NP and DEX with almost identical efficacy. Free CHR was less efficient as expected (Fig 11B).

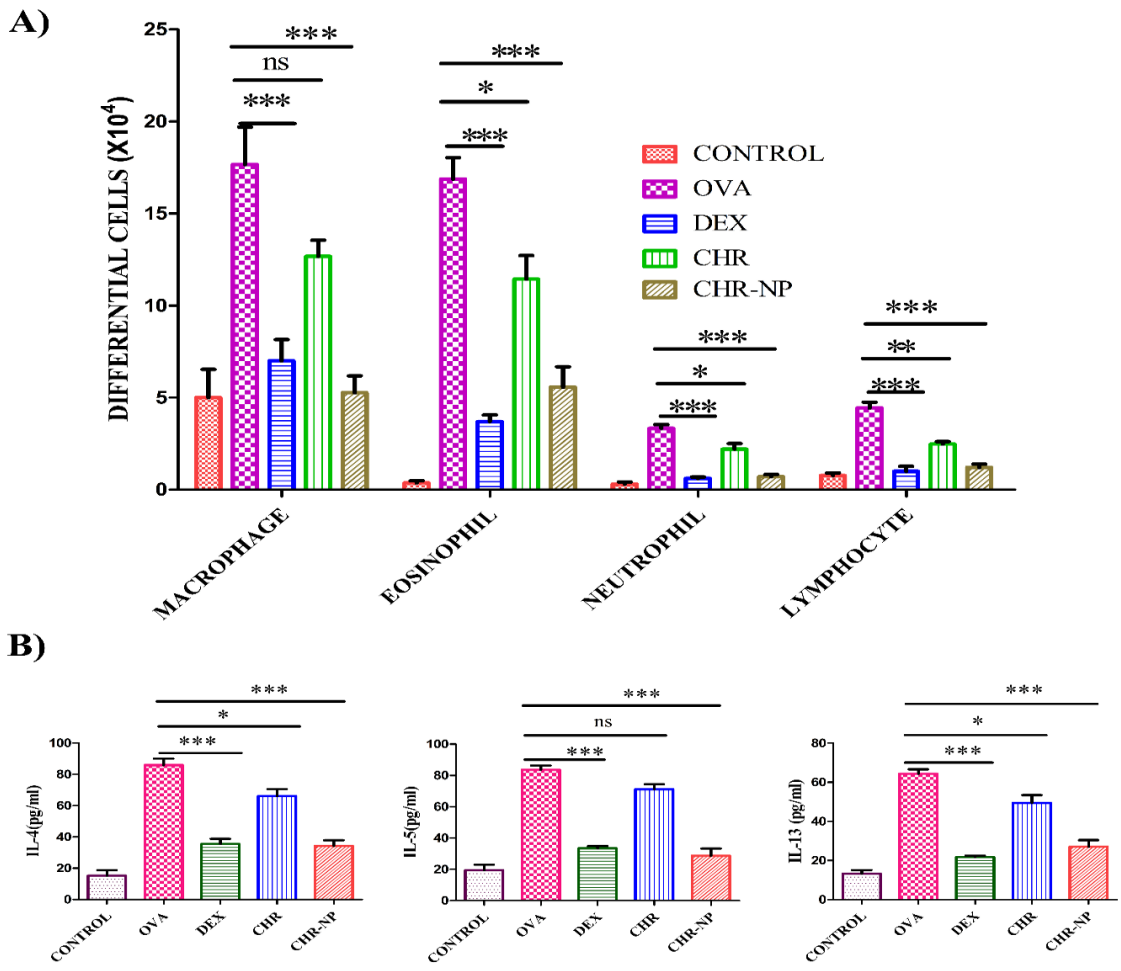

Fig 11:A) inflammatory cell differential count in BALF.

B) Th2 cytokine levels in BALF were assessed using ELISA. Values are presented as means ±SEM among five mice. (P < 0.05) Bronchoalveolar Lavage Fluid (BALF)

OVA-induced pro-inflammatory cytokines production were reduced by CHR-NP

In serum, the activity of CHR-NP on pro-inflammatory cytokines such as tumour necrosis factor (TNF-α), IL-6, IL-18, and IL-1β were analysed. The cytokine levels in the OVA group serum were notably higher than those in the Control group, as shown in (Fig 12 A). CHR-NP administration significantly reduced the levels of these pro-inflammatory cytokines,

approximately identical to the effect of DEX. Protein expression of these cytokines evaluated by Western blot in the lung tissue of experimental mice was consistent with the results of their level in the sera, as shown in (Figure 12 B).

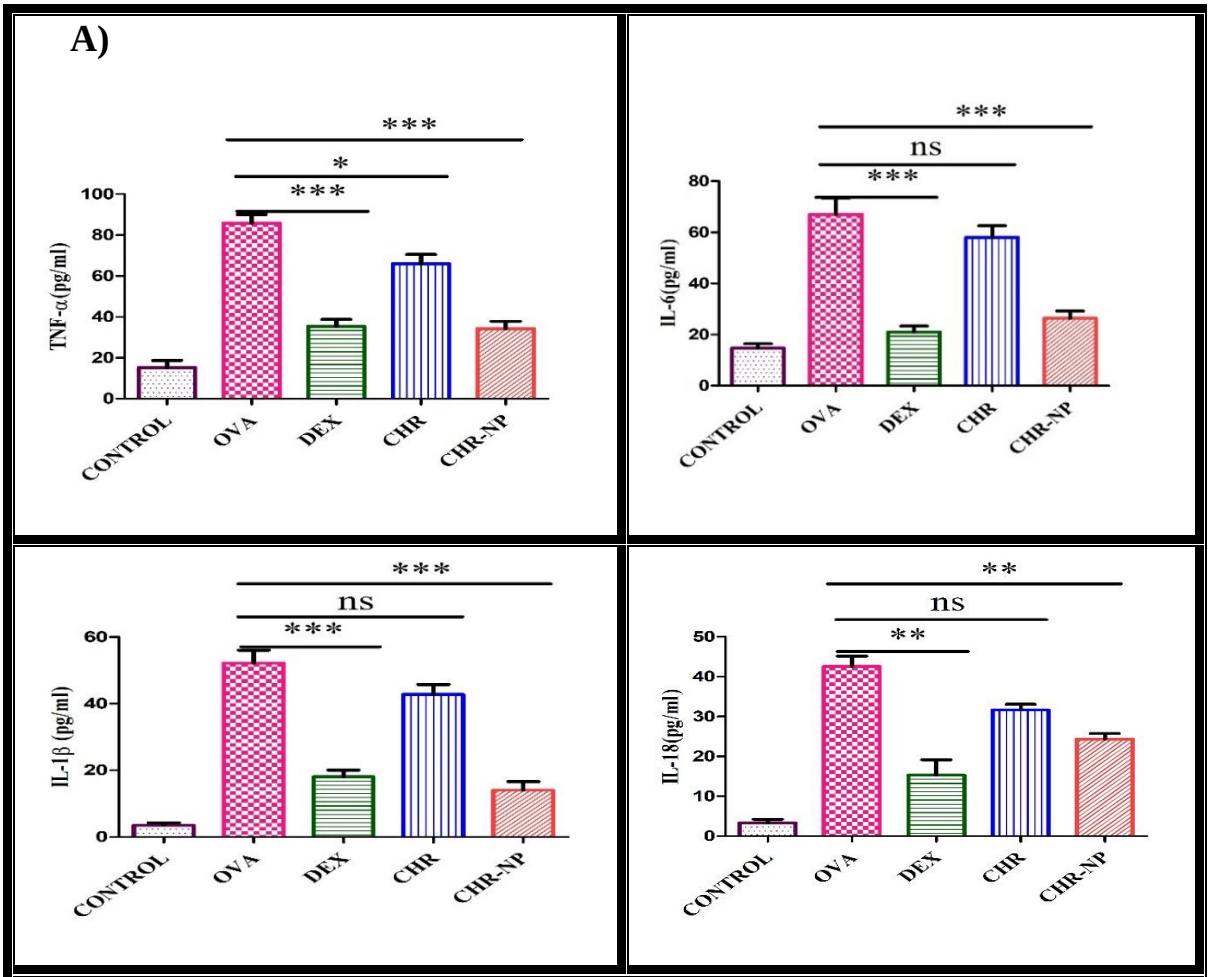

Fig 12: A) Pro-inflammatory cytokines (IL6, TNF-α, IL-1β, and IL-18) were observed by ELISA in the serum of mice from all test group. Values are presented as means ±SEM among five mice. (P < 0.05).

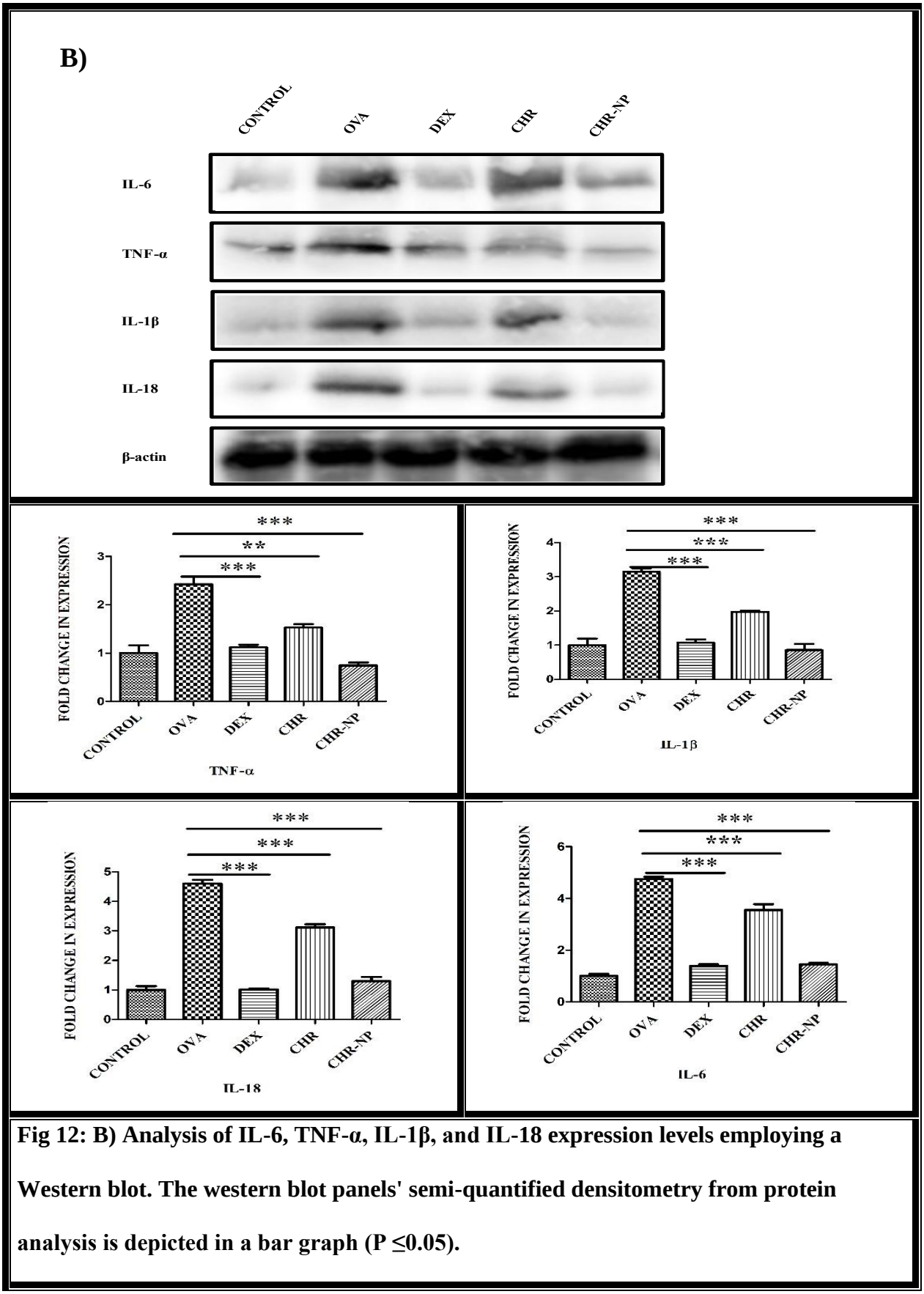

Fig 12: B) Analysis of IL-6, TNF-α, IL-1β, and IL-18 expression levels employing a Western blot. The western blot panels' semi-quantified densitometry from protein analysis is depicted in a bar graph (P ≤0.05).

OVA-induced NF- κB translocation were curtailed by CHR-NP

The transcription factor NF-**κ**B is a master inflammatory regulator that has been widely identified in the onset of inflammation. (Schuliga, 2015b) The upstream signals I-κB have a strong influence on NF- κB activation. As a result, we examined the levels of NF-κB, and I-κB in the lung tissue of OVA-challenged treated and untreated mice. An immunofluorescence investigation demonstrated an elevated level of p-p65 following OVA stimulation, although CHR-NP significantly lowered the levels of p- p65 and I-κB phosphorylation, whereas free CHR failed to lower the levels (Fig 13 A). CHR-NP therapy decreased phosphorylated I-κB, limiting nuclear translocation of NF-κB as observed from western blot (Fig 13B).

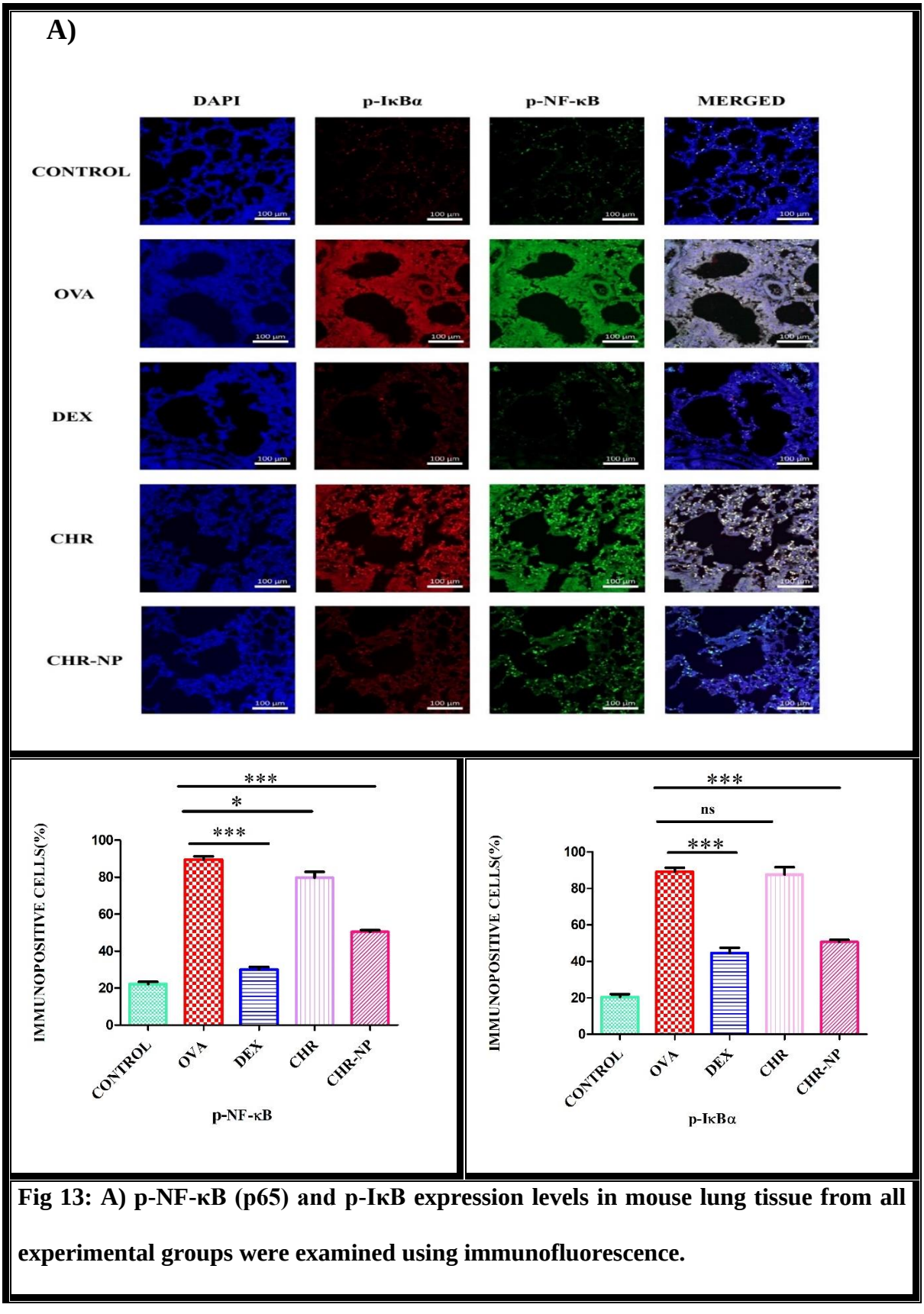

Fig 13: A) p-NF-κB (p65) and p-IκB expression levels in mouse lung tissue from all experimental groups were examined using immunofluorescence.

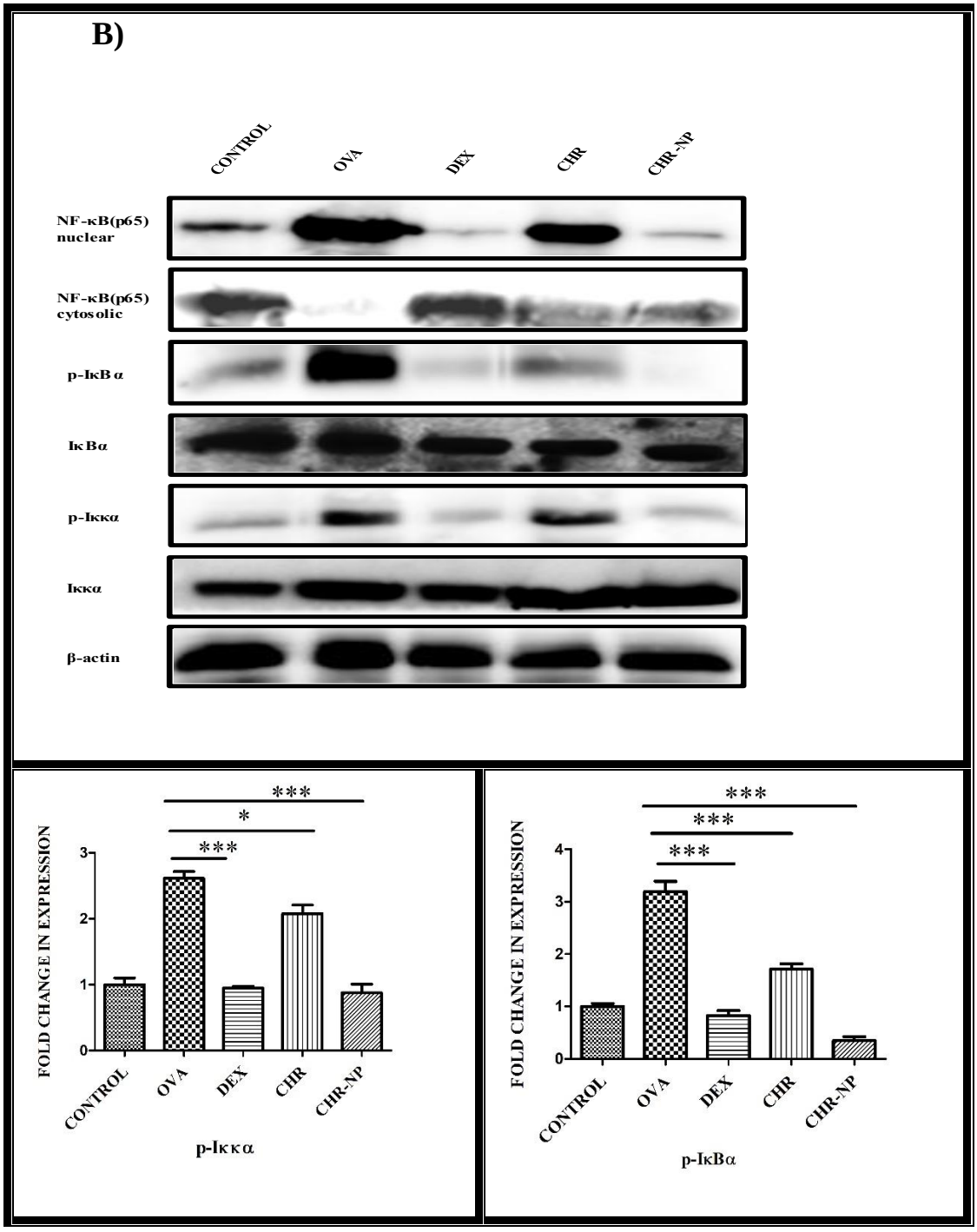
B)
CONTROL
OVA
DEX
CHR
CHR-NP
NF-κB(p65) nuclear
NF-κB(p65) cytosolic
p-IκBα
IκBα
p-Ικκα
Ικκα
β-actin
FOLD CHANGE IN EXPRESSION
***
*
***
CONTROL
OVA
DEX
CHR
CHR-NP
p-Ικκα
FOLD CHANGE IN EXPRESSION
***
***
***
CONTROL
OVA
DEX
CHR
CHR-NP
p-IκBα

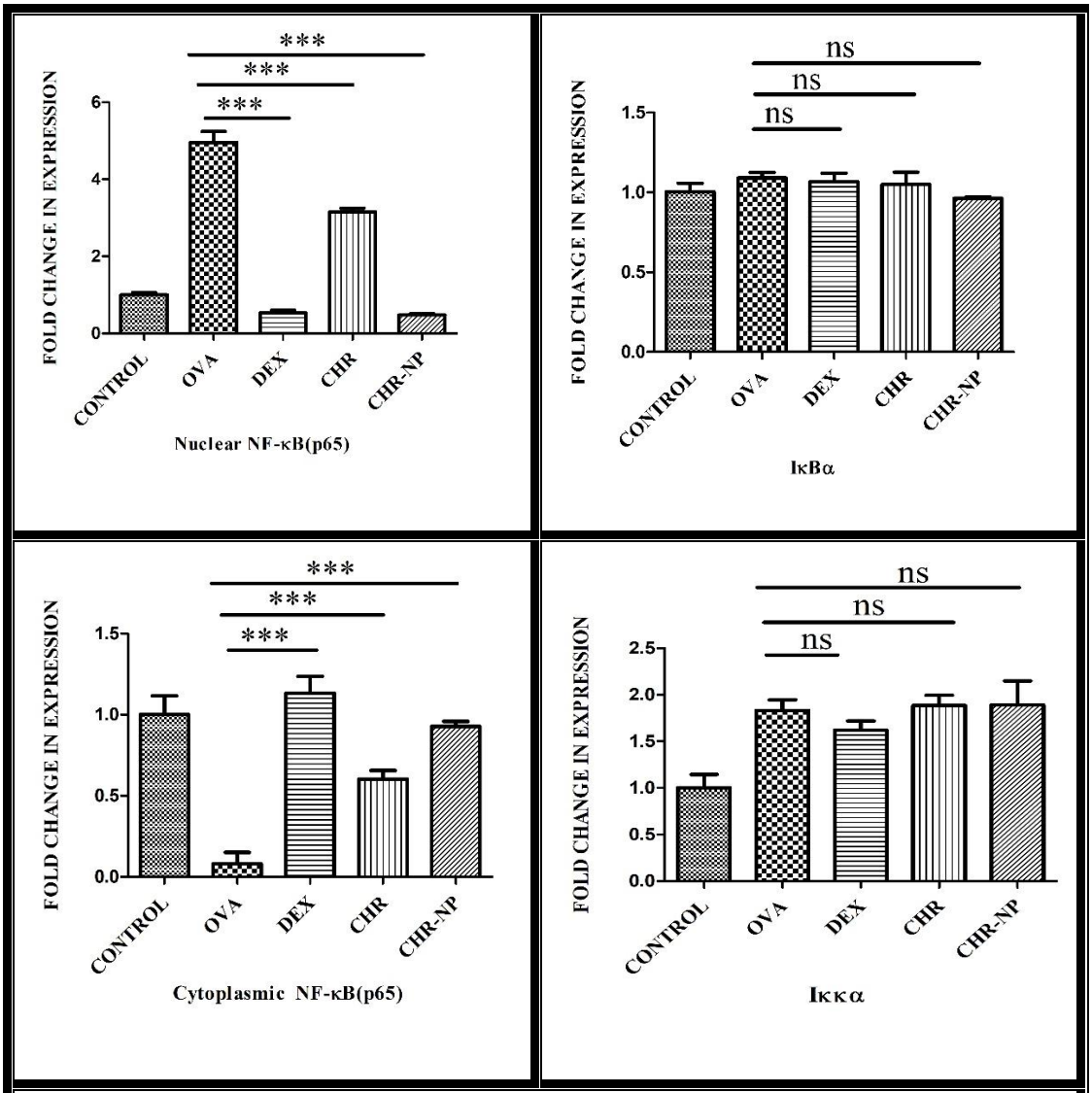

Fig 13: B) Expression levels of nuclear and cytosolic NF-κB (p65), p-IκB, I-κB, Ικκα, and p-Ικκα were analysed using Western blot. The western blot panels' semi-quantified densitometry from protein analysis is displayed in a bar graph (P≤ 0.05).

TLR 2/4 expression was lowered by CHR-NP.

TLR4 and TLR2 mediated NF-kB signalling has been reported in recent researches to elicit inflammatory responses in OVA-induced allergic asthma (Luo et al., 2017).(Helal et al., 2019) We used immunofluorescence to look at the protein expression levels of TLR4 and TLR2 in

lung tissue. TLR4 and TLR2 levels in the OVA group were seen to be lowered following treatment with CHR-NP (Fig 14 A). In the immunoblotting investigation, a comparable outcome was detected (Fig 14 B). CHR-NP was observed to be more efficacious than free CHR.

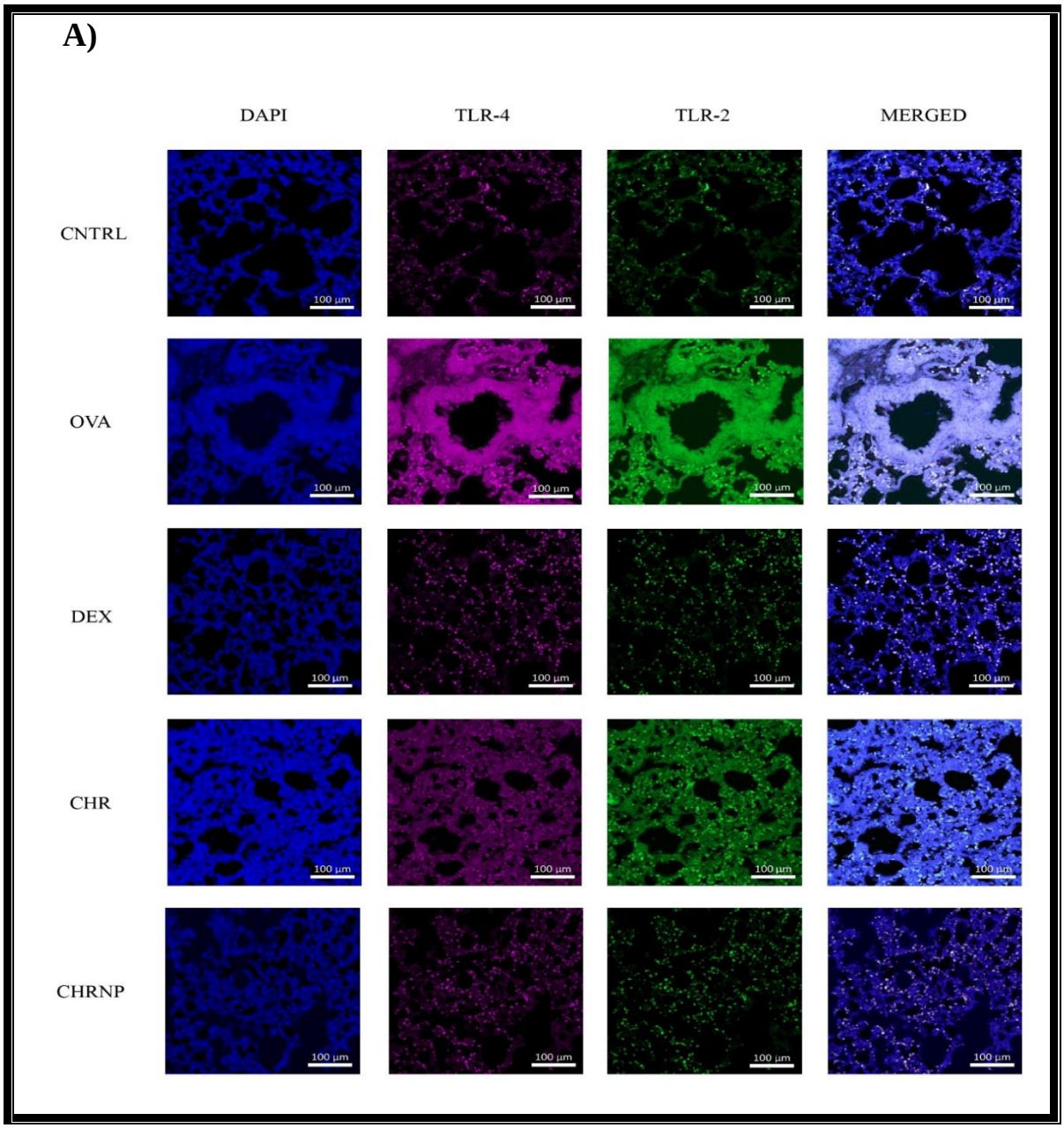

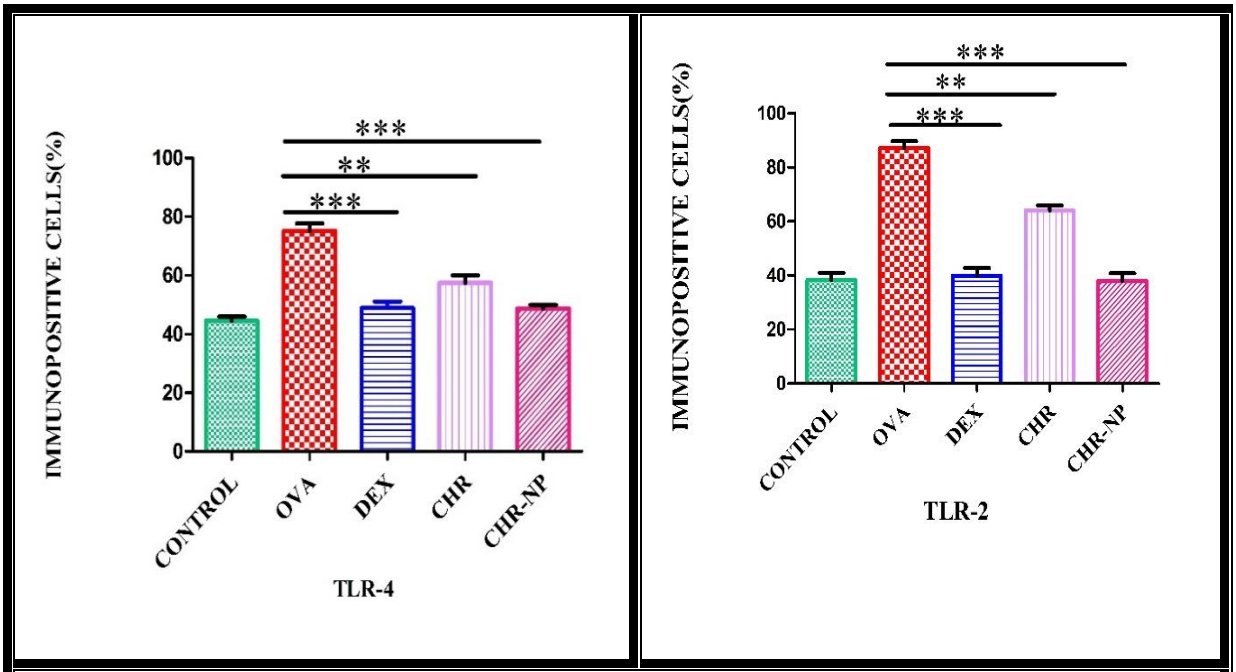

Fig 14: A) TLR-2 and TLR-4 expression levels were examined using immunofluorescence in the lung tissue of mice from all experimental groups.

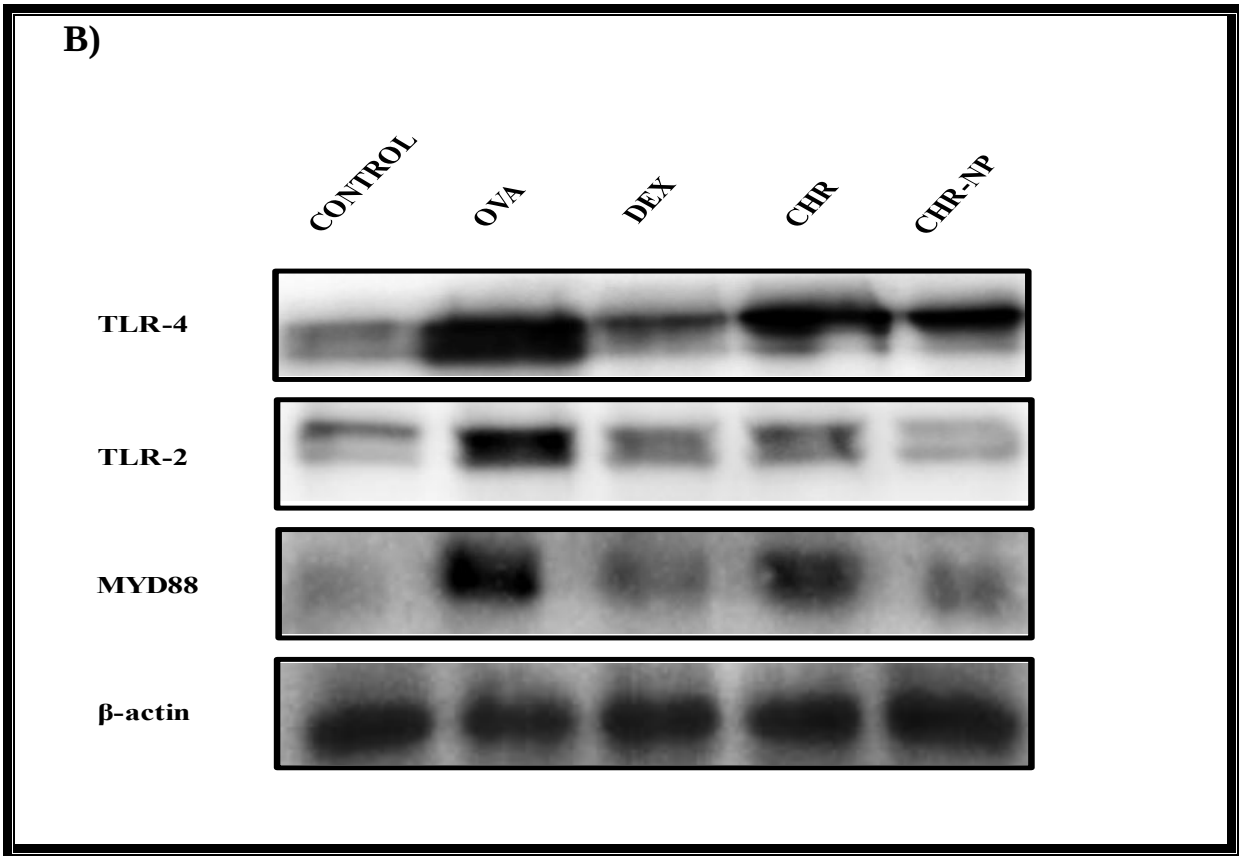

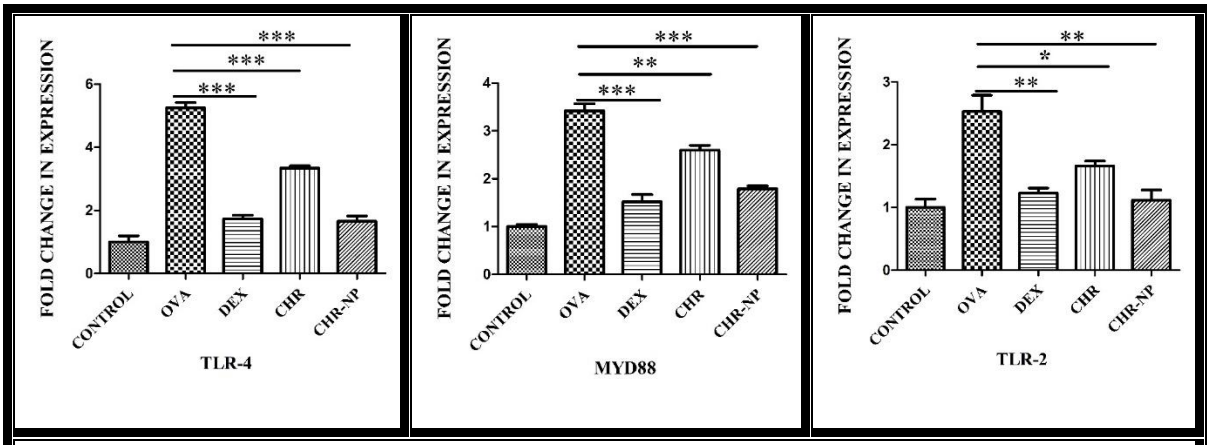

Fig 14: B) TLR-2, TLR-4, and MyD88 expression levels were analysed using a Western blot. The western blot panels' semi-quantified densitometry from protein analysis is portrayed in a bar graph (P≤ 0.05).

CHR-NP inhibits the activation of the NLRP3 inflammasome.

TLR2/TLR4 activation of NF-kB promotes the formation of the NLRP3 inflammasome complex, which contributes to the caspase-1-dependent release of pro-inflammatory cytokines IL-1 and IL-18. Mounting data indicates that NLRP3 activation is closely connected to asthma pathogenesis. We used immunofluorescence to examine the expression patterns of NLRP3 inflammasome components in lung tissue. It was examined that NLRP3 and ASC were significantly upregulated in the lungs of OVA group mice (Fig 15 A). These elevations were significantly reversed by CHR-NP therapy, which was consistent with the effects on NF-κB. (Fig 15 A).

Finally, immunoblot examination of lung tissues indicated that NLRP3, ASC, and Caspase-1 β levels were higher in OVA group mice compared to Control group mice, demonstrated in (Fig 15 B). Furthermore, CHR-NP treatment lowered the levels in OVA-sensitized mice.

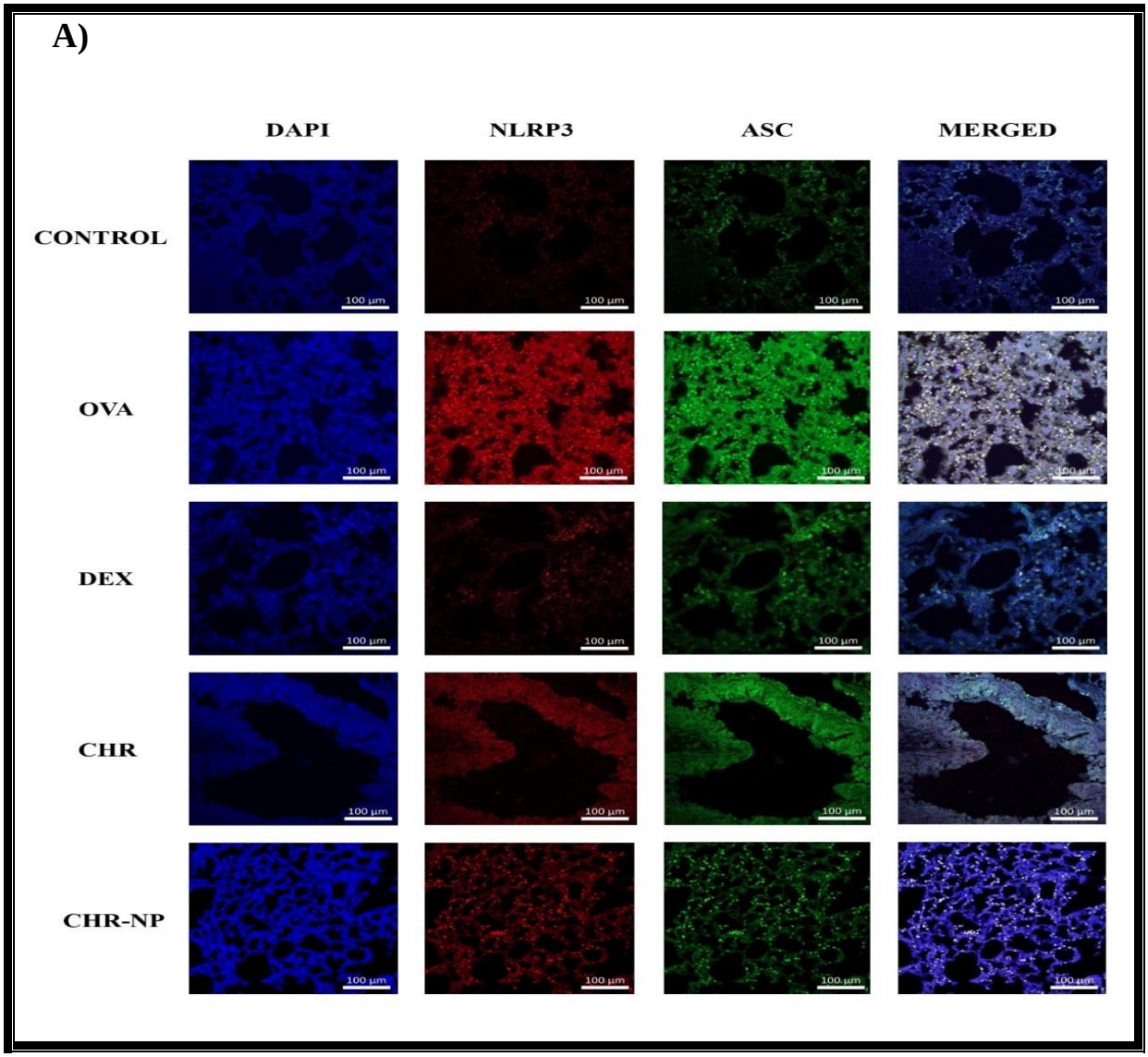
A)
DAPI
NLRP3
ASC
MERGED
CONTROL
OVA
DEX
CHR
CHR-NP
100 µm

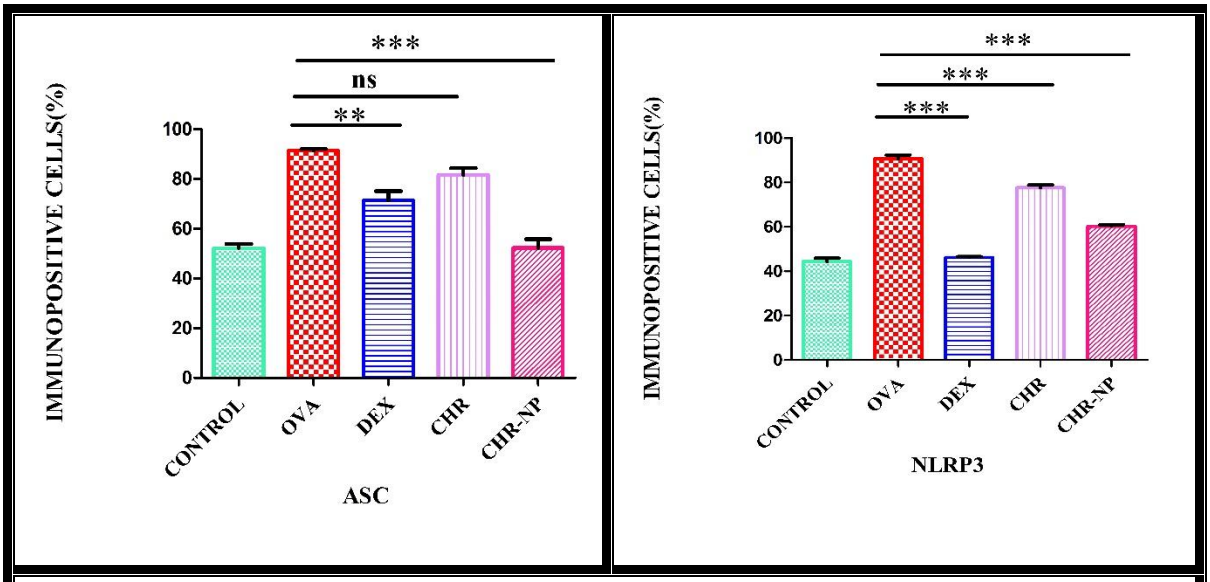

Fig 15:A) NLRP3 and ASC level of expression in mouse lung tissue from all experimental and control group were examined using immunofluorescence.

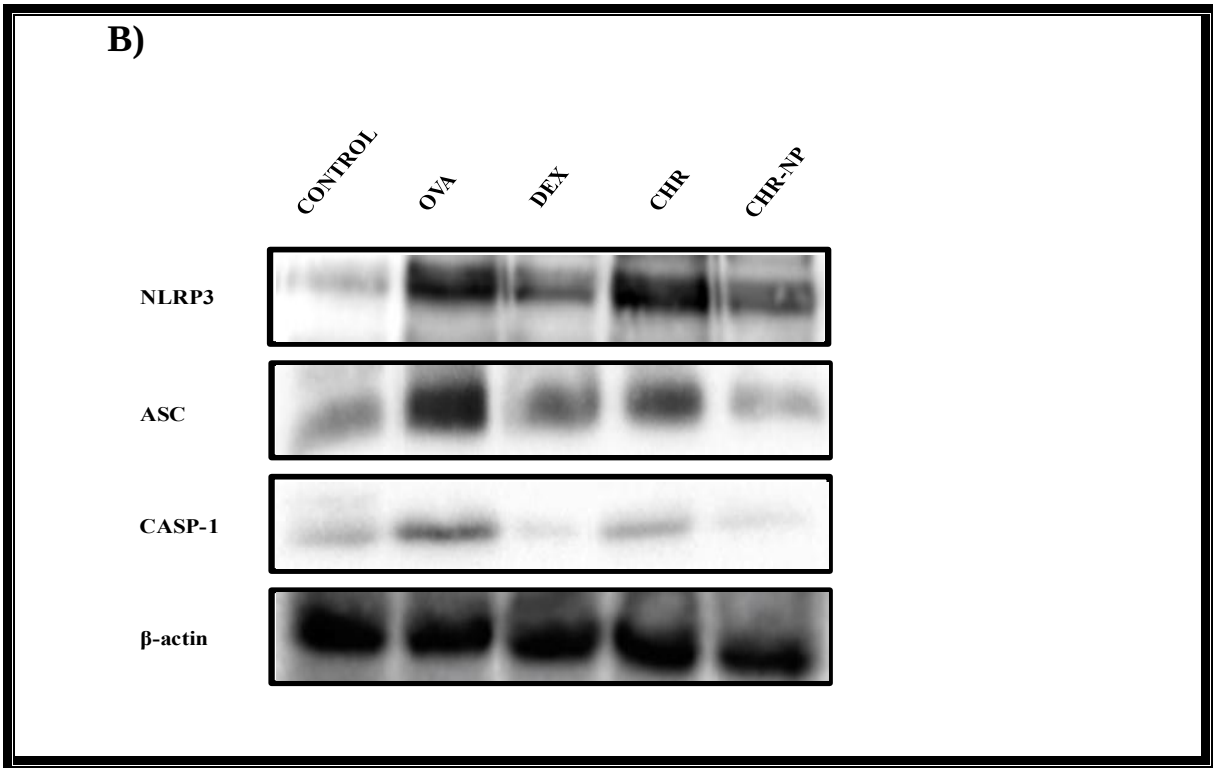

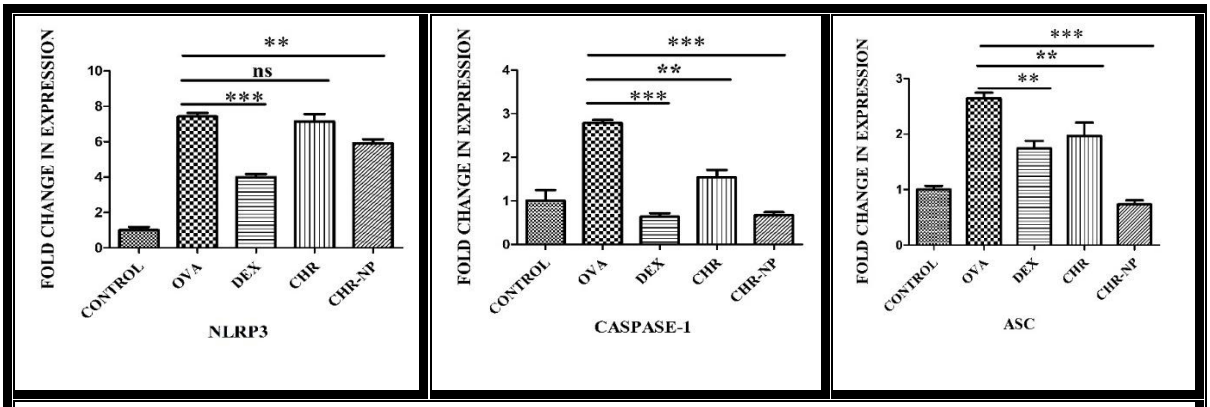

Fig 15:B) Analysis of NLRP3, ASC, and Caspase-1 expression levels utilizing Western blot. The western blot panels' semi-quantified densitometry from protein analysis is displayed in a bar graph (P ≤0.05).

DISCUSSION

We employed PLGA to make CHR-loaded nanoparticles (CHR-NP) with the aim of developing an oral delivery method for CHR, a promising anti-asthmatic drug with a low water solubility. Preclinical in vivo tests were used to assess the therapeutic potential of the particles, which were created using the nanoprecipitation process (Fessi et al., 1989b).

The nanoparticles that were synthesized had no discernible grooves on the surface and were round shaped. In biological systems, polymeric nanoformulation with microscopic sizes and sustained or progressive release patterns shows non immunogenicity, innocuity, and biodegradability(Panyam & Labhasetwar, 2003). In order to decrease phagocytosis, PLGA plays a crucial role by altering the size and thus affecting macrophage ingestion(Wang et al., 2018). Drug release, cellular uptake, and drug stability are all influenced by the size distribution and particle size of the nanoparticle. The small size of the drug greatly improves its ability to be absorbed in the body. The synthesized nanoparticles (CHR-NP) were within 100 nm and had slow sustained release accomplishing it as a better substitute than crude CHR.

Inflamed lungs have vascular leakage as an outcome of inflammation, and CHRNPs accumulate in the lung as a consequence of higher permeability of the capillary endothelium. This property has been well documented in the treatment of cancer utilizing nanoparticles.

This study also sought to investigate the efficacy of CHR-NP in allergic asthma model along with elucidation of the probable underlying cellular mechanism .

CHR-NPs suppressed OVA-induced lung histological alterations, inflammatory cell infiltration, and cytokine levels in BALF and serum more robustly than free CHR. The findings might be explained by the greater accumulation of CHR-NP in the inflamed lung compared to free CHR. Complex signalling networks coordinate airway inflammation. As a result, we still don't completely comprehend the molecular processes involved in it. TLR2/TLR-4 recognizes the allergen during its entrance into the lungs and influences the expression of downstream inflammatory molecules .The level of TLR2/4 were upsurged in our experimental OVA group which diminished after treatment with CHR-NP. NF-κB is present ubiquitously in nearly all types of cells and imposes immunological response in asthma(Schuliga, 2015a). In unstimulated cells , I-κB sequesters NF-κB in the cytoplasm(Solt & May, 2008). Nevertheless, NF-κB translocates into the nucleus via phosphorylation and degradation of I-κB , where it modulates transcription of target genes encoding various inflammatory proteins such as pro-inflammatory cytokines TNF-α, IL-6, and pro-IL-1β, all of which are connected to the pathophysiology of asthma. It has become increasingly clear that IL-6, in addition to being a B cell growth factor, is an important modulator of CD4 T cells. IL-6 stimulates autocrine IL-4 production during antigen stimulation of CD4 T cells(Rincón et al., 1997), which enhances Th2 differentiation via an autocrine feedback loop. Because the cytokine environment dictates the fate of effector CD4 + T cells, cytokines secreted by epithelial cells may impact local immune response.

It is consistent with the current study's findings that NF κB was overexpressed in lung tissue's nuclear fraction in the allergic asthma disease group. CHR-NP treatment decreased dramatically the degradation of I- κB, as well as the translocation of the NF-κ B p65 subunit into the nucleus. Thus, by suppressing the NF-κB pathway, IL-6 release is curbed. As a result, the Th2 differentiation of CD4 + T cells, which results in the production of IL-4, IL-5, and IL-13, is repressed.

Aside from NF-κB signalling, it has been proposed that NLRP3 inflammasome-mediated cytokine production plays a role in the pathogenesis of allergic airway inflammation (Latz et al., 2013), (Im & Ammit, 2014). CHR-NP effectively suppressed the NLRP3 inflammasome and its downstream proinflammatory cytokines.

As a result of our findings, it was inferred that CHR-NP is more effective than crude CHR in treating allergic asthma by addressing the underlying inflammation.

REFERENCES

Bousquet, J., Jeffery, P. K., Busse, W. W., Johnson, M., & Vignola, A. M. (2000). State of the Art Asthma From Bronchoconstriction to Airways Inflammation and Remodeling. In *Am J Respir Crit Care Med* (Vol. 161). www.atsjournals.org

Bousquet, J., Mantzouranis, E., Cruz, A. A., Aït-Khaled, N., Baena-Cagnani, C. E., Bleecker, E. R., Brightling, C. E., Burney, P., Bush, A., Busse, W. W., Casale, T. B., Chan-Yeung, M., Chen, R., Chowdhury, B., Chung, K. F., Dahl, R., Drazen, J. M., Fabbri, L. M., Holgate, S. T., … Zuberbier, T. (2010). Uniform definition of asthma severity, control, and exacerbations: Document presented for the World Health Organization Consultation on Severe Asthma. *Journal of Allergy and Clinical Immunology*, *126*(5), 926–938. https://doi.org/10.1016/j.jaci.2010.07.019

Du, Q., Gu, X., Cai, J., Huang, M., & Su, M. (2012). Chrysin attenuates allergic airway inflammation by modulating the transcription factors T-bet and GATA-3 in mice. *Molecular Medicine Reports*, *6*(1), 100–104. https://doi.org/10.3892/mmr.2012.893

Fessi, H., Puisieux, F., Devissaguet, J. P., Ammoury, N., & Benita, S. (1989a). Rapid Communication Nanocapsule formation by interfacial polymer deposition following solvent displacement. In *International Journal of Pharmaceutics*.

Fessi, H., Puisieux, F., Devissaguet, J. P., Ammoury, N., & Benita, S. (1989b). Rapid Communication Nanocapsule formation by interfacial polymer deposition following solvent displacement. In *International Journal of Pharmaceutics*.

Global Asthma Network The Global Asthma Report. (2018). www.globalasthmanetwork.org

Helal, M. G., Megahed, N. A., & Abd Elhameed, A. G. (2019). Saxagliptin mitigates airway inflammation in a mouse model of acute asthma via modulation of NF-kB and TLR4. *Life Sciences*, *239*. https://doi.org/10.1016/j.lfs.2019.117017

Im, H., & Ammit, A. J. (2014). The NLRP3 inflammasome: Role in airway inflammation. *Clinical and Experimental Allergy*, *44*(2), 160–172. https://doi.org/10.1111/cea.12206

Kawai, T., & Akira, S. (2011). Toll-like Receptors and Their Crosstalk with Other Innate Receptors in Infection and Immunity. In *Immunity* (Vol. 34, Issue 5, pp. 637–650). https://doi.org/10.1016/j.immuni.2011.05.006

Latz, E., Xiao, T. S., & Stutz, A. (2013). Activation and regulation of the inflammasomes. In *Nature Reviews Immunology* (Vol. 13, Issue 6, pp. 397–411). https://doi.org/10.1038/nri3452

Luo, X., Yu, Z., Deng, C., Zhang, J., Ren, G., Sun, A., Mani, S., Wang, Z., & Dou, W. (2017). Baicalein ameliorates TNBS-induced colitis by suppressing TLR4/MyD88 signaling cascade

and NLRP3 inflammasome activation in mice. *Scientific Reports*, *7*(1). https://doi.org/10.1038/s41598-017-12562-6

Marandi, Y., Farahi, N., & Hashjin, G. S. (2013). Asthma: Beyond corticosteroid treatment. *Archives of Medical Science*, *9*(3), 521–526. https://doi.org/10.5114/aoms.2013.33179

Mogensen, T. H. (2009). Pathogen recognition and inflammatory signaling in innate immune defenses. In *Clinical Microbiology Reviews* (Vol. 22, Issue 2, pp. 240–273). https://doi.org/10.1128/CMR.00046-08

Nakajima, H., & Takatsu, K. (2007). Role of cytokines in allergic airway inflammation. In *International Archives of Allergy and Immunology* (Vol. 142, Issue 4, pp. 265–273). https://doi.org/10.1159/000097357

Naz, S., Imran, M., Rauf, A., Orhan, I. E., Shariati, M. A., Iahtisham-Ul-Haq, IqraYasmin, Shahbaz, M., Qaisrani, T. B., Shah, Z. A., Plygun, S., & Heydari, M. (2019). Chrysin: Pharmacological and therapeutic properties. In *Life Sciences* (Vol. 235). Elsevier Inc. https://doi.org/10.1016/j.lfs.2019.116797

Panyam, J., & Labhasetwar, V. (2003). Biodegradable nanoparticles for drug and gene delivery to cells and tissue. In *Advanced Drug Delivery Reviews* (Vol. 55, Issue 3, pp. 329–347). Elsevier. https://doi.org/10.1016/S0169-409X(02)00228-4

Park, H. S., Kim, S. R., Kim, J. O., & Lee, Y. C. (2010). The roles of phytochemicals in bronchial asthma. *Molecules*, *15*(10), 6810–6834. https://doi.org/10.3390/molecules15106810

Peng, S., Gao, J., Liu, W., Jiang, C., Yang, X., Sun, Y., Guo, W., & Xu, Q. (2016). Andrographolide ameliorates OVA-induced lung injury in mice by suppressing ROS-mediated NF-κB signaling and NLRP3 inflammasome activation. In *Oncotarget* (Vol. 7, Issue 49). www.impactjournals.com/oncotarget/

Rincón, M., Anguita, J., Nakamura, T., Fikrig, E., & Flavell, R. A. (1997). Interleukin (IL)-6 Directs the Differentiation of IL-4-producing CD4 T Cells. In *J. Exp. Med* (Vol. 185, Issue 3).

Salazar, F., & Ghaemmaghami, A. M. (2013). Allergen recognition by innate immune cells: Critical role of dendritic and epithelial cells. In *Frontiers in Immunology* (Vol. 4, Issue NOV). Frontiers Media SA. https://doi.org/10.3389/fimmu.2013.00356

Schuliga, M. (2015a). NF-kappaB signaling in chronic inflammatory airway disease. In *Biomolecules* (Vol. 5, Issue 3, pp. 1266–1283). MDPI AG. https://doi.org/10.3390/biom5031266

Schuliga, M. (2015b). NF-kappaB signaling in chronic inflammatory airway disease. In *Biomolecules* (Vol. 5, Issue 3, pp. 1266–1283). MDPI AG. https://doi.org/10.3390/biom5031266

Solt, L. A., & May, M. J. (2008). The IκB kinase complex: Master regulator of NF-κB signaling. In *Immunologic Research* (Vol. 42, Issues 1–3, pp. 3–18). https://doi.org/10.1007/s12026-008-8025-1

Stompor-gorący, M., Bajek-bil, A., & Machaczka, M. (2021). Chrysin: Perspectives on contemporary status and future possibilities as pro-health agent. In *Nutrients* (Vol. 13, Issue 6). MDPI. https://doi.org/10.3390/nu13062038

Tran, H. B., Lewis, M. D., Tan, L. W., Lester, S. E., Baker, L. M., Ng, J., Hamilton-Bruce, M. A., Hill, C. L., Koblar, S. A., Rischmueller, M., Ruffin, R. E., Wormald, P. J., Zalewski, P. D., & Lang, C. J. (2012). Immunolocalization of NLRP3 Inflammasome in Normal Murine Airway Epithelium and Changes following Induction of Ovalbumin-Induced Airway Inflammation. *Journal of Allergy*, *2012*, 1–13. https://doi.org/10.1155/2012/819176

Wang, K., Feng, Y., Li, S., Li, W., Chen, X., Yi, R., Zhang, H., & Hong, Z. (2018). Oral delivery of bavachinin-loaded PEG-PLGA nanoparticles for asthma treatment in a murine model. *Journal of Biomedical Nanotechnology, 14*(10), 1806–1815. https://doi.org/10.1166/jbn.2018.2618

CHAPTER 5

STUDY ON ANTICANCER POTENTIAL OF CHRYSIN FUNCTIONALIZED GOLD NANOPARTICLE

Background

Lung cancer is the fastest - growing cause of cancer fatality in both men and women globally, with non-small-cell lung cancer (NSCLC) accounting for roughly 85 % of cases (Thai et al., 2021). Mostly, the patients with NSCLC are detected in late stages, making surgery unfeasible (Howington et al., 2013). Chemotherapy is the treatment modality for the majority of individuals with advanced lung cancer ; however, the toxicity caused by chemotherapy has limited its usage in clinical settings. Furthermore, despite the fact that chemotherapy alleviate cancer symptoms and improves quality of life, it can only extend patient survival for a few months at most in patients with late-stage malignancies. For advanced NSCLC, third-generation chemotherapeutic drugs like paclitaxel (PTX) in conjunction with a platinum compound is currently the prescribed first-line treatment.(Planchard et al., 2018) The systemic toxicity of PTX, on the other hand, is a concern. That being said, the systemic toxicity of PTX or platinum, as well as treatment resistance, has resulted in a high percentage of NSCLC mortality. As a result, it is crucial to establish novel NSCLC therapy strategies. When assorted therapeutics are used in conjunction to target multiple mechanisms during carcinogenesis, lung cancer prevention becomes more pragmatic and promising (Alkhatib et al., 2018; Kyakulaga et al., 2020).

Because of their implied biomedical uses, green synthesis of gold nanoparticles (AuNPs) has sparked a lot of attention. Green chemistry has garnered attention because it leverages plant extracts and other bioresources to create a nontoxic, clean, ecologically sound, and environmentally friendly alternative to the conventional physiochemical methodologies (Muniyappan et al., 2021).Chrysin is a naturally derived flavone that has been identified to have anti-tumor properties (Samarghandian et al., 2014).The goal of this investigation was to delve at lung cancer chemoprevention utilising a mechanism-based approach that included

low doses of paclitaxel (PTX) in combination with chrysin functionalized gold nanoparticle (CHR-AuNP).

Materials and Methods:

Chemical ingredients used in this study:

S. No.	Name	Source
1.	DMEM medium	HiMedia Laboratories, Mumbai, India
2.	Acridine Orange (AO)	Invitrogen (California).
3.	Ethidium bromide (EtBr)	Invitrogen (California).
4.	Tetrachloroauric acid (HAuCl4)	Sigma-Aldrich Co, St Louis, MO, USA
5.	Chrysin (CHR) (purity ≥ 97.0%)	Sigma-Aldrich Co, St Louis, MO, USA
6.	Propidium iodide (PI)	Sigma-Aldrich Co, St Louis, MO, USA
7.	Caspase-3/9 assay kit	Santacruz Biotechnology (Santa Cruz, CA, USA)
8.	Cytochrome-c assay kit	Invitrogen Corporation, Camarillo, CA USA
9.	3-(4,5-Dimethylthiazol-2-yl)-2,5-diphenyltetrazolium bromide	Calbiochem
10.	4,6 -diamidino-2-phenylindole (DAPI)	Sigma-Aldrich Co, St Louis, MO, USA
11.	Fetal bovine serum (FBS	Sigma-Aldrich Co, St Louis, MO, USA
12.	Penicillin-Streptomycin	Hi Media Laboratories, Mumbai, India
13.	primary antibodies	Santa Cruz Biotechnology (Santa Cruz, CA)

14.	Secondary antibodies	Santa Cruz Biotechnology (Santa Cruz, CA)
15.	Annexin-V/FITC kits	Calbiochem
16.	Rhodamine 123	Calbiochem
17.	A549 cell line	National Centre for Cell Science (Pune, India)
18.	Trypsin	Gibco BRL(Grand Island, USA)
19.	Cell culture plastic	NUNC(Denmark)
20.	Protein assay reagent, BCA	Pierce
21.	Dimethylsulfoxide (DMSO)	Merck Life Science Pvt. Ltd., Bengaluru
22.	Bovine serum albumin (BSA)	Sigma-Aldrich Co, St Louis, MO, USA
23.	Cell lysis buffer	Abcam

Methods

Green synthesis of CHR-AuNP

Gold nanoparticles (CHR-AuNP) were synthesized in this study by reducing the gold salt (HAuCl4) with CHR, as previously mentioned in the literature with some minor modification.

In brief, the following steps were followed to synthesis of CHR-AuNP. 20 ml of aqueous Chrysin (CHR)(1mM) solution was prepared firstly with the addition of a few drops of 0.1N NaOH to increase CHR solubility. The CHR solution was then added dropwise to a 20 mL

aqueous solution of HAuCl4 (1 mM) and stirred for 30 minutes. The aqueous HAuCl4 solution changed its colour from pale yellow to ruby red, confirming the synthesis of CHR-AuNPs (Ahmed et al., 2016).

Characterization of CHR-AuNP

The synthesized CHR-AuNP were characterised utilising UV absorbance spectroscopy, DLS, AFM, and FTIR methods in accordance with the conventional procedure.

UV-visible spectral analysis

The synthesis of CHR-AuNPs was verified by analysing the absorption spectra between 400 to 700 nm. The absorbance band of AuNPs is directly dependent on the nanoparticle size. A UV-Visible spectrophotometer (Lambda 35, Perkin Elmer) was used to record the UV-Visible spectra of CHR-AuNPs utilizing 1 cm quartz cuvette.

Analysis of Particle Size

The particle size and zeta potential were determined using a Malvern, Nano-ZS 90. The mean nanoparticle diameter was estimated using differential light scattering (DLS) on 12 mm cells at 90 ° and 25°C. The nanoparticles were diluted in distilled water prior to the measurements, and 500 µl of the nanoparticle were filtered via a syringe filter (0.45 m) and collected and loaded into the cuvette for DLS.

Fourier transform infrared spectral analysis (FT-IR)

An FTIR spectroscopic analysis was carried out using a Perkin Elmer FT-IR spectrometer (MA, USA) to investigate molecular absorption and transmission bands or peaks caused by the vibration frequencies of atomic bonds. FTIR spectroscopy was used to analyse CHR-

AuNP and compared with CHR. The FTIR spectrum was obtained between 400 and 4000 -1 cm range.

Atomic force microscopy (AFM)

Atomic force microscopy (AFM) was employed to investigate the physical topography of CHR-AuNP in contact mode on an Agilent Technologies 5500 (CA). After diluting the nano particles in distilled water, a 5 µl test drop was placed on the mica sheet. The sample solution was then allowed to dry on the mica sheet for 15-25 minutes before being analysed with AFM.

Cell culture

A549 cultures were maintained in tissue culture flasks. DMEM medium was used for cell culture.10% FBS and 1% antibiotic was supplemented in the media for cell growth and optimum temperature of 37°C was maintained in a CO2 incubator with 5% CO2.

Cell viability assay

The cytotoxicity of CHR-AuNP, CHR, and PTX on A549 was explored by performing MTT assay and compared with untreated cells. The investigational drugs were administered in varied doses to confluent cells after growing them overnight and then incubated for 24 hours. Each well, including the control well, received a 20µl MTT solution. The crystals that were produced at the end of 4 hours incubation at 37°C were thereby dissolved in DMSO. The absorbance was measured at 595 nanometers (nm).

Annexin V Assay

The cytotoxicity of CHR-AuNP, CHR, and PTX on the carcinoma cell line was investigated. The Annexin-V test was used to assess the degree of apoptosis in cells. To measure PS

(phosphatidyl serine) exposure, A549 cells were double stained with Annexin-V/PI. The lung cancer cells were incubated in a predetermined ratio of CHR-AuNP, PTX, and their combination. The control cells were not treated. For the analysis, all cells were washed with PBS and trypsinized before staining with Annexin-V-FITC and PI, as specified by the manufacturer. Flow-cytometric analysis was used to determine the percentages of living and necrotic cells.

Mitochondrial Membrane Potential (MMP)Quantitation

MMP regulation is important for homeostasis, and its depolarization indicates apoptosis, as typically measured with the JC-1 dye. A drop in the red to green ratio suggests mitochondrial depolarization. The treated and untreated A549 cells were preincubated for 30 minutes with 2 µl of JC-1 dye (Invitrogen) before being detected. JC-1 aggregates were observed at excitation/emission wavelengths of 590/610 nm, while monomers were discovered at excitation/emission wavelengths of 485/535 nm. BD LSR fortessa flow cytometry (Becton Dickinson, San Jose, California, USA) were used to examine the samples. Spectroflourometrically, Rhodamine-123 dye was used and the emission was measured at 535 nm.

AO/EtBr staining

DNA dyes AO and EtBr are used extensively to study morphological characteristics of cellular apoptosis. Both live and dead cells might be stained by AO. EtBr enters necrotic cells with permeable membranes and turns them red. Because of AO penetration, live cells appear uniformly green. Cells in the early stages of apoptosis appear vivid green. This vividity is owing to chromatin condensation and chromatin DNA cleavage into internucleosomal fragments. The Orange staining is associated with late apoptotic cells due to EtBr absorption. Control and treated cells were stained with AO/EtBr to draw a distinction between live,

apoptotic, and necrotic cells. This investigation of nuclear damage or chromatin condensation of the cells was carried out under a fluorescence microscope (Olympus, Tokyo, Japan). Cells seeded in six-well plates for 24 hours were exposed to CHR- AuNP, PTX individually and in combination. Following the treatment, 20 µL of acridine orange/ethidium bromide dye mixture was administered in each well. The cells were then counterstained with DAPI and inspected under a fluorescence microscope.

ROS assay: DCF-DA was used to monitor reactive oxygen species accumulation. DCF-DA is an oxidation sensitive reagent. Following treatment with CHR-AuNP, PTX, and their combinations, the cell samples were kept in incubation for 15 minutes at 37 °C with 20mM DCF-DA. The cell pellets from treated and untreated group had to be harvested and resuspended in PBS solution (0.5 ml). The fluorescent chemical 2′,7′-dichlorofluorescein was formed as a result of oxidation of DCF-DA by intracellular reactive oxygen species (ROS). The samples were then examined using BD LSR fortessa flow cytometry. The wavelength of excitation was 480 nm, while the wavelength of emission was 525 nm.

Cell Death Assay

Enzyme linked Immunoassay was performed to measure histone-associated DNA fragments in the cytoplasm of treated and untreated cells according to the supplier's (Sigma-Aldrich, St. Louis, USA) instructions.

Caspases 3/9 and Cytochrome C assay

Colorimetric Assay Kits were employed to detect caspase 3/9 and cytochrome C. In brief, cells were plated and cultured at 37°C for 24 hours before being treated with CHR-AuNP, PTX and their combination for 48 hours with untreated cells serving as controls. Both treated

and untreated cells were collected, and then lysates were prepared to be utilised in the study as directed by the manufacturer.

Western blot

A549 cells were treated with CHR, CHR-AuNP and PTX. Cells were then lysed and protein were estimated with the help of BCA reagent. Cell lysates from drug-treated and untreated cells were then mixed with loading dye (4:1) and electrophoresed on a 10 – 15% SDS polyacrylamide gel. After the protein separation the gel was transferred to PVDF membranes and blocked with 5% BSA, washed with washing buffer, and lastly incubated overnight with primary antibodies to particular proteins which were to be analysed. After the overnight incubation, the membranes were washed with wash buffer. The membranes were then further incubated with secondary antibodies which were conjugated with horseradish peroxidase for 2 hours in the next day. Finally, protein expression was measured in a chemidoc system using the horseradish peroxidase substrate (peroxidase/luminol).

Confocal microscopy

The effect of CHR-AuNP, PTX and their combination on different protein expression in A549 cells were explored using immunocytochemical techniques using Olympus FV10i automated laser scanning confocal microscope.

Synergism analysis by Compusyn software

The CompuSyn Software was used to determine the fraction affected (Fa) and combination index (CI) values for synergism and statistical analysis (www.combosyn.com). Synergism, additive effect, and antagonism were signified by CI values of 1, 1, and >1. The mean of at least three different experiments was used to obtain the results, and the error bars reflected

the standard deviation (SD). To analyze two distinct groups, a two-tailed Student's t test was applied, with significance determined as *P 0.05, **P 0.01 and ***P 0.001. (Chou, 2010)

Result

Physical characterisation of CHR-AuNP

CHR-AuNP had a distinctive wine red colour (Fig. 1A) Nanoparticle formation was ascertained with the appearance of band at 540 nm (Fig.1B). According to AFM tests, the surface architecture of CHR-AuNP particles was uniform, with a spherical shape and sizes spanning from 40 to 60 nm (Fig. 1E and 1F). The differential light scattering (DLS) study indicated that the size of CHR-AuNP particles ranged between 35 and 70 nm (Fig. 1C), and the zeta potential observed was -22 mV (Fig.1D), indicating that the particle is relatively stable. The zeta potential is regarded as an important parameter of the stability of the produced CHR-AuNPs. The zeta potential assesses the extent of electrostatic interaction between adjoining particles and particles having zeta potential ±10 to ±30 are typically stable.

Hence our formulated nanoparticles were not only uniformly nanosized but also stable in nature.

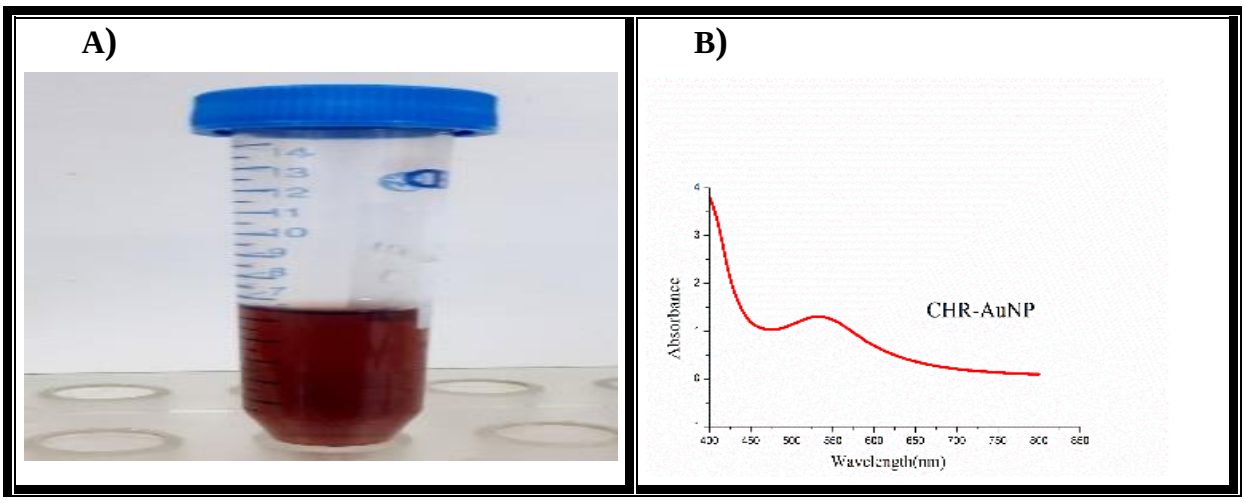

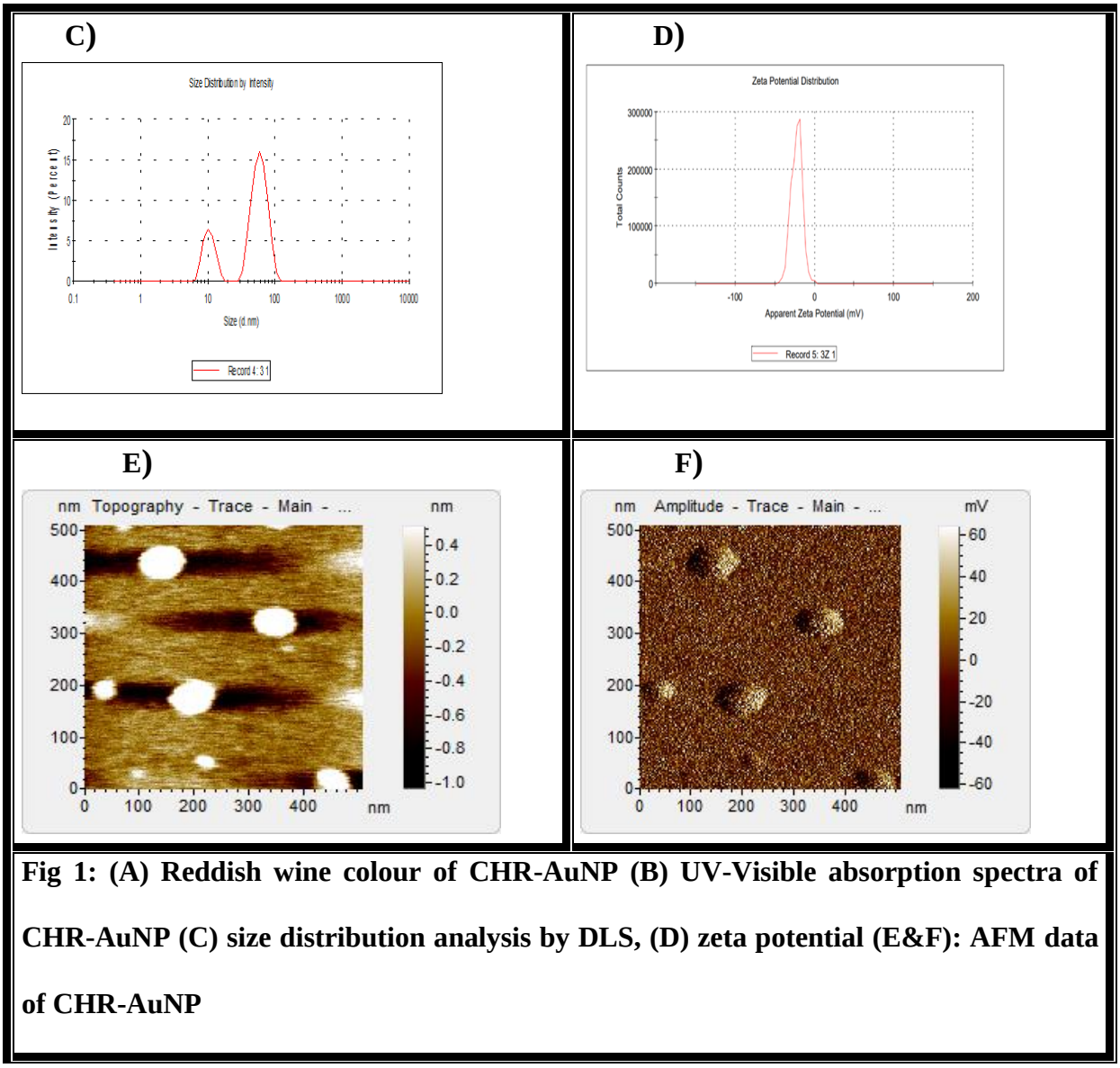

Fig 1: (A) Reddish wine colour of CHR-AuNP (B) UV-Visible absorption spectra of CHR-AuNP (C) size distribution analysis by DLS, (D) zeta potential (E&F): AFM data of CHR-AuNP

FTIR analysis

The existence of distinct functional groups in free CHR and CHR-AuNP was investigated using FTIR analysis. The bands 3500-3000 correspond to symmetrical and assymetrical O-H stretching modes. There is an alteration in the amount of transmittance at 3500-3000 after reduction. The intensity variation represents a loss of one -OH group during coordination to a metal ion. The shift of the strong band at 1648 to 1618 reflects the functionalization of CHR on CHR-AuNP via the C=0 oxygen atom. (Fig 2)

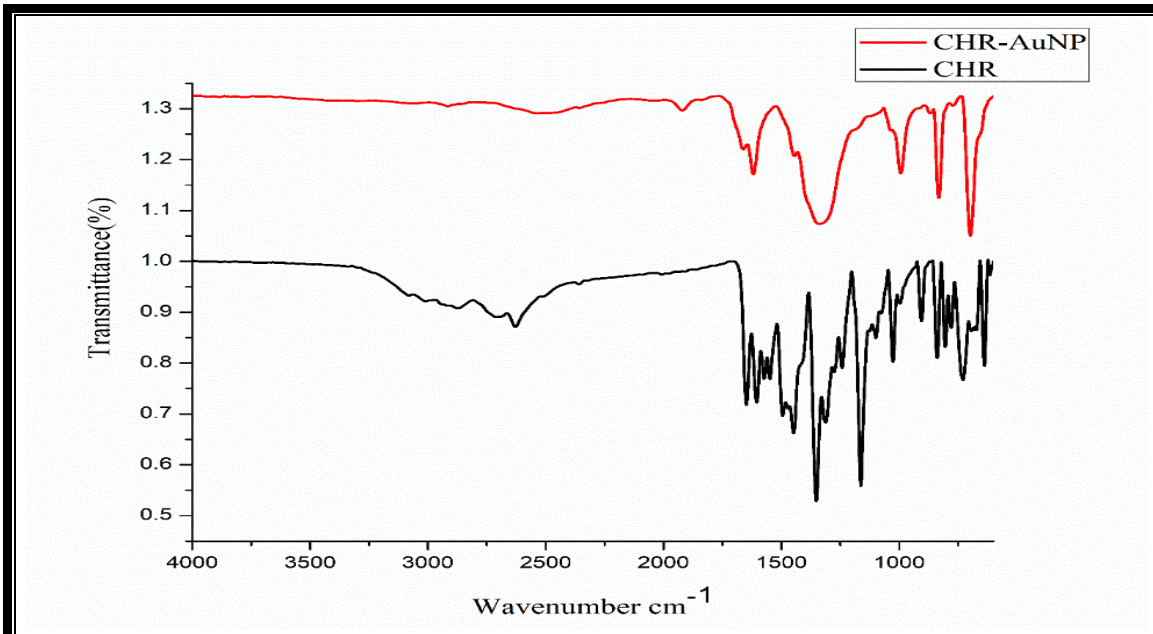

Fig 2: FTIR analysis of CHR and CHR-AuNP

Cell viability study

In this investigation, the MTT test was used to examine the cytotoxic effects of CHR, CHR-AuNP, and PTX on the lung cancer cell line A549. All three compounds inhibited cell growth time and dose dependently (Fig. 3A-3C), but not in normal human bronchial epithelial cells (NHBE) (data not shown). When combined, CHR-AuNP inhibited CHR cell growth approximately twice as much as CHR alone, and it also significantly increased the cytotoxicity of PTX (Fig. 3D). Pharmacotherapy of CHR-AuNP IC20 (2.5 mg/ml) with PTX IC20 (2.5 nM) resulted in an estimated 58.6 % cytotoxicity. The combination of IC20 CHR-AuNP and PTX IC30 has a cytotoxicity of around 72% (4 n M).

Similarly, an increase in cytotoxicity was seen following treatment with PTX IC30 and CHR-AuNP IC30 (Fig. 3E). As a result, the findings suggest that CHR-AuNP can promote the cytotoxic potential of PTX.

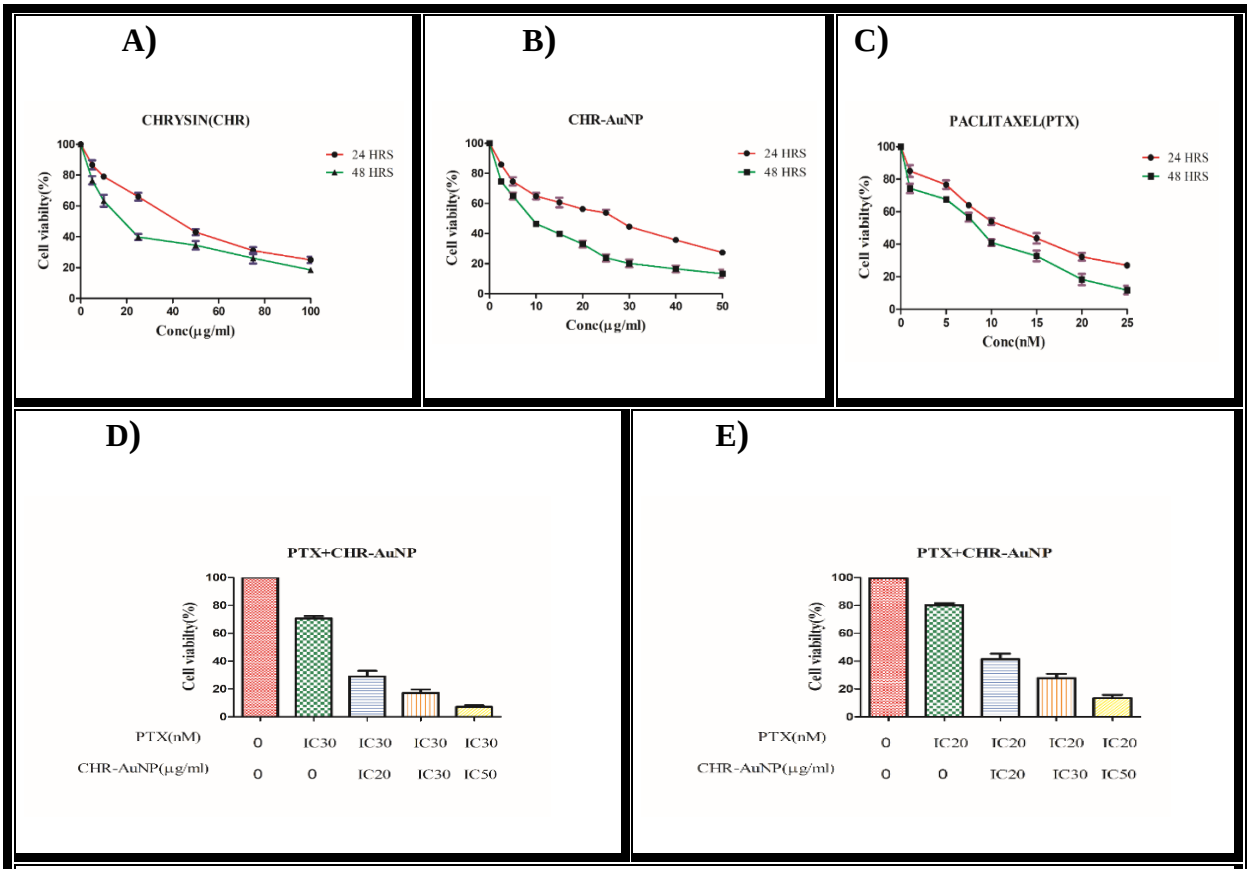

Fig 3: MTT assay of (A) CHR, (B) CHR-AuNP, and (C) Paclitaxel (PTX) for 24 hrs and 48 hrs respectively (D) IC20 of PTX in combination with different doses of CHR-AuNP, E) IC 30 of PTX in combination with different doses of CHR-AuNP for 48 hrs.

Cytotoxic Synergy

We evaluated the combined impact of CHR-AuNP and PTX in different ratios to assess the level of synergism between these two drugs. Cell viability was considerably decreased after treatment, and the effects were more severe in the co therapy compared to individual therapy (Fig 4 A). The combination index values (CI) for various treatment ratios in A549 cells were further analysed using the Isobologram analysis method. (Fig 4 B)

A) CI Data : (CHR-AuNP+ PTX)

CHR-AuNP	PTX	Effect	CI
2.5	2.5	0.586	0.49079
4.5	2.5	0.721	0.35642
9.5	2.5	0.865	0.24165
2.5	4.0	0.71	0.36946
4.5	4.0	0.84	0.21323
9.5	4.0	0.925	0.14218

Fig 4: A) Combination index

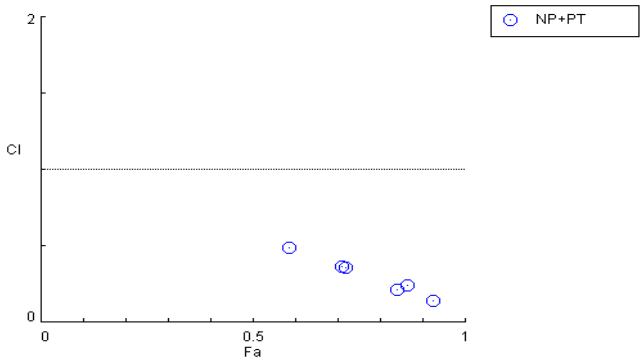

Fig 4: B) Fa-CI plot depicts the synergism between CHR-AuNP and PTX

The combined effect of CHR-AuNP and PTX promoted apoptosis

Apoptosis is a well-coordinated process with distinct morphological and molecular changes. Dual staining was performed in A549 cells after treatment with acridine orange / ethidium bromide (AO/EtBr) to monitor various types of apoptosis-induced morphological changes and visualised under a light microscope. The cells treated with CHR-AuNP (IC20) + PTX(IC20) for 48 hours exhibited apoptosis-like rounding and shrinkage. Control cells counterstained with DAPI exhibited intact blue nuclei whereas the treated cells showed brighter fragmented nuclei. Complete green nuclei in control group cells were indicated by AO/EtBr staining. When stained, live cells showed green because they had only taken up AO. However in treated cells yellow, orange, and reddish fragmented nuclei were seen. Due to the predominance of EtBr absorption, late apoptotic cells have orange to red nuclei with constricted or broken chromatin. When cells were treated with a CHR-AuNP+PTX combination rather than the IC20 of individual medicines alone, the impact of apoptosis was more pronounced.

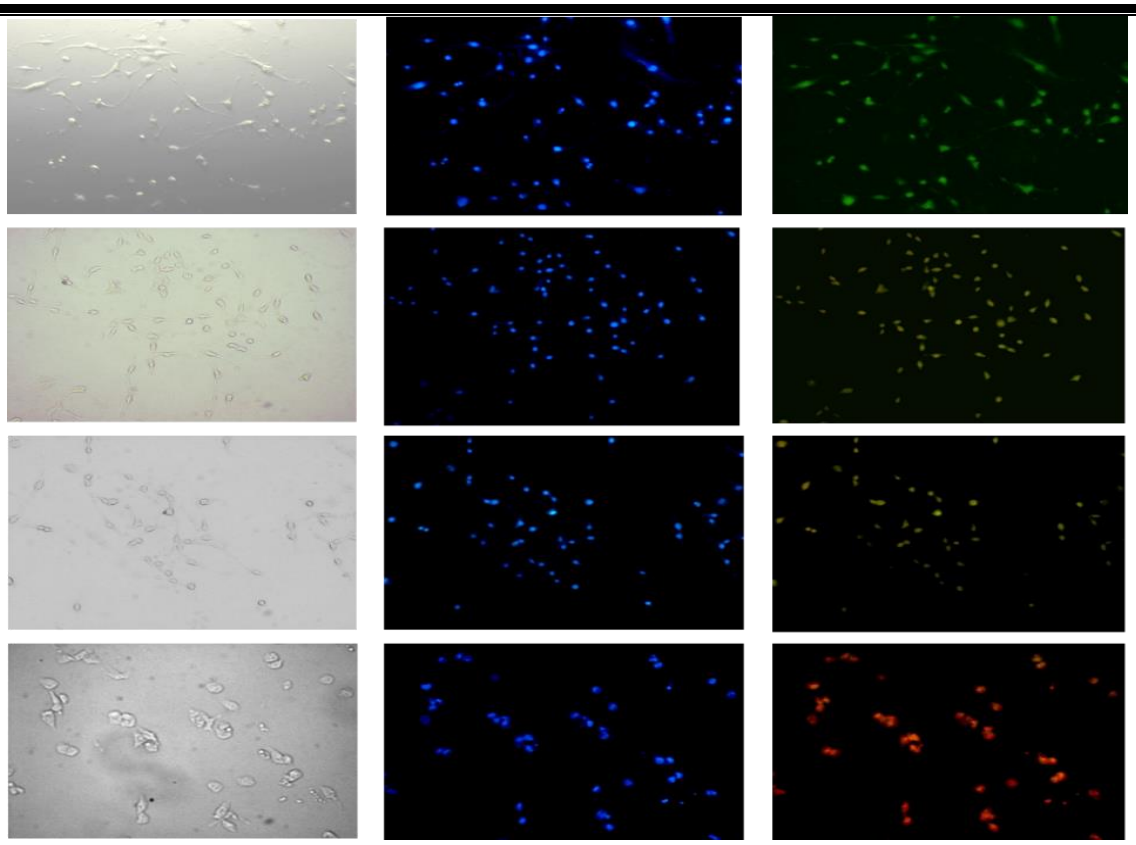

Fig 5: AO/EtBr dual staining of A549 cells untreated and treated with IC 20 concentration of CHR-AuNP, PTX and their IC20 combination. The images were taken with fluorescent microscope and represent one of the three independent experiments.

A549 cells treated with CHR-AuNP, PTX, and CHR-AuNP+ PTX increased Annexin V positive cells

When apoptosis happens, PS is released out from inner membrane to outside membrane. The concentration of PS in the outer membrane of A549 cells following treatment with IC20 of PTX , CHR-AuNP and CHR-AuNP (IC20) + PTX(IC20) combination for 24 h was examined by Annexin-V/FITC assay kit. The percentage of apoptotic cells (determined by the annexin positive cells) quantified by flow cytometry was greater in CHR-AuNP, PTX, and CHR-

AuNP+PTX treated cells than in control cells (Fig. 6A). Thus, apoptosis is associated in CHR-AuNP and CHR-AuNP+ PTX- induced cell death**.** The graphical representation of the same represented in (Fig. 6B).

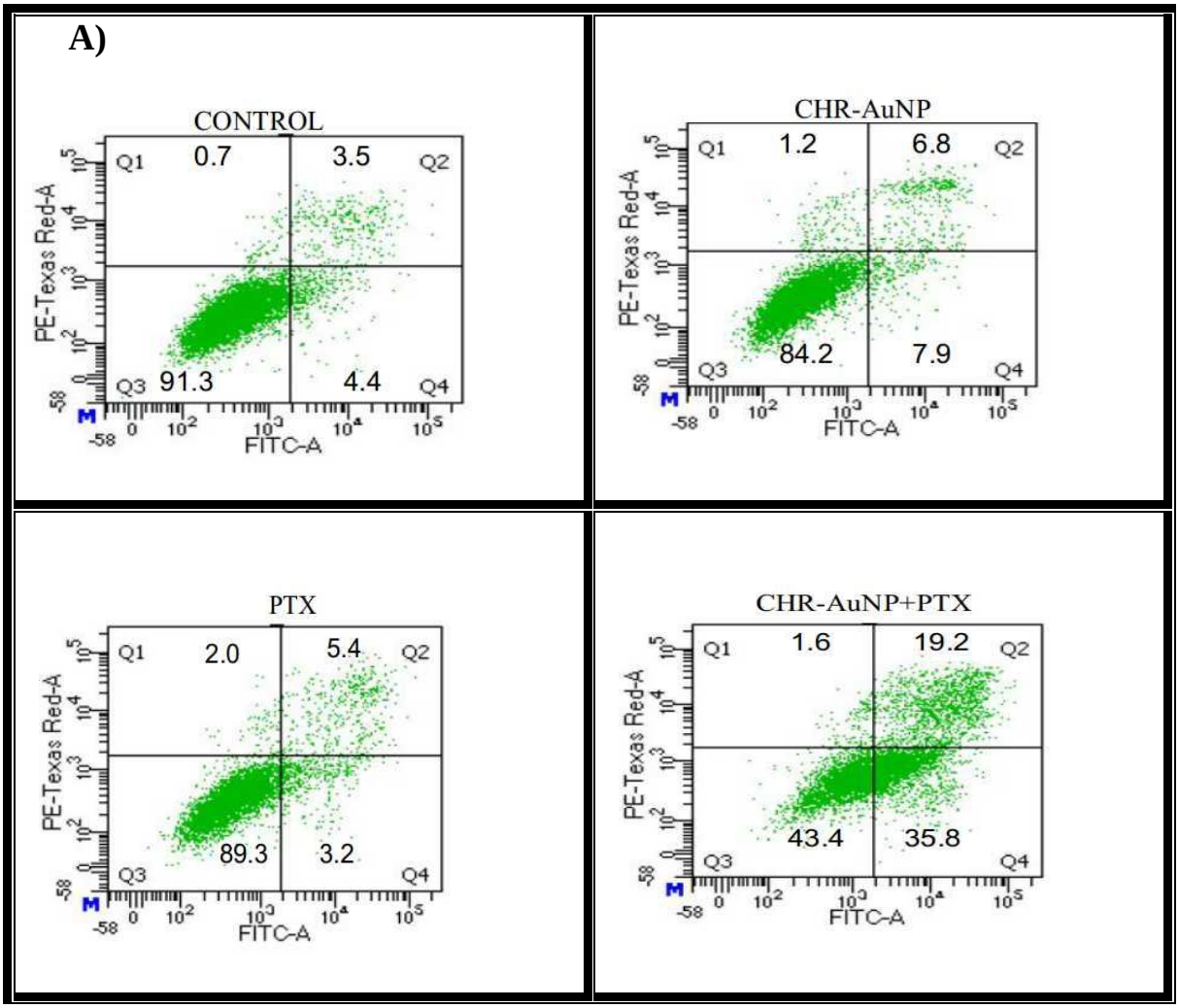

B)

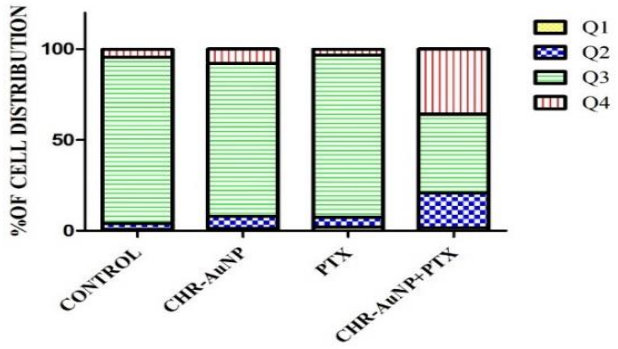

Fig 6: Comparative study of apoptotic death induced by CHR-AuNP, PTX and CHR-AuNP+PTX on A549 cells.

(A) A549 cells were treated with CHR-AuNP, PTX and combined doses CHR-AuNP+PTX and were analyzed by Flow-cytometry using Annexin-PI staining.

(B) represents the graphical parameters of these. Data presented here are the representation of three independent experiments.

CHR-AuNP+PTX augments ROS accumulation:

ROS generation triggered by gold nanoparticles plays a prominent role in cancer cell death.

ROS were generated in A549 cells by CHR-AuNP, PTX, and their combinations (Fig. 7A). The combined therapy of CHR-AuNP+PTX increased ROS production. Flow cytometry studies revealed that NAC (1mM) reduced ROS generation by CHR-AuNP, PTX, and their combinations.(Fig 7 B) Spectrofluorimetrically ROS formation was also determined (Fig 7C) and it was discovered that the treatment of A549 cells with combined drug therapy boosted production of ROS.

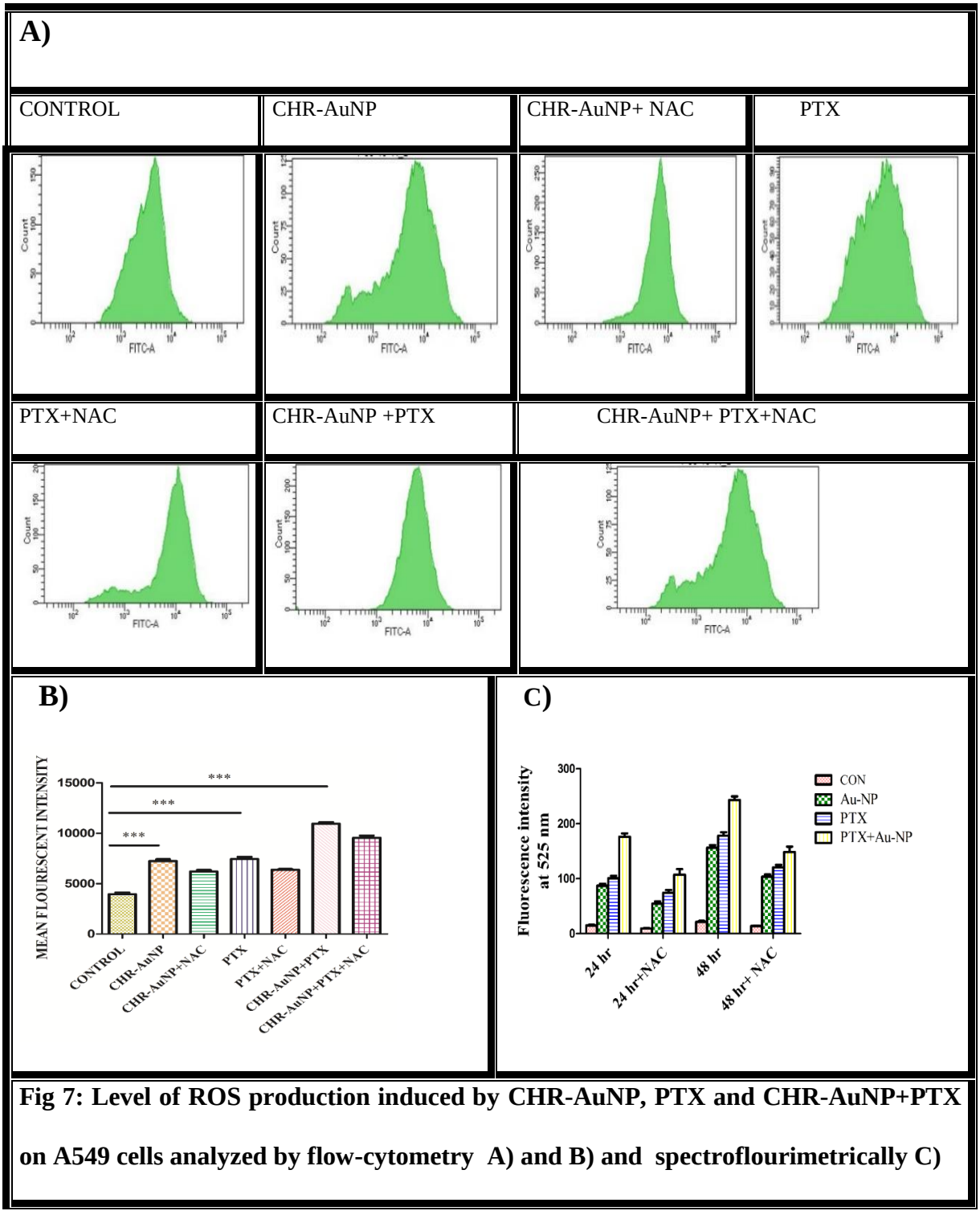

Fig 7: Level of ROS production induced by CHR-AuNP, PTX and CHR-AuNP+PTX on A549 cells analyzed by flow-cytometry A) and B) and spectroflourimetrically C)

CHR-AuNP and PTX combination generated ROS-dependent DNA damage.

ROS have the potential to trigger DNA damage in cells. DNA fragmentation was analyzed using a spectrofluorimeter after A549 cells were incubated with CHR-AuNP, PTX, and their combination. It was seen that with combination therapy DNA damage was escalated. Fig 8

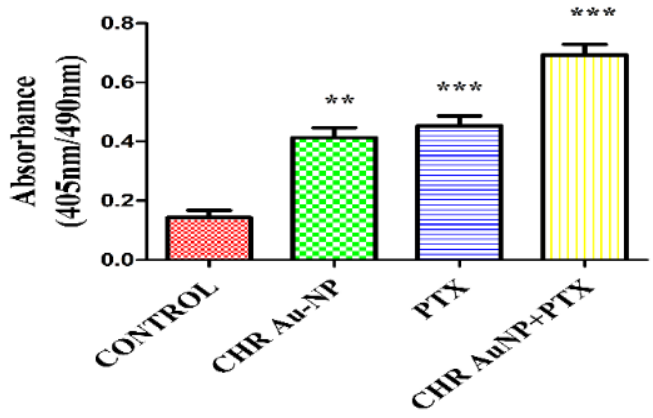

Fig 8: DNA fragmentation study in A549 cell colorimetrically

CHR-AuNP and PTX co -therapy promote cell death in A549 cells by the mitochondrial route of apoptosis

Cellular apoptosis occurs by an intrinsic (mitochondrial) or extrinsic pathway, or both. The downward shift of mitochondrial membrane potential (MMP) occurs very early in the apoptotic pathway because the opening of the mitochondrial membrane permeability transition pore (MPTP) is essential to commence the mitochondrial apoptotic pathway. This may be determined by using JC-1 dye . The quantification is done via flow cytometry by measuring the reduction in the ratio of red to green fluorescence caused by the conversion of

JC-1 aggregates to monomers. Also by the employment of Rhodamine 123 dye mitochondrial membrane potential can be determined spectroflourimetrically.

Flow cytometry and spectroflourimetric analysis revealed that CHR-AuNP, PTX, and their combination reduced mitochondrial membrane potential (MMP) and increased cytosolic cytochrome c levels (Fig 9 A, B, C) 24 hr after the administration of CHR-AuNP, PTX, and their combination. Caspase-9 and caspase-3 levels were measured to determine where the apoptosis was through mitochondrial or non-mitochondrial pathway. (9D,9E).

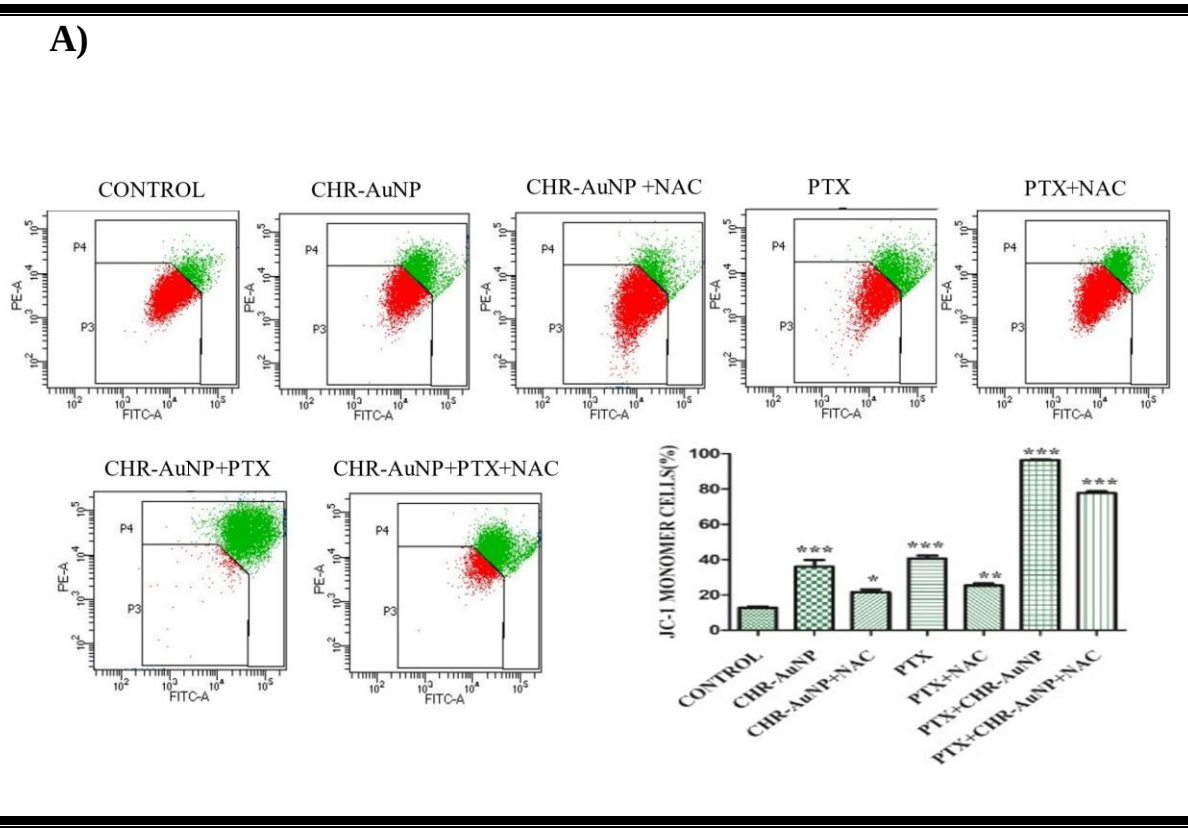

Fig 9: A) Mitochondrial membrane potential of A549 cell treated with CHR-AuNP, PTX and their comibination in presence and absence of 1mM NAC was analyzed by flow cytometry

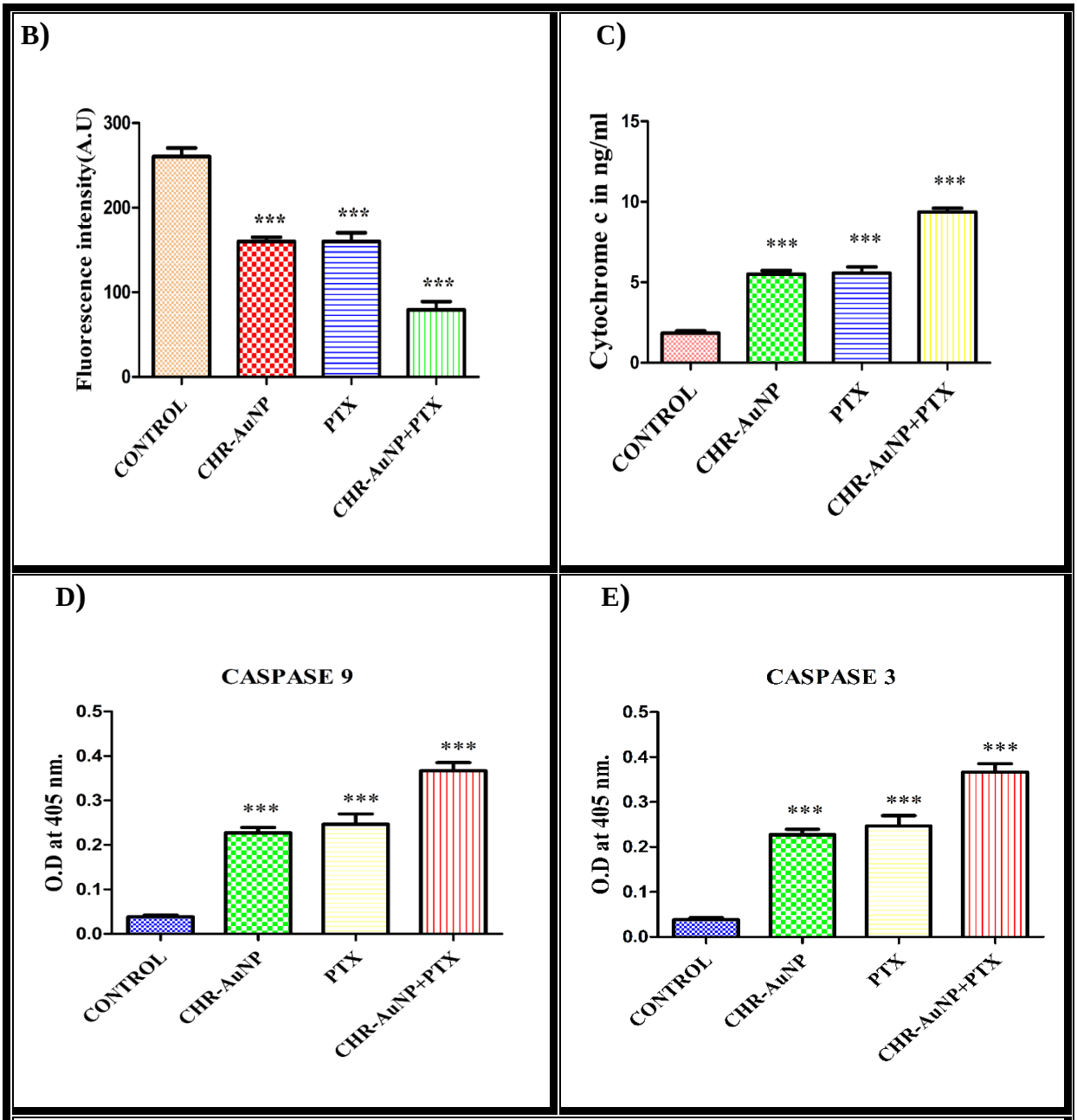

Fig 9: B) Mitochondrial membrane potential of A549 cell treated with CHR-AuNP, PTX and their combination was measured by spectroflourimetry using Rhodamine 123 and change in O.D is evaluated. C) Cytochrome C level alteration determined via spectroflourimetric assay. D)&E) Levels of activated Caspase-3 and Caspase-9 were assayed colorimetrically by ELISA kits

CHR-AuNP, in conjunction with PTX alters the expression of pro- and anti-apoptotic proteins in A549 cells

The initiation of apoptosis is accompanied by a significant contribution of pro- and anti-apoptotic markers . In western blot examination, CHR-AuNP, PTX, and combination enhanced the levels of pro-apoptotic Bax, Bcl2 protein expression, and enhanced cytosolic cytochrome C releasev compared to the untreated control (Fig. 10A). Furthermore, overexpression of p- p53 and p21 were identified in immunofluorescence investigation (Fig10 B). These findings imply that CHR-AuNP+ PTX-induced cytotoxicity is caused by an increase in pro-apoptotic /anti-apoptotic protein ratio. The relative expression of the proteins obtained in western blot were plotted graphically and represented in (Fig. 10 C)

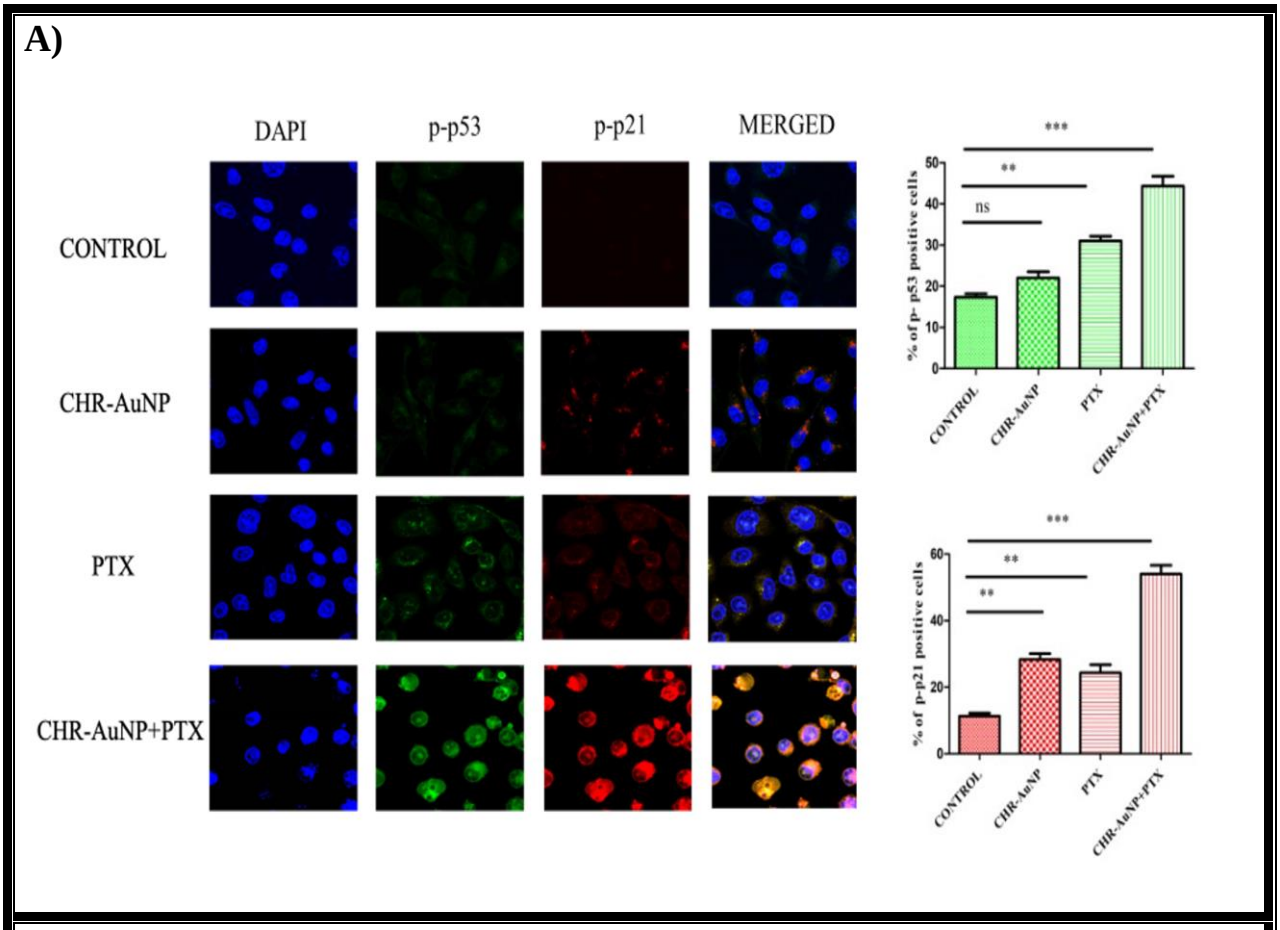

Fig 10: A) Immunoflourescence analysis of p-p53, p-p21 expression on A549 cells treated with CHR-AuNP, PTX, CHR-AuNP+ PTX

B)

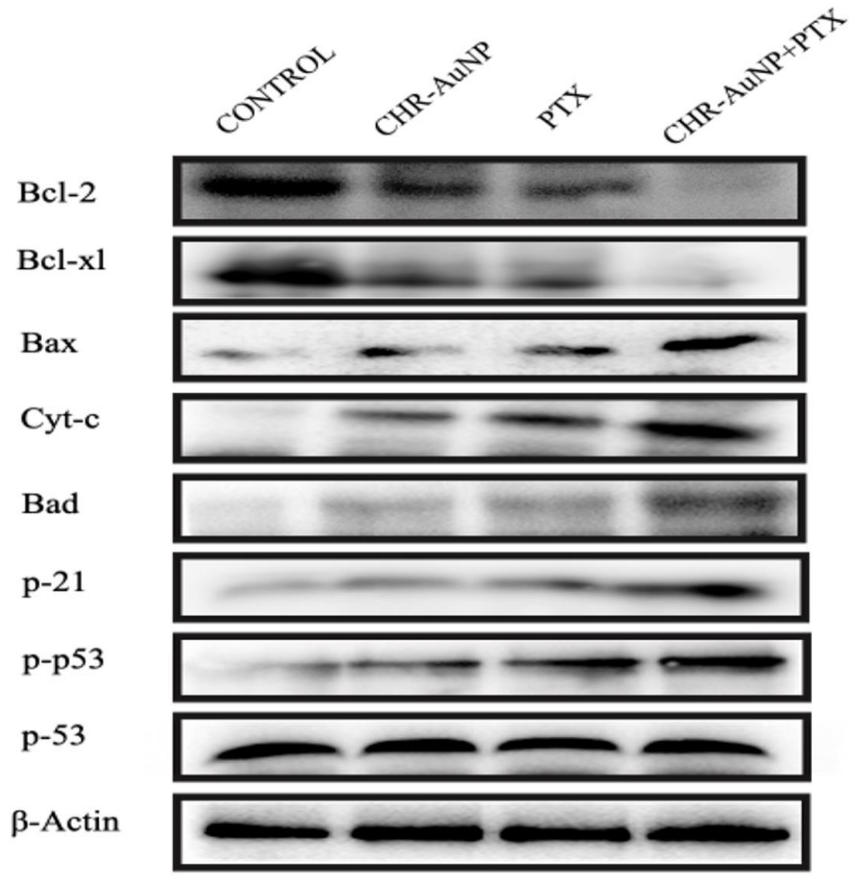

Fig 10: B) Western blot analysis were performed on A549 cells treated with CHR-AuNP, PTX, and CHR-AuNP+ PTX to detect the pro-apoptotic and anti-apoptotic molecules

C)

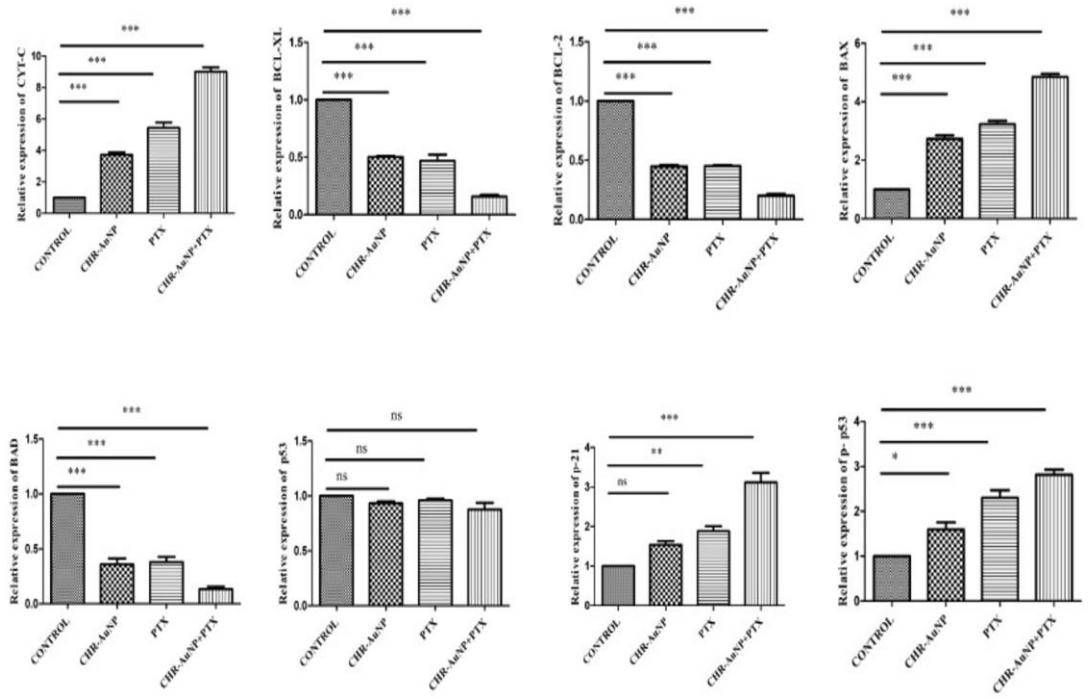

Fig 10: C) Relative expression of pro and antiapoptotic molecules in A549 cells treated with CHR-AuNP, PTX, and CHR-AuNP+ PTX

CHR-AuNP combined with PTX activates PPAR-ϒ via blocking the PI3k-Akt pathway

Overactivated PI3K/Akt pathway is implicated in cancer cell growth. The PI3K/Akt pathway is mostly inhibited by PTEN. PTEN is a non-redundant phosphatase that modulates the toxic and carcinogenic pro-survival PI3K-Akt signalling pathway. Earlier research found that PPAR-ϒ agonists' tumour suppressor and anti-inflammatory functions were mediated by PTEN overexpression in colorectal and breast cancer cells (Patel et al., 2001). (To et al., 2018) PTEN was also reported to be upregulated by PPAR-ϒ agonists, blocking the PI3K-Akt signalling pathway in lung cancer cells (Salmena et al., 2008).

Western blot assay of A549 cells treated with CHR-AuNP, PTX, and CHR-AuNP +PTX revealed increased PPAR-ϒ, PTEN and decreased PI3K-AKT expression. (Fig11B) The similar finding regarding expression of PPAR-ϒ and p-AKT was reported in the Immunoflourescence investigation. (Fig 11A). The relative expression of the proteins obtained in western blot were plotted graphically and represented in (Fig. 11 C)

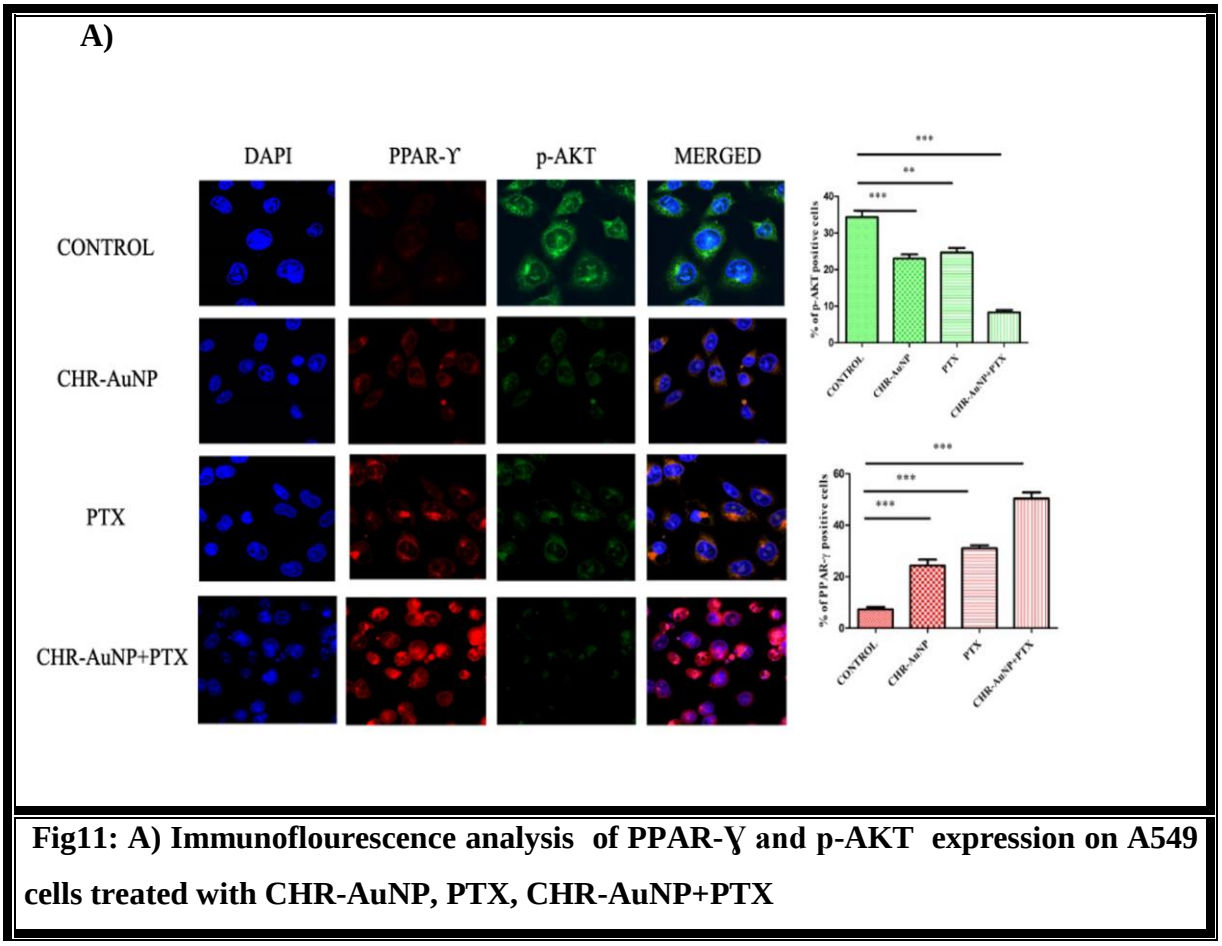

Fig11: A) Immunoflourescence analysis of PPAR-ϒ and p-AKT expression on A549 cells treated with CHR-AuNP, PTX, CHR-AuNP+PTX

B)

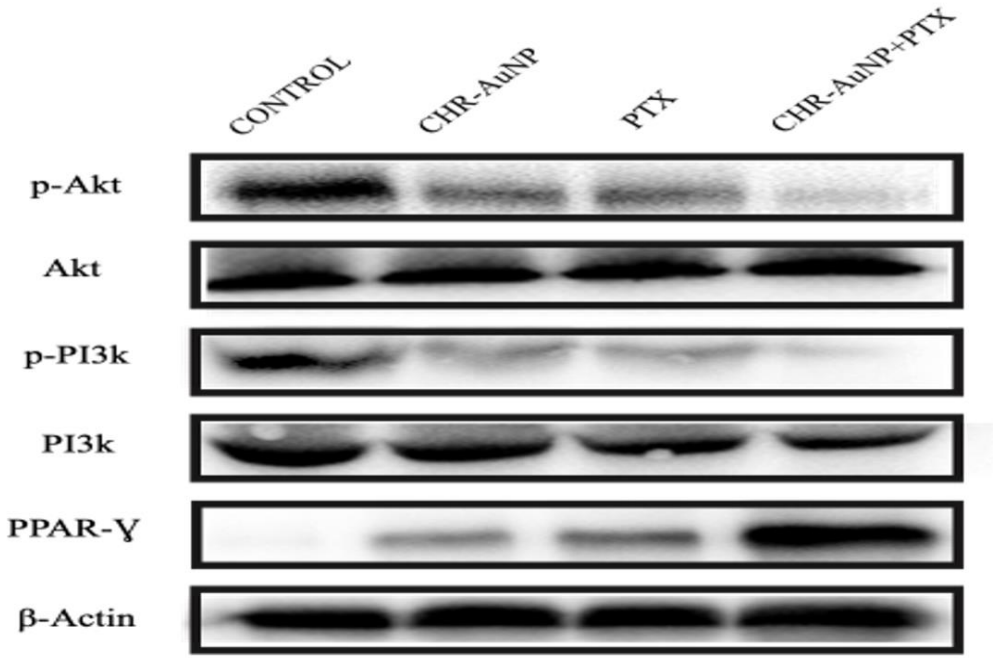

Fig 11: B) Western Blot analysis of AKT, p-AKT, PPAR-ϒ, PI3K, p-PI3K on A549 cells treated with CHR-AuNP, PTX, CHR-AuNP+ PTX

C)

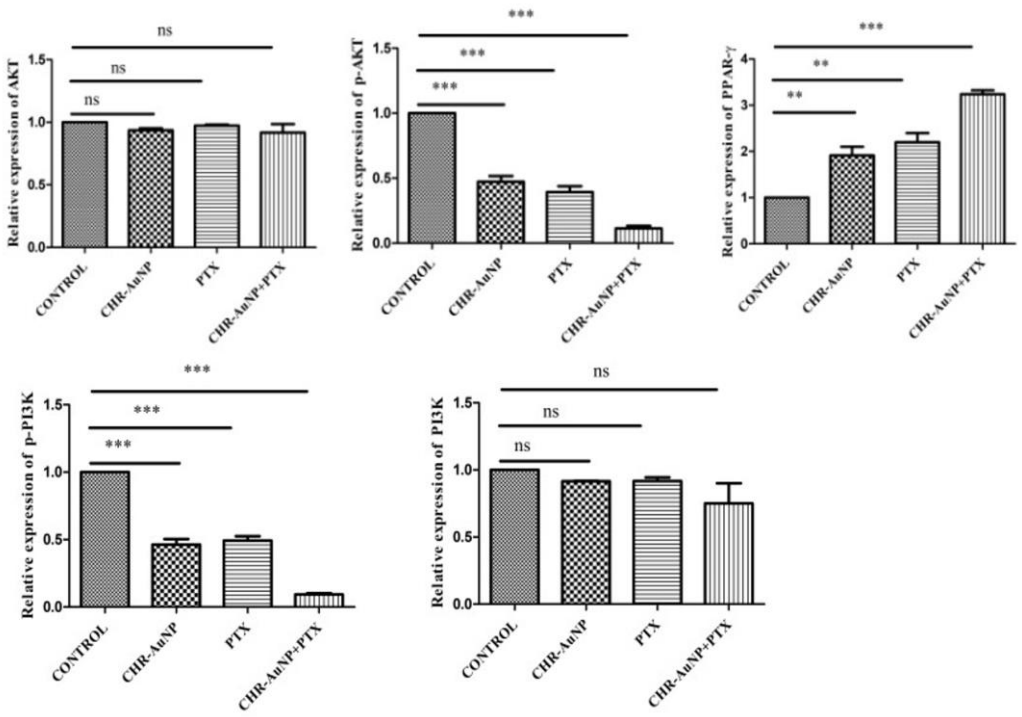

Fig 11: C) Relative expression of AKT, p-AKT, PPAR-ϒ, PI3K, p-PI3K in A549 cells treated with CHR-AuNP, PTX and CHR-AuNP+ PTX

The combination of CHR-AuNP and PTX inhibits the Wnt/ β-Catenin pathway

WNT/β-catenin signalling is escalated in inflammatory processes and oxidative stress, as well as in many malignancies. PPAR-ϒ, on the other hand, is frequently significantly attenuated during inflammation and oxidative stress, as well as in many malignancies.

PPAR-ϒ inhibits carcinogenesis and Wnt signalling in physiological cells by directing phosphorylated β-catenin to the proteasome via a process involving the PPAR-ϒ/β -catenin binding domain. The results of Western blot and immunofluorescence evaluation on A549 cells treated with CHR-AuNP, PTX, and CHR-AuNP+ PTX combination revealed that these

drugs efficiently enhanced the PPAR-ϒ level while decreased the β-catenin level. Fig(12A,12B) The relative expression of the proteins obtained in western blot were plotted graphically and represented in (Fig. 12 C)

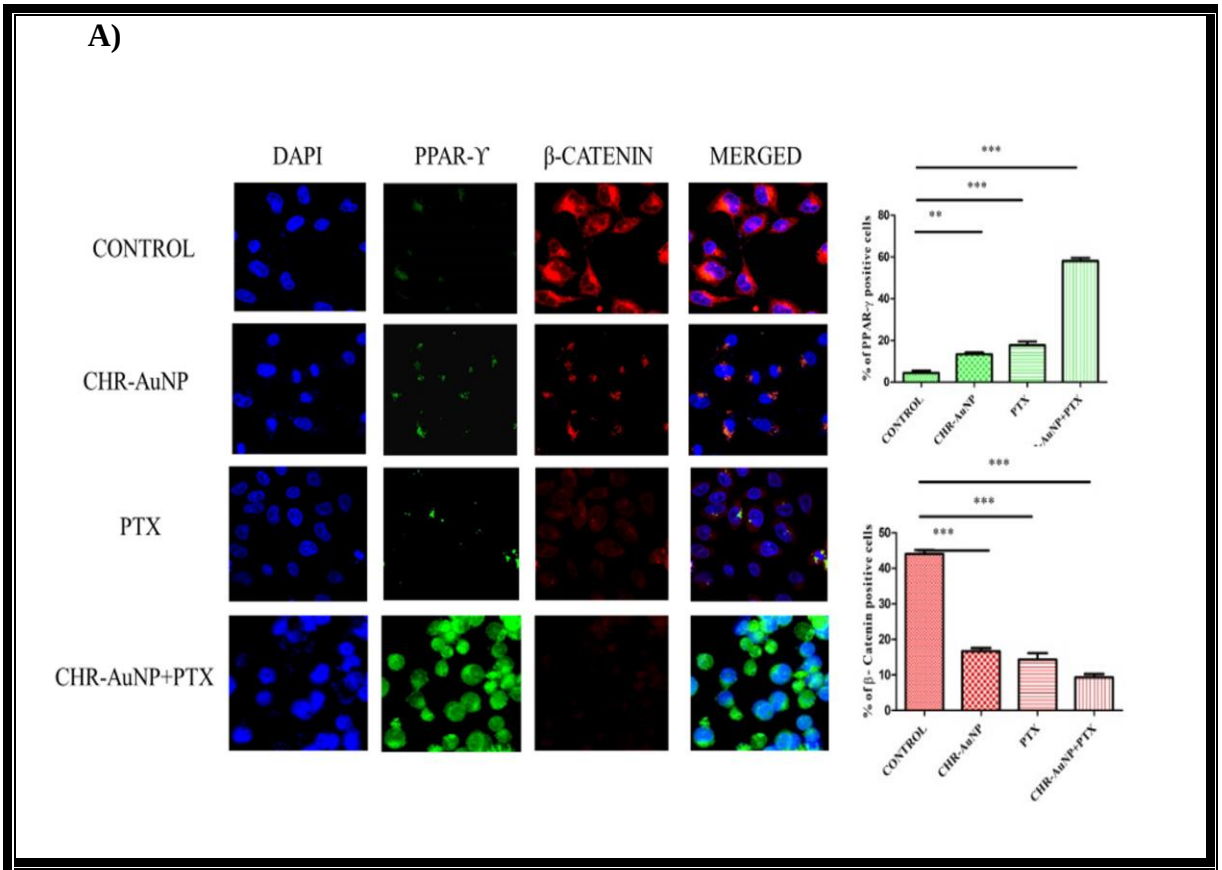

Fig12: A) Immunoflourescence study of PPAR-ϒ and β-catenin protein expression on A549 cells treated with CHR-AuNP, PTX, CHR-AuNP+ PTX

B)

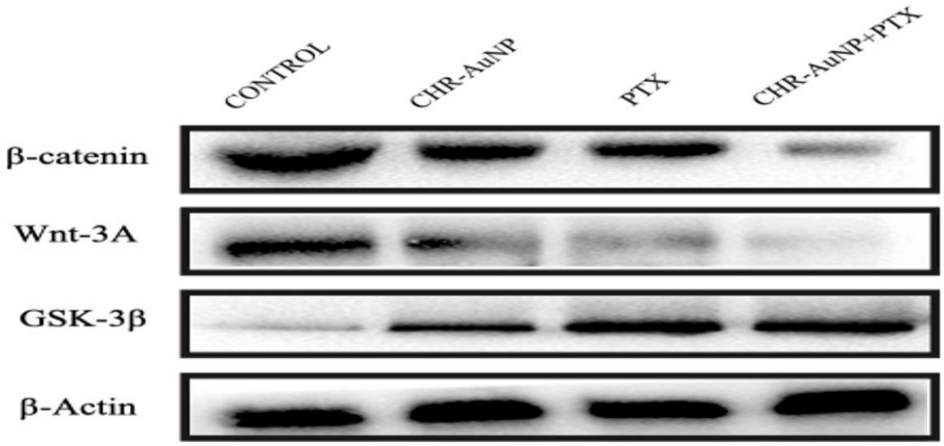

Fig 12: B) Western blot analysis were performed on A549 cells treated with CHR-AuNP, PTX, and CHR-AuNP +PTX to detect the molecules involved in Wnt pathway.

C)

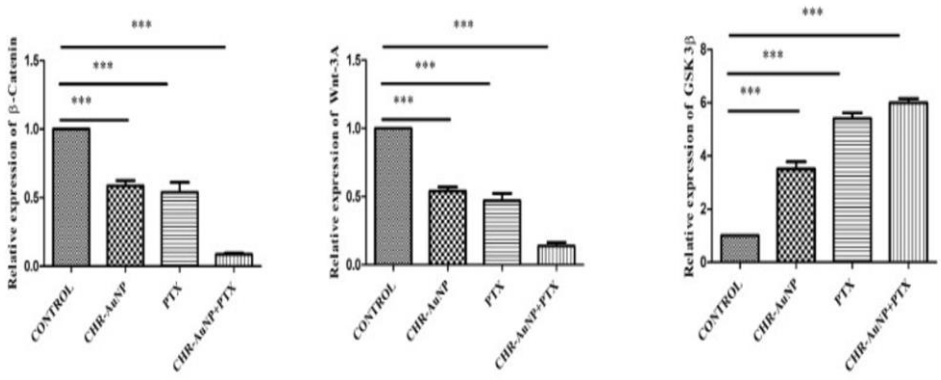

Fig12:C) Relative expression of β-catenin, Wnt-3A and GSK-3β in A549 cells treated with CHR-AuNP, PTX and CHR-AuNP+ PTX.

Discussion

In this investigation, we synthesized Chrysin-functionalized gold nanoparticles (CHR-AuNP) to be used in conjunction with PTX. The goal was to reduce the dosage of the chemotherapeutic medicine PTX, hence minimising the side effects. The cytotoxic action of CHR-AuNP augments the therapeutic impact of paclitaxel. Chrysin has anticancer properties as well, but also has poor pharmacokinetics. As a result, producing chrysin functionalized gold nanoparticles (CHR-AuNP) improved Chrysin's cytotoxicity.

The wine red colouration as well as the plasmonic band at 540 nm observed in UV spectroscopy confirmed the successful formulation of CHR-AuNP. As determined by AFM microscopy and corroborated by DLS analysis, the nanoparticles (CHR-AuNP) generated were found in the nano range (40-60) nm. The particles were spherical and moderately stable, with a zeta potential of -22 mV. The anticancer potential of CHR-AuNP was further evaluated in invitro A549 lung carcinoma cells. MTT assay revealed that CHR-AuNP was found to be more cytotoxic than crude CHR. The co-treatment of CHR-AuNP and PTX also resulted in a reduction in PTX dosage and found to be synergistic. The co-therapy was also found to more efficiently cause ROS-mediated apoptosis than the monotherapy. It was also observed by JC-1 assay and Rhodamine 123 assay that the apoptosis was mediated through intrinsic pathway. The combination therapy efficiently boosted pro-apoptotic molecule expression while decreasing anti-apoptotic molecule expression. The likely signalling pathways by which apoptosis eventuated was investigated further.

PI3K/Akt pathway is upregulated in majority of the cancer and likewise found in our experimental studies. Upregulation of PTEN on the other hand inhibits the PI3K/Akt pathway. Our studies unveiled that the combination therapy downregulated the PI3K/Akt pathway by upregulating PTEN more prominently than CHR-AuNP and PTX alone.

The peroxisome proliferator activator receptor-gamma (PPAR-ϒ) is a transcriptional factor that is activated by ligands and is implicated in tumour growth. PPAR-ϒ stimulates the synthesis of proteins involved in apoptosis and cell growth regulation, such as Bax (BCL2-associated X), Bid (BH3 interacting-domain), and the tumour suppressor p53. PPAR-ϒ expression is found to be repressed whereas classical Wnt/β-catenin pathway is overexpressed in most malignancies. Canonical Wnt/β-catenin pathway activation induces PPAR-ϒ inactivation in many tissues, whereas PPAR-ϒ activation inhibits canonical Wnt/ β-catenin signalling. Our experimental analysis revealed that CHR-AuNP + PTX co therapy effectively inhibited the Wnt /β-catenin pathway by activating PPAR-ϒ and thus suppressing carcinogenesis.

REFERENCES

Ahmed, S., Annu, Ikram, S., & Yudha S., S. (2016). Biosynthesis of gold nanoparticles: A green approach. *Journal of Photochemistry and Photobiology B: Biology, 161,* 141–153. https://doi.org/10.1016/j.jphotobiol.2016.04.034

Alkhatib, S., Kandemiş, E., Gizir, G., & Bulut, G. (2018). *Synergistic Effect of YK-4-279 and Paclitaxel on A549 Cell Line*. 1588. https://doi.org/10.3390/proceedings2251588

Chou, T.-C. (2010). Drug Combination Studies and Their Synergy Quantification Using the Chou-Talalay Method. *Cancer Research*, *70*(2), 440–446. https://doi.org/10.1158/0008-5472.CAN-09-1947

Howington, J. A., Blum, M. G., Chang, A. C., Balekian, A. A., & Murthy, S. C. (2013). Treatment of Stage I and II Non-small Cell Lung Cancer. *Chest*, *143*(5), e278S-e313S. https://doi.org/10.1378/chest.12-2359

Kyakulaga, A. H., Aqil, F., Munagala, R., & Gupta, R. C. (2020). Synergistic combinations of paclitaxel and withaferin A against human non-small cell lung cancer cells. In *Oncotarget* (Vol. 11, Issue 16). www.oncotarget.com

Muniyappan, N., Pandeeswaran, M., & Amalraj, A. (2021). Green synthesis of gold nanoparticles using Curcuma pseudomontana isolated curcumin: Its characterization, antimicrobial, antioxidant and anti- inflammatory activities. *Environmental Chemistry and Ecotoxicology*, *3*, 117–124. https://doi.org/10.1016/j.enceco.2021.01.002

Patel, L., Pass, I., Coxon, P., Downes, C. P., Smith, S. A., & Macphee, C. H. (2001). Tumor suppressor and anti-inflammatory actions of PPARγ agonists are mediated via upregulation of PTEN. *Current Biology*, *11*(10), 764–768. https://doi.org/10.1016/S0960-9822(01)00225-1

Planchard, D., Popat, S., Kerr, K., Novello, S., Smit, E. F., Faivre-Finn, C., Mok, T. S., Reck, M., van Schil, P. E., Hellmann, M. D., & Peters, S. (2018). Metastatic non-small cell lung cancer: ESMO Clinical Practice Guidelines for diagnosis, treatment and follow-up. *Annals of Oncology*, *29*, iv192–iv237. https://doi.org/10.1093/annonc/mdy275

Salmena, L., Carracedo, A., & Pandolfi, P. P. (2008). Tenets of PTEN Tumor Suppression. *Cell*, *133*(3), 403–414. https://doi.org/10.1016/j.cell.2008.04.013

Samarghandian, S., Nezhad, M., & Mohammadi, G. (2014). Role of Caspases, Bax and Bcl-2 in Chrysin-Induced Apoptosis in the A549 Human Lung Adenocarcinoma Epithelial Cells. *Anti-Cancer Agents in Medicinal Chemistry*, *14*(6), 901–909. https://doi.org/10.2174/1871520614666140209144042

Thai, A. A., Solomon, B. J., Sequist, L. v, Gainor, J. F., & Heist, R. S. (2021). Lung cancer. *The Lancet*, *398*(10299), 535–554. https://doi.org/10.1016/S0140-6736(21)00312-3

To, K. K. W., Wu, W. K. K., & Loong, H. H. F. (2018). PPARgamma agonists sensitize PTEN-deficient resistant lung cancer cells to EGFR tyrosine kinase inhibitors by inducing autophagy. *European Journal of Pharmacology*, *823*, 19–26. https://doi.org/10.1016/j.ejphar.2018.01.036

CHAPTER 6

SUMMARY AND CONCLUSION

SUMMARY AND CONCLUSION

Chrysin (CHR) a is an inherently endogenous flavonoid with anticancer, anti-inflammatory, and anti-asthmatic activities. It's restricted water solubility impairs bioavailability and, as a consequence, therapeutic advantages. As a corollary, nanotechnology may be invaluable in combating its limitations and augmenting its bioavailability.

Incidence of Asthma is growing at an alarming rate which is primarily treated with inhaled corticosteroid along with bronchodilators and mast cell inhibitor. Inhaled corticosteroids have serious adverse effect in long run. Hence alternative therapy is of utmost need. Reports of effectively using phytochemicals as alternate therapy in asthma model are plenty. So CHR ,a phytochemical was chosen as alternate drug in treating allergic asthma in one of our studies. Also, Chrysin was loaded in PLGA to overcome its poor pharmacokinetics.

CHR loaded PLGA nanoparticles (CHR-NP) were formulated following nanoprecipitation technique. The nanoparticles were uniformly spherical in shape with diameter ranging from (65-90 nm) with smooth surface. The synthesised nanoparticles' encapsulation effectiveness and drug loading were determined to be 91.45 ±1.4 and 8.37±0.12, respectively. The zeta potential (ZP) recorded was to be -13.1±2.9 mV at pH 7.4 and -9.33±0.5 mV and -6.10±0.7 mV at pH 6.8 and pH 2 respectively. DSC, XRD, FTIR analysis confirmed the encapsulation of chrysin in the nanoparticle. The FITC tagged CHR-NP was observed to be effectively up taken by A549 cells after incubating for 4 hours. The in vitro release study showed slow and sustained release of CHR from CHR-NP.

The efficacy of CHR-NP was evaluated in vivo employing a number of biochemical tests, including differential cell counts in BAL fluids using Giemsa staining, cytokines (IL-4, IL-5, IL-13) and serum immunoglobulin (IgE) level detection using ELISA. Western blot and

immunofluorescence studies revealed that CHR-loaded PLGA nanoparticles significantly alleviated OVA-induced allergic asthma by modulating TLR2/4, NF-κB, and NLRP3 pathways. Also because NF-κB and NLRP3 pathways are vital for the production of pro-inflammatory cytokines, efficient downregulation of these pathways by CHR-NP reduces inflammation during allergic asthma. Based on our findings, CHR-NP may be a viable alternative treatment for mitigating allergic asthma and its associated inflammation.

Lung cancer is becoming more pervasive, and the standard line of drug-like platinum compounds, paclitaxel (PTX) is exhibiting resistance. Along with that chemotherapeutic drug infers major side effect.The usage of natural compounds as chemosensitizers to boost the efficacy of these chemotherapeutic drugs and minimising the toxicity on the other hand, is a possible approach. PTX was employed as the conventional chemotherapeutic agent in our investigation. We employed CHR-functionalized gold nanoparticles (CHR-AuNP) to boost its cytotoxicity. Gold nanoparticles were chosen for two reasons: firstly, they have cytotoxic properties, and secondly, they increase CHR bioavailability and solubility.

In our second study we formulated CHR functionalized gold nanoparticles (CHR-AuNP) with spherical shape in nanosize range (35-70 nm) and negative ZP -22 mV suggesting stability. The physicochemical characterization by UV-Vis spectroscopy, FT-IR as well as visual evidence of the wine red coloured hue of the formulation also confirmed the nanoparticle formation. MTT assay illustrated that CHR-AuNP is more effective than CHR, and co - treatment of PTX and CHR-AuNP was synergistic, also verified by Compusyn software. When the drugs were taken together in low doses, they elicited more significant morphological changes in the cancer cell, triggering apoptosis, as observed by AO/ETBr staining and quantitative determination of apoptosis by Annexin V. The combined treatment exacerbated ROS production and MMP destabilization. The expression of pro-apoptotic and anti-apoptotic protein molecules in co-therapy group were found to be comparatively variable with the

monotherapy. The co -treatment downregulated the anti -apoptotic molecules and upregulated the pro apoptotic molecules more profoundly. We also explored the plausible mechanism via which apoptosis eventuated. It was revealed that CHR-AuNP+ PTX elevated PPAR-ϒ expression by suppressing Akt and overexpressing the PTEN protein. In turn, the PPAR-ϒ impeded the Wnt /βcatenin pathway, which is frequently upregulated in lung cancer. Thus, our study concluded that low-dose combination therapy with PTX and CHR-AuNP is a promising option for addressing the inadequacies in the standard treatment plan.

REPRINTS OF PUBLICATIONS

Nanomedicine: Nanotechnology, Biology, and Medicine
30 (2020) 102292

nanomedicine
Nanotechnology, Biology, and Medicine

nanomedjournal.com

Chrysin-loaded PLGA attenuates OVA-induced allergic asthma by modulating TLR/NF-κB/NLRP3 axis

Saheli Roy, M.S. (Pharm.)[a], Krishnendu Manna, PhD[b], Tarun Jha, PhD[c], Krishna Das Saha, PhD[a,*]

[a]*Cancer Biology & Inflammatory Disorder, Indian Institute of Chemical Biology (CSIR-IICB), Kolkata, West Bengal, India*
[b]*Department of Food & Nutrition, University of Kalyani, Kalyani, West Bengal, India*
[c]*Natural Science Laboratory, Division of Medicinal and Pharmaceutical Chemistry, Department of Pharmaceutical Technology, Jadavpur University, Kolkata, West Bengal, India*

Revised 23 June 2020

Abstract

Asthma, one of the significant public health problems, is triggered by certain inflammatory processes in the airways that are not addressed propitiously by current therapies. Though pieces of evidence on allergic asthma mitigation by the anti-inflammatory bioflavonoid chrysin (CHR) are accumulating, poor bioavailability, and low solubility curtail drug development. To overcome these shortcomings, CHR loaded nanoparticle (CHR-NP) was formulated, and its salutary effect in preclinical murine allergic asthma model via the peroral route was evaluated. The spherical nanosized particles showed slow, sustained release in vitro. Moreover, CHR-NP dramatically reduced the serum IgE, ovalbumin (OVA)-induced lung histological alteration, as well as Th2 (T-helper 2) cytokines in the bronchoalveolar lavage fluid (BALF). It also suppressed the elevated serum pro-inflammatory cytokines and their upstream TLR/NF-κB/NLRP3 pathway activation in lung superior to CHR and almost identical to dexamethasone (DEX). Thus this study suggests the potentiality of CHR-NP in ameliorating allergic asthma progression.

Key words: Chrysin; Murine allergic asthma model; Th2 cytokines; TLR/NF-κB/NLRP3 pathway

Asthma is a complex heterogeneous disease marked by chronic inflammation of the airways, wheezing, shortness of breath, chest tightness, and dyspnea due to congestion of the airways.[1] The World Health Organization (WHO) reports that asthma impacts 300 million people globally.[2,3] Nascent approaches to the management of asthma focused on relieving bronchoconstriction with a bronchodilator. However, the discovery of airway inflammation as a crucial pathophysiological component of asthma eventually led to the use of inhaled corticosteroids as the central element of asthma therapy. Airway inflammation is typically associated with T helper-2 (Th2)-related responses. There is eosinophil overproduction, elevation in Th2 cytokine levels notably, interleukins (IL)–4, IL-5, and IL-13, and immunoglobulin-E (IgE) secretion. Both IL- 4 and IL-13 foster acute inflammatory processes and underlining respiratory tract alterations. Th2 cytokine stimulation triggers B cells to secrete IgE and the substitution of leukocytes in the lung tissue.[4–6]

The Global Asthma Initiative (GINA) launched new guidelines regarding asthma treatment in April 2019, where the intake of inhaled corticosteroids was made compulsory along with bronchodilators and leukotriene receptor antagonists.[7] It is necessary to improve existing therapies in terms of lower side effect profile or oral formulations and to avoid recurrence after treatment discontinuation, which is prevalent with corticosteroids.[8–10]

Chrysin (CHR), also known as 5,7-dihydroxyflavone is a bioflavonoid widely disseminated in a plethora of natural sources,[11,12] and possesses multimodal pharmacological activities including anti-inflammatory, anti-proliferative, anti-allergic, etc.[13,14,15] However, it has poor bioavailability following oral administration[16,17] and low solubility (2–5 μg/mL),[18] which is a bottleneck for its pharmaceutical application. Hence, numerous strategies like (cosolvents, salt formation, complexes with cyclodextrins are applied to overcome its solubility problem.[19]

Funding Source: This work was supported by the National Medicinal Plant Board (NMPB), Ministry of AYUSH & Department of Biotechnology, North Eastern Region (DBT-NER), Government of India partially along with a research fellowship of ICMR-SRF granted by the Indian Council of Medical Research (ICMR), Government of India.

Disclosure: The authors of this article declare no conflicts of interest.

*Corresponding author at: Cancer Biology & Inflammatory Disorder Division, CSIR-Indian Institute of Chemical Biology (CSIR-IICB), Kolkata -700032, West Bengal, India.

E-mail address: krishna@iicb.res.in. (K.D. Saha).

https://doi.org/10.1016/j.nano.2020.102292
1549-9634/

ACS OMEGA

Article

Cite This: ACS Omega 2018, 3, 16134−16142

http://pubs.acs.org/journal/acsodf

Synthesis of Triazole-Substituted Quinazoline Hybrids for Anticancer Activity and a Lead Compound as the EGFR Blocker and ROS Inducer Agent

Biswadip Banerji,*[,†,‡] Kadaiahgari Chandrasekhar,[†,‡] Kancham Sreenath,[§] Saheli Roy,[∥] Sayoni Nag,[∥] and Krishna Das Saha[∥]

[†]Organic & Medicinal Chemistry Division, [‡]Academy of Scientific and Innovative Research (AcSIR), and [∥]Cancer Biology & Inflammatory Disorder, Indian Institute of Chemical Biology (CSIR-IICB), 4 Raja S. C. Mullick Road, Kolkata 700032, India

[§]National Institute of Pharmaceutical Education and Research (NIPER)—Kolkata, 4, Raja S. C. Mullick Road, Kolkata 700032, India

Supporting Information

ABSTRACT: A series of triazole-substituted quinazoline hybrid compounds were designed and synthesized for anticancer activity targeting epidermal growth factor receptor (EGFR) tyrosine kinase. Most of the compounds showed moderate to good antiproliferative activity against four cancer cell lines (HepG2, HCT116, MCF-7, and PC-3). Compound **5b** showed good antiproliferative activity (IC_{50} = 20.71 μM) against MCF-7 cell lines. Molecular docking results showed that compound **5b** formed hydrogen bond with Met 769 and Lys 721 and π−sulfur interaction with Met 742 of EGFR tyrosine kinase (PDB ID: 1M17). Compound **5b** decreases the expression of EGFR and p-EGFR. It also induces apoptosis through reactive oxygen species generation, followed by the change in mitochondrial membrane potential.

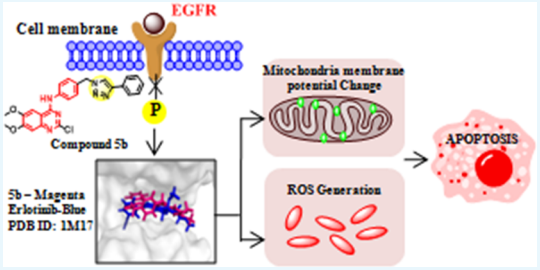

INTRODUCTION

Cancer is one of the most devastating diseases in the developing countries.[1] The epidermal growth factor receptor (EGFR) plays an important role in cell survival, growth, differentiation, and tumorigenesis. Dysregulation of EGFR is a common mechanism in cancer progression especially in nonsmall cell lung cancer (NSCLC). Also, overexpression of EGFR has been observed in different types of cancers such as breast, ovarian, head and neck, colon, and so forth.[2] Some FDA-approved drugs, EGFR inhibitors such as erlotinib[3] (i), gefitinib[4] (ii), icotinib[5] (iii), lapatinib[6] (iv), and afatinib[7] (v), are used for the treatment of the above-mentioned cancers (Figure 1). The interplay of reactive oxygen species (ROS) and the EGFR plays an important role in cancer progression. Excessive ROS can induce negative responses such as growth inhibition or death of cancer cells. Mitochondrial dysfunction is also the major mechanism inducing oxidative stress. Higher ROS levels can trigger overoxidation of the Met residue of EGFR T790M and shut down the EGFR downstream survival pathway.[8] Therefore, direct EGFR inhibition or inhibition of EGFR function via excessive ROS generation or both may be a feasible therapeutic approach for cancer treatment.

Side effects are major problems with the current EGFR inhibiting anticancer drugs. For example, erlotinib significantly reduced the levels of white blood cells, red blood cells (RBCs), and hemoglobin. It increased liver function markers, aspartate aminotransferase and alanine aminotransferase levels, and damaged the internal organs in an experimental rat model.[9] Similarly, unusual hematologic complications were detected after erlotinib was administered in patients with advanced NSCLC.[10] Therefore, it is important to design new EGFR inhibitors as anticancer agents with low toxicity on normal organs and blood cells.

Quinazoline is an important heterocyclic moiety used in drug discovery because of its diverse biological activities.[11] Especially, 4-aminoquinazoline moiety showed good efficacy against various cancers. The structure−activity relationship (SAR) of EGFR inhibitors such as erlotinib and lapatinib revealed a quinazoline moiety to play an important role in antitumor activity, especially 4-aminoquinazoline moiety. 4-Aminoquinazoline moiety seemed particularly very important for activity and showed diverse biological activities such as anticancer,[12] antitubercular,[13] antimalarial,[14] antileishmanial,[15] and antibacterial and antifungal activities.[16]

1,2,3-Triazole is another important pharmacophore in medicinal chemistry and it can form hydrogen bonding with biological targets,[17] which will be useful for the activity. Also, triazole moiety-containing molecules (vi−ix, Figure 1) are known to show various pharmacological activities such as anticancer,[18] anti-human immunodeficiency virus,[19] antituber-

Received: August 9, 2018
Accepted: October 26, 2018
Published: November 28, 2018

DOI: 10.1021/acsomega.8b01960
ACS Omega 2018, 3, 16134−16142

Nanomedicine: Nanotechnology, Biology, and Medicine
20 (2019) 102006

nanomedjournal.com

Therapeutic potential of andrographolide-loaded nanoparticles on a murine asthma model

Shreyasi Chakraborty, M.Pharm[a], Iman Ehsan, M.Pharm[a], Biswajit Mukherjee, Ph.D[a,*], Laboni Mondal, M.Pharm[a], Saheli Roy, M.Pharm[b], Krishna Das Saha, Ph.D[b], Brahamacharry Paul, M.Pharm[c], Mita Chatterjee Debnath, Ph.D[c], Tanmoy Bera, Ph.D[a]

[a]*Department of Pharmaceutical Technology, Jadavpur University, Kolkata, India*
[b]*Cancer and Inflammatory Disorder Division, CSIR-Indian Institute of Chemical Biology, Kolkata, India*
[c]*Infectious Diseases and Immunology Division, CSIR-Indian Institute of Chemical Biology, Kolkata, India*

Revised 27 February 2019

Abstract

Corticosteroids commonly prescribed in asthma show several side-effects. Relatively non-toxic andrographolide (AG) has an anti-asthmatic potential. But its poor bioavailability and short plasma half-life constrain its efficacy. To overcome them, we encapsulated AG in nanoparticle (AGNP) and evaluated AGNP for anti-asthmatic efficacy on murine asthma model by oral/pulmonary delivery. AGNP had 5.47% drug loading with a sustained drug release *in vitro*. Plasma and lung pharmacokinetic data showed predominantly improved AG-bioavailability upon AGNP administered orally/by pulmonary route. Cell numbers, IL-4, IL-5, and IL-13 levels in broncho-alveolar lavage fluid and serum IgE content were reduced significantly after administration of AGNP compared to free-AG treatment. AGNP-mediated suppression of NF-κβ was predominantly more compared to free-AG. Further, pulmonary route showed better therapeutic performance. In conclusion, AGNP effectively controlled mild and severe asthma and the pulmonary administration of AGNP was more efficacious than the oral route.

Key words: Andrographolide; Nanoparticle; Murine asthma model; Ovalbumin; Eosinophilia

Allergic asthma is a chronic airway disorder characterized by airway inflammation, mucus hyper-secretion, airway hyper-responsiveness followed by shortness in breathing[1] and approximately three hundred million people around the world suffer from asthma.[2] Many inflammatory cells such as Th2 cells, B-cells, mast cells and a number of cytokines are involved in the allergic cascade.[1,3] Allergen induces crosslinking of IgE with IgE-receptor (FcεRI) on mast cells, releasing histamine, leukotrienes, interleukins (ILs) and other inflammatory mediators.[4,5] Airway eosinophilia together with Th2 cytokines, IL-4, IL-5 and IL-13, may ultimately contribute to airway hyper-responsiveness in asthma.[6] Treatment with corticosteroids is a common therapeutic strategy for asthma but has severe side-effects.[7–9] Novel therapeutic agents with their effective route of administration and prolonged action may be an alternative to corticosteroids for management of asthma.

Nanoparticles are frequently used for loading different types of drug due to the several advantages such as improved bioavailability, sustained release, tissue targeted delivery, improved permeability to biological membranes, and usefulness in different routes of administration.[10–14] In the past few decades, biodegradable polylactide-co-glycolide (PLGA), approved by the US Food and Drug Administration and European Medicine Agency, has been extensively used to develop sustained release nanoparticles to treat various diseases including pulmonary diseases in animals [15–17] and humans.[18,19]

Andrographolide (AG), a labdane diterpene lactone,[20] attenuates ovalbumin (OVA) induced allergic asthma.[21–24] But poor water solubility,[25] and very short biological half-life in gastrointestinal acidic and alkaline conditions due to its

Funding Source: This work was supported by Department of Science and Technology, Government of India [NSTMIS/Inspire Fellowship/2015/150019]. and [NSTMIS/NSTMIS/05/207-1/2016-17].

*Corresponding author at: Department of Pharmaceutical Technology, Jadavpur University, Kolkata, India.
E-mail addresses: biswajit.mukherjee@jadavpuruniversity.in biswajit55@yahoo.com (B. Mukherjee).

https://doi.org/10.1016/j.nano.2019.04.009
1549-9634/

Saheli Roy